BINARY GALAXIES

AND

GROUPS OF GALAXIES

Thesis by

Edwin Lewis Turner

In Partial Fulfillment of the Requirements

for the Degree of

Doctor of Philosophy

California Institute of Technology

Pasadena, California

1976

(Submitted October 13, 1975)

To Joyce

ACKNOWLEDGEMENTS

It is not possible to adequately thank my thesis advisor, Wal Sargent, for the many roles he has played in my graduate education. He has provided enormous amounts of scientific advice, moral support and practical assistance. His approach to astronomical research has, I hope, deeply influenced the formation of my own.

Richard Gott will be a co-author of the papers represented by Chapters 3 and 4. I could not have wished for a more stimulating collaborator or a better friend.

Jim Gunn, who acted as a sort of secondary thesis advisor, often supplied a patient ear, valuable insights, and infectious enthusiasm. Also, his help with financial and administrative matters smoothed over many rough spots in my graduate career.

It is a pleasure to thank Ted Williams for teaching me to use the digital microphotometer and related data reduction programs, providing many interesting discussions, and easing the strain of the past months by his friendship during a parallel struggle.

Paul Schechter provided several useful conversations and computer programs dealing with the luminosity function of galaxies.

In addition to the above, there are many others from

whom I have received intellectual and/or personal benefit. These include Richard Green, Paul Hickson, John Huchra, Bob Kirshner, Gill and Steve Knapp, Phil Morrison, Gus Oemler, Jerry Ostriker, Allan Sandage, Anneila Sargent, Maartin Schmidt, Linda Schweizer, Steve Shectman, Trinh Thuan, Alar Toomre, Barry Turnrose, and particularly Doug Richstone.

Helen Holloway, Marilyn Rice, Elsa Titchenell, and especially Janet Williams have generously provided their time and expert skills to type the manuscript.

Without the early encouragement and help of my parents, I could not have begun either this thesis or any other.

In addition to providing unflagging and indispensable emotional support, Joyce Turner helped extensively in the compilation of data and preparation of tables for Chapters 1 and 3.

Finally, I offer my thanks and apologies to anyone I have unintentionally omitted.

The financial support for my graduate studies consisted of an NSF Graduate Fellowship for 3 years and a Virginia Steele Scott Fellowship for 13 months.

ABSTRACT

Using precisely defined identification criteria, a sample of 156 binary galaxy systems is selected from the Zwicky Catalog of Galaxies and Clusters of Galaxies. Data on their magnitudes, morphological types, radial velocities, angular separations, et cetera are presented. Accurate, new radial velocities for both components of 66 of the pairs have been measured. Substantial effort is directed towards establishing a sample of binary galaxies in which all sources of systematic bias and statistical error are well understood.

With particular attention to the removal of selection effects, extensive statistical and dynamical analyses of these data lead to several conclusions: The ratio of the mass-to-light ratio in early-type galaxies to that in late-types is 2.0 ± 0.5. The distribution of spatial separations r between binary galaxies has an approximately $r^{-1/2}$ dependence. A variety of dynamical models for binary galaxy systems are viable; however, they all require total mass-to-light ratios for spirals far larger than conventional (rotation curve) values. The most plausible interpretation of the binary galaxy data requires that spiral galaxies possess halos containing ~10 times the disk mass and have total mass-to-light ratios ~65 $M_\odot/L_\odot$ (H_o= 50 km

s^{-1} Mpc^{-1}). It is shown that previous studies of binary galaxies have probably underestimated masses by a factor $\gtrsim$10 primarily because selection biases (particularly those toward small projected separations) were ignored. There is some evidence against halos containing significant mass on scales very large compared to 100 kpc. Orbits of moderate eccentricity are more consistent with the present data than either purely circular or purely radial (probably excluded) ones.

A catalog of small groups of galaxies is generated by identifying regions of the sky in which the surface number-density of galaxies is enhanced. The determinations of both group existence and membership are accomplished by well-defined procedures and are based entirely on the distribution of galaxies in the sky. A variety of data on the groups, their component galaxies, and those galaxies not assigned to groups (i.e. field galaxies) is presented. The generally small velocity dispersions of the groups validate the group identification algorithm.

Using the available data, statistical analyses of the galaxy luminosity function in groups, the group dynamics, and the multiplicity function are described. The luminosity function is shown to be similar to that in rich clusters, well fit by a Schechter function with α=-1

and $L^*=3.4 \times 10^{10} L_\odot$, and useful for estimating group distances. The dynamical analysis indicated that the groups are bound and relaxed, and gives typical mass-to-light ratios of $\sim 90\ M_\odot/L_\odot$. A crude estimate of the group multiplicity function (distribution of total group luminosities) suggests a power-law ($\sim L^{-7/3}$) for groups brighter than $\sim L^*$.

TABLE OF CONTENTS

INTRODUCTION

As required by the new Astronomy Department regulations, each chapter of this thesis is intended to represent an independent paper written in a form suitable for direct submission to the Astrophysical Journal. For this reason, the chapters may seem somewhat disjoint and, in a few places, redundant. The purpose of this introduction is to provide an overview of the work, hopefully offsetting these problems.

The text can be effectively divided into two parts. The first part concerns binary galaxies and is made up of Chapters 1 and 2. The second part deals with groups of galaxies and is comprised of Chapters 3 and 4. Chapters 1 and 3 report the generation of complete and well-defined samples (i.e., catalogs) of binary galaxies and groups of galaxies, respectively. In addition, Chapter 1 details the results of new observations of binary systems. Chapters 2 and 4 present statistical analyses of these samples (catalogs). Chapter 2 is concerned with the dynamical properties of the binary galaxies, while Chapter 4 describes studies of the galaxy luminosity function, dynamics, and multiplicity function of the groups. When Chapters 3 and 4 appear as papers, Richard Gott will be a co-author.

All four chapters are basically attempts to determine the statistical properties of small aggregates of galaxies. Also, both the binary and the group investigations take as their starting points the invaluable general catalogs of galaxies compiled by Zwicky *et al.* and by Nilson.

CHAPTER 1

BINARY GALAXIES:

A WELL-DEFINED STATISTICAL SAMPLE

I. INTRODUCTION

The occurrence of apparently bound pairs of galaxies permits a statistical estimation of galaxian masses and mass-to-light ratios. Such estimates are superior in some ways to those obtained from rotation curve and velocity dispersion studies of individual galaxies and virial theorem analyses of groups and clusters. Unlike the former, binary galaxy mass determinations can measure material well outside the optical object (e.g., a dark halo). And, unlike groups and clusters, binary systems are simple enough to permit the use of an explicit model of the individual galaxy orbits.

Despite these advantages, the binary galaxy method has not been as fully developed as the others. Page (1952, 1961, 1966, and references cited therein) and Holmberg (1954) made pioneering contributions, and more recently a number of authors (Wolf and Bahcall 1972; Noerdlinger 1975; Jenner 1974; and Smart 1973) have used or attempted to improve these methods and data.

Because the method is fundamentally a statistical one, it is critically important that the binary systems used in the analysis represent a well-defined statistical sample and that the analysis take into account any biases in the selection of the sample. Evidence supporting this claim in detail is given in the second paper in this series (Turner 1976, hereafter PII). The data previously compiled by Page

and others suffers somewhat from a lack of well-defined selection criteria. In this paper a rigorous definition of binary galaxy systems is used to choose a suitable statistical sample (§II). Various data are given for the sample (§III), and the results of radial velocity measurements performed on a part of the sample are presented (§IV). A summary is given in §V, and the Appendix describes the radial velocity reduction procedure. A dynamical analysis of these data is the subject of PII.

II. SELECTION CRITERIA

The problem of defining criteria for the selection of binary systems is a central one. The selection criteria should have the following properties:

1) They should identify as large a fraction of true binary systems as possible without including too many accidentally projected (i.e., optical) pairs.

2) It should be possible to take any resulting selection effects into account during the analysis.

3) They must make use of data available from some general catalog or survey of galaxies.

For the present study, a number of sets of criteria were considered. The most satisfactory set was adopted and is given by the requirements that

$$\theta_{12} \leq \theta_c \qquad (1)$$

and

$$\theta_{12,3} \geq x\, \theta_{12} \qquad (2)$$

where θ_{12} is the angular distance from a galaxy 1 to its nearest neighbor 2 and $\theta_{12,3}$ is the angular distance from the middle of the 1-2 system to the next nearest galaxy 3. θ_c is a cut-off radius chosen such that two galaxies are unlikely to satisfy equation (1) a by chance projection. x is a number chosen such that there is only a small chance that the second nearest neighbor to a point is $\geq$ x times farther away than the nearest, if the nearby points are distributed randomly (a probability which is independent of the local density). Essentially, criterion (1) selects pairs which are probably physically associated in some way, while criterion (2) rejects those which are associated through common membership in a group or cluster. If galaxies were distributed randomly with a mean density of $\bar{\rho}$ galaxies per steradian, the probabilities of a random galaxy satisfying criteria (1) and (2) are

$$P_1(\theta_c) = 1 - \exp[-2\pi\bar{\rho}\ (1 - \cos\ \theta_c)] \qquad (3)$$

and

$$P_2(x) = e^{-2} \int_0^{2\pi/x} \sin\ \theta\ \exp[\cos\ \theta + \cos\ x\theta]\, d\theta \qquad (4)$$

respectively.

These criteria have been applied to galaxies listed in the Catalog of Galaxies and Clusters of Galaxies (Zwicky

et al. 1961-1968, hereafter CGCG) which satisfy

$$\delta \geq 0°$$
$$|b^{II}| \geq 40° \qquad (5)$$
$$m_{pg} \leq 15.0$$

with $\theta_c = 8'$ and $x = 5$. All position and magnitude data were taken from the CGCG, which contains $\sim$ 4400 galaxies satisfying (5) (giving a mean density $\bar{\rho} = 1960$). This search yielded a sample of 156 candidate pairs. These systems constitute the sample with which the remainder of this paper and PII will be concerned.

It is of considerable interest to estimate the number of projected pairs in this sample. Unfortunately, as the following discussion shows, this number depends heavily on the degree of clustering of the CGCG galaxies. If all of the galaxies were distributed randomly about the sky, we would only expect $\sim$ 8 accidental pairs since $P_1(\theta_c = 8') = 0.033$ and $P_2(x = 5) = 0.054$. At the other extreme, if all of the galaxies were concentrated in a single cluster with $\rho >> \bar{\rho}$, criterion (1) is always satisfied and $\sim$ 240 accidental pairs would result. The real situation is clearly intermediate but much closer to the former case than the latter. Examination of available velocity data (PII) suggests that $\sim$ 12% ($\sim$ 19) of the pairs are optical.

III. BINARY GALAXY DATA

Table I gives various data for the 156 binary galaxy systems. Except for the new radial velocity material (described in §IV), the nature and source of these data are described below:

Column 1: Identification. Each system is assigned a number, and the two components are indicated by the letters A and B. The western or (if both components have the same right ascension) southernmost galaxy is labeled A. In addition, other designations for the individual galaxies are given.

Column 2: The 1950 coordinates of the system center. These are obtained from the CGCG positions of the components.

Column 3: Apparent magnitudes. These are the CGCG magnitudes of the components except in cases where the CGCG only gives one combined magnitude. In the latter case, the luminosity ratio of the two components was estimated from a comparison of the galaxy images on a glass copy of the Palomar Sky Survey plate and combined with the total CGCG magnitude to give individual magnitudes; these magnitudes are enclosed in parentheses and may be uncertain by $\sim$ 0.5 mag.. An overall 0.3 mag. accuracy of the CGCG magnitudes has recently been verified by extensive photoelectric photometry by Huchra (1975).

Column 4: Morphological types. Approximate types were obtained from the Uppsala General Catalog (Nilson 1973,

TABLE I

BINARY GALAXY DATA

(1) IDENTIFICATION		(2) ALPHA	DELTA	(3) MAG	(4) TYPE	(5) VEL	(6) ERR	(7) SEP	(8) ERR	(9) AP
1A		8 53.2	52 17	13.6	S	3715	14	3.30	0.10	6
B	NGC2692			14.1	S	3803	15			
2A	NGC2719	8 57.1	35 55	(15.0)	(I)	0	0	0.49	0.05	8
B	ARP 202			(14.1)	S	(3073)	100			
3A	NGC2778	9 9.4	35 10	13.1	E	2017	21	7.40	0.10	4
B	NGC2780			14.2	S	2173	22			
4A	NGC2802	9 13.9	19 10	(15.0)	(E)	8519	27	0.80	0.10	8
B	NGC2803			(15.0)	(E)	8718	30			
5A	NGC2831	9 16.8	33 58	(14.7)	E	5005	26	0.31	0.15	2
B	NGC2832			(13.6)	E	6762	30			
6A	NGC2852	9 20.0	40 24	14.0	QS	1881	40	2.30	0.10	5
B	NGC2853			14.6	S	1793	39			
7A	NGC2939	9 35.4	9 47	13.5	S	3209	66	5.80	0.10	5
B	NGC2940			14.8	EO	2824	65			
8A	NGC2944	9 36.4	32 36	(13.6)	S	(6747)	100	0.47	0.10	7
B	ARP 129			(14.8)	S	0	0			
9A	APP 255	9 50.7	8 7	14.8	S	0	0	4.30	0.10	3
B				15.0	S	0	0			
10A	IC577	9 53.5	10 43	14.4	S	0	0	3.10	0.10	6
B	IC578			14.7	S	0	0			

TABLE I (CONTINUED)

BINARY GALAXY DATA

(1) IDENTIFICATION		(2) ALPHA	DELTA	(3) MAG	(4) TYPE	(5) VEL	(6) ERR	(7) SEP	(8) ERR	(9) AP
11A	IC2530	9 58.6	37 27	15.0	(OS)	0	0	3.30	0.10	5
B				14.9	S	0	0			
12A	IC590	10 3.3	0 53	(15.0)	(E)	6025	31	0.22	0.10	8
B				(15.0)	(E)	6192	35			
13A	NGC3168	10 13.3	60 30	14.6	(E)	9382	37	4.80	0.10	4
B				14.9	(S)	9118	43			
14A	IC601	10 15.6	7 17	15.0	(SI)	3480	36	1.30	0.10	4
B	IC602			13.4	(I)	3646	31			
15A	VV 312	10 20.6	53 21	(15.0)	(S)	9740	14	0.56	0.10	8
B				(15.0)	(S)	9416	26			
16A	NGC3226	10 20.7	20 7	13.3	E	1441	42	2.20	0.10	9
B	NGC3227			12.2	S	1148	38			
17A	NGC3286	10 33.1	58 51	14.6	(E)	7678	61	4.00	0.10	5
B	NGC3288			15.0	(S)	7682	52			
18A		10 36.7	48 11	14.4	S	0	0	3.50	0.10	6
B				14.5	S	0	0			
19A		10 45.6	50 17	14.9	(S)	0	0	5.50	0.10	5
B				14.9	(S)	0	0			
20A	NGC3395	10 47.0	33 14	12.1	S	(1622)	100	1.30	0.10	8
B	NGC3396			12.6	I	(1611)	100			

TABLE I (CONTINUED)

BINARY GALAXY DATA

(1) IDENTIFICATION		(2) ALPHA	DELTA	(3) MAG	(4) TYPE	(5) VEL	(6) ERR	(7) SEP	(8) ERR	(9) AP
21A		10 47.3	0 37	14.9	(OS)	0	0	5.20	0.10	3
B				14.8	(S)	0	0			
22A	NGC3394	10 47.4	66 0	13.1	S	0	0	4.10	0.10	5
B	NGC3392			14.8	E	0	0			
23A	NGC3419	10 48.7	14 16	13.4	(S)	0	0	4.80	0.10	5
B				14.9	(S)	0	0			
24A		10 48.8	51 18	(14.1)	E	0	0	0.31	0.20	3
B				(14.9)	(E)	0	0			
25A	NGC3454	10 51.8	17 34	14.1	S	(1060)	100	3.70	0.10	6
B	NGC3455			13.1	S	0	0			
26A	NGC3473	10 55.5	17 22	14.8	(S)	0	0	2.00	0.10	4
B	NGC3474			14.9	(OS)	0	0			
27A		10 56.9	50 18	14.8	(S)	0	0	2.70	0.10	6
B				14.4	E	0	0			
28A		11 0.8	3 36	14.4	(S)	7291	22	5.20	0.10	5
B				15.0	(S)	7130	69			
29A	ARP 301	11 7.1	24 31	14.5	S	6107	61	0.76	0.15	8
B	VV 229			14.6	S	6083	46			
30A	NGC3577	11 11.1	48 34	14.7	S	5271	78	5.20	0.10	6
B	NGC3583			11.6	S	4887	126			

TABLE I (CONTINUED)

BINARY GALAXY DATA

(1) IDENTIFICATION		(2) ALPHA	DELTA	(3) MAG	(4) TYPE	(5) VEL	(6) ERR	(7) SEP	(8) ERR	(9) AP
31A	NGC3609	11 15.4	26 54	14.1	S	5622	90	5.40	0.10	5
B	NGC3612			15.0	SI	5470	150			
32A		11 15.6	19 4	13.6	(S)	0	0	6.80	0.10	4
B				14.9	D	0	0			
33A		11 15.6	28 31	14.8	S	0	0	2.20	0.10	5
B				14.7	D	0	0			
34A		11 18.2	31 31	14.8	S	0	0	5.60	0.10	4
B				15.0	S	0	0			
35A		11 21.7	0 57	14.8	(D)	0	0	4.20	0.10	5
B				14.7	(S)	0	0			
36A	IC694	11 25.7	58 50	(12.6)	S	(3212)	100	0.62	0.20	9
B	NGC3690			(12.6)	(S)	(3097)	100			
37A	NGC3719	11 29.7	1 5	13.8	S	0	0	2.20	0.10	6
B	NGC3720			13.7	(S)	0	0			
38A	NGC3769	11 35.0	48 10	11.7	S	(804)	100	1.20	0.10	4
B				14.7	S	(768)	100			
39A	NGC3786	11 37.0	32 12	13.5	S	(2737)	100	1.40	0.10	8
B	NGC3788			13.2	S	(2327)	100			
40A	NGC3799	11 37.6	15 37	14.4	S	(3434)	100	1.30	0.10	7
B	NGC3800			13.1	S	(3469)	100			

TABLE I (CONTINUED)

BINARY GALAXY DATA

(1) IDENTIFICATION		(2) ALPHA	DELTA	(3) MAG	(4) TYPE	(5) VEL	(6) ERR	(7) SEP	(8) ERR	(9) AP
41A	NGC3808	11 38.2	22 43	(14.7)	(S)	(6989)	100	1.10	0.10	8
B	ARP 87			(15.0)	(SI)	(7138)	100			
42A	NGC3824	11 40.4	53 2	14.6	(OS)	0	0	7.60	0.10	6
B	NGC3829			15.0	S	0	0			
43A	NGC3873	11 43.1	20 2	14.2	E	0	0	0.87	0.10	7
B	NGC3875			14.8	OS	0	0			
44A	NGC3894	11 46.2	59 43	12.9	O	0	0	2.10	0.10	5
B	NGC3895			14.0	S	0	0			
45A	NGC3933	11 49.5	17 6	14.2	S	0	0	3.70	0.10	4
B	NGC3934			15.0	(S)	0	0			
46A	NGC3991	11 54.9	32 36	(14.2)	(S)	0	0	0.34	0.30	2
B	ARP 313			(15.0)	(S)	0	0			
47A	NGC3990	11 55.1	55 43	13.6	O	(817)	100	3.00	0.10	4
B	NGC3998			11.2	O	(1177)	100			
48A	NGC4003	11 55.4	23 26	14.8	OS	0	0	4.90	0.10	5
B	NGC4002			14.7	O	0	0			
49A	IC749	11 56.1	42 59	13.4	S	0	0	3.40	0.10	6
B	IC750			12.7	S	0	0			
50A		11 59.7	30 7	14.3	S	0	0	4.20	0.10	5
B				14.4	S	0	0			

TABLE I (CONTINUED)

BINARY GALAXY DATA

(1) IDENTIFICATION		(2) ALPHA	DELTA	(3) MAG	(4) TYPE	(5) VEL	(6) ERR	(7) SEP	(8) ERR	(9) AP
51A		12 0.8	16 46	14.6	(S)	3434	150	2.20	0.10	3
B				14.0	(OS)	3834	19			
52A	NGC4061	12 1.6	20 30	14.4	E	1545	83	1.10	0.10	1
B	NGC4065			14.0	E	1122	152			
53A	IC2989	12 2.0	2 4	14.8	(S)	5725	104	1.30	0.10	2
B	NGC4077			14.5	E0	6783	140			
54A		12 2.8	18 10	14.1	S	4423	56	2.10	0.10	5
B				14.6	S	4630	68			
55A		12 3.1	9 16	15.0	(SI)	6222	47	1.50	0.10	5
B				14.8	S	6058	54			
56A	NGC4121	12 5.6	65 25	14.6	(S)	1599	20	3.80	0.10	4
B	NGC4125			10.9	E	1523	36			
57A	NGC4151	12 8.1	39 43	11.2	S	907	61	5.20	0.10	6
B	NGC4156			14.3	S	758	63			
58A	NGC4227	12 14.0	33 49	13.8	OS	6524	43	2.60	0.10	5
B	NGC4229			14.3	S	6671	62			
59A	NGC4232	12 14.3	47 43	14.6	S	0	0	1.20	0.10	7
B	NGC4231			14.5	(OS)	0	0			
60A	NGC4284	12 18.1	58 22	14.7	S	0	0	4.70	0.10	6
B	NGC4290			12.8	S	0	0			

TABLE I (CONTINUED)

BINARY GALAXY DATA

(1) IDENTIFICATION		(2) ALPHA	DELTA	(3) MAG	(4) TYPE	(5) VEL	(6) ERR	(7) SEP	(8) ERR	(9) AP
61A	NGC4294	12 18.9	11 47	12.6	S	(306)	100	5.60	0.10	7
B	NGC4299			12.8	I	(103)	100			
62A	NGC4298	12 19.1	14 53	12.2	S	0	0	2.20	0.10	8
B	NGC4302			13.4	S	0	0			
63A	NGC4305	12 19.6	13 3	13.8	S	0	0	2.90	0.10	6
B	NGC4306			14.4	0	0	0			
64A	NGC4333	12 20.9	6 20	14.8	S	0	0	4.00	0.10	2
B	NGC4339			13.1	E	(1173)	100			
65A	NGC4340	12 21.2	16 59	12.4	OS	0	0	5.70	0.10	7
B	NGC4350			11.5	0	(1123)	100			
66A	NGC4382	12 23.1	18 29	10.2	0	(712)	100	7.80	0.10	6
B	NGC4394			11.9	S	(719)	100			
67A	NGC4430	12 24.9	6 31	13.4	S	0	0	2.50	0.10	4
B	NGC4432			15.0	S	0	0			
68A	NGC4458	12 26.5	13 30	13.3	E	(311)	100	3.90	0.10	6
B	NGC4461			12.2	0	(1815)	100			
69A	NGC4485	12 28.0	41 57	12.4	I	(848)	100	4.00	0.10	8
B	NGC4490			10.1	S	(622)	100			
70A	NGC4512	12 30.5	64 12	14.7	(SI)	0	0	4.10	0.10	4
B	NGC4521			13.0	OS	0	0			

TABLE I (CONTINUED)

BINARY GALAXY DATA

(1) IDENTIFICATION		(2) ALPHA	DELTA	(3) MAG	(4) TYPE	(5) VEL	(6) ERR	(7) SEP	(8) ERR	(9) AP
71A	NGC4550	12 33.0	12 31	12.5	O	(279)	100	3.20	0.10	6
B	NGC4551			13.1	E	(907)	100			
72A	NGC4568	12 34.0	11 31	12.5	S	(2204)	100	1.10	0.20	9
B	NGC4567			12.5	S	(2197)	100			
73A		12 36.4	32 19	14.6	S	0	0	6.50	0.10	3
B				14.0	S	0	0			
74A	NGC4606	12 38.6	12 10	12.7	S	0	0	3.90	0.10	6
B	NGC4607			14.7	S	0	0			
75A	NGC4614	12 39.0	26 19	14.2	OS	0	0	2.30	0.10	3
B	NGC4615			13.8	S	0	0			
76A	NGC4627	12 39.6	32 50	13.3	E	0	0	2.50	0.20	7
B	NGC4631			9.8	S	(646)	100			
77A	NGC4633	12 40.1	14 36	14.7	(I)	0	0	3.80	0.10	4
B	NGC4634			13.6	S	0	0			
78A	NGC4647	12 41.0	11 51	12.5	S	(1328)	100	2.80	0.10	9
B	NGC4649			10.3	E	(1200)	100			
79A		12 41.5	55 10	(14.7)	(S)	(5062)	100	0.58	0.15	5
B				(15.0)	(U)	0	0			
80A	NGC4676	12 43.7	31 0	(14.9)	(U)	(6515)	100	0.60	0.10	9
B				(14.9)	(U)	(6620)	100			

TABLE I (CONTINUED)

BINARY GALAXY DATA

(1) IDENTIFICATION		(2) ALPHA	DELTA	(3) MAG	(4) TYPE	(5) VEL	(6) ERR	(7) SEP	(8) ERR	(9) AP
81A	NGC4809	12 52.3	2 55	14.8	(SI)	0	0	0.78	0.10	7
B	NGC4810			14.9	I	(794)	100			
82A	NGC4841	12 55.1	28 45	(14.0)	E	0	0	0.54	0.10	7
B				(14.6)	E	0	0			
83A		12 59.0	29 35	(15.0)	(OS)	(7376)	100	0.38	0.15	6
B				(15.0)	(SI)	0	0			
84A	IC881	13 17.6	16 9	14.8	S	6815	34	3.80	0.10	5
B	IC882			15.0	(OS)	6754	47			
85A	NGC5194	13 27.8	47 29	8.8	S	(552)	20	4.60	0.10	9
B	NGC5195			10.6	I	(634)	29			
86A		13 34.4	17 43	15.0	(O)	6728	87	0.89	0.10	6
B				15.0	(S)	6695	88			
87A	NGC5257	13 37.5	1 5	13.7	S	6632	62	1.80	0.10	9
B	NGC5258			13.8	S	6564	26			
88A	NGC5278	13 39.8	55 56	(13.7)	(U)	7711	69	0.58	0.15	7
B	NGC5279			(15.0)	(S)	7726	42			
89A	NGC5273	13 39.9	35 53	12.7	U	1089	22	3.30	0.10	5
B	NGC5276			14.6	S	5346	44			
90A	NGC5296	13 44.2	44 6	15.0	(S)	2323	107	1.50	0.10	4
B	NGC5297			12.3	S	2683	44			

TABLE I (CONTINUED)

BINARY GALAXY DATA

(1) IDENTIFICATION		(2) ALPHA	DELTA	(3) MAG	(4) TYPE	(5) VEL	(6) ERR	(7) SEP	(8) ERR	(9) AP
91A	NGC5331	13 49.8	2 20	(15.0)	(S)	0	0	0.49	0.15	8
B				(15.0)	(S)	0	0			
92A		13 54.7	12 16	14.9	(S)	0	0	1.50	0.10	3
B	IC962			14.0	(OS)	0	0			
93A	NGC5394	13 56.5	37 41	13.7	S	(3648)	100	1.90	0.10	9
B	NGC5395			12.6	S	0	0			
94A		13 56.6	15 50	15.0	(S)	0	0	4.60	0.10	4
B				14.5	S	0	0			
95A	NGC5421	13 59.5	34 4	(15.0)	(U)	0	0	0.27	0.20	8
B				(15.0)	(U)	0	0			
96A	NGC5480	14 4.7	50 59	12.6	S	2165	40	3.20	0.10	7
B	NGC5481			13.5	E	2475	102			
97A		14 4.9	15 22	14.6	(S)	7419	56	4.60	0.10	1
B				15.0	(U)	12021	41			
98A		14 10.6	45 55	(14.9)	(S)	8175	15	0.49	0.10	8
B				(14.9)	(S)	8397	24			
99A	IC988	14 12.1	3 23	14.5	(S)	7052	73	5.00	0.10	3
B	IC989			13.4	E	7454	34			
100A	NGC5536	14 14.3	39 46	14.5	S	5247	50	5.50	0.10	4
B	NGC5541			13.4	S	7582	41			

TABLE I (CONTINUED)

BINARY GALAXY DATA

(1) IDENTIFICATION		(2) ALPHA	DELTA	(3) MAG	(4) TYPE	(5) VEL	(6) ERR	(7) SEP	(8) ERR	(9) AP
101A	NGC5544	14 15.0	36 48	(14.2)	S	3222	53	0.65	0.15	8
B	NGC5545			(13.8)	S	3356	68			
102A	IC999	14 17.2	18 5	14.5	O	0	0	2.20	0.10	3
B	IC1000			14.4	O	0	0			
103A	NGC5619	14 24.9	5 1	14.0	S	0	0	3.70	0.10	3
B	IC4424			14.8	OS	0	0			
104A	IC1017	14 26.0	26 4	14.9	O	0	0	2.40	0.10	1
B	NGC5629			14.2	O	0	0			
105A	NGC5636	14 27.1	3 28	14.6	S	0	0	2.10	0.10	4
B	NGC5638			12.5	E	1710	61			
106A	NGC5648	14 28.3	14 13	14.1	S	0	0	5.50	0.10	5
B	NGC5649			14.0	S	0	0			
107A		14 31.8	40 17	15.0	S	0	0	0.87	0.10	6
B				14.8	S	0	0			
108A	NGC5707	14 35.9	51 48	(13.4)	S	0	0	1.50	0.10	4
B				(15.0)	(EO)	0	0			
109A	NGC5730	14 38.1	42 59	14.7	I	0	0	4.00	0.10	6
B	NGC5731			14.0	S	0	0			
110A	IC1042	14 38.1	3 40	14.9	O	0	0	1.10	0.10	6
B	NGC5718			14.6	EO	0	0			

TABLE I (CONTINUED)

BINARY GALAXY DATA

(1) IDENTIFICATION		(2) ALPHA	DELTA	(3) MAG	(4) TYPE	(5) VEL	(6) ERR	(7) SEP	(8) ERR	(9) AP
111A		14 39.5	44 43	14.8	(U)	0	0	3.40	0.10	5
B				13.9	S	0	0			
112A	NGC5752	14 43.3	38 56	(15.0)	(SI)	0	0	1.20	0.10	7
B	NGC5754			(14.7)	S	0	0			
113A		14 49.0	35 46	14.5	(U)	(1232)	100	4.10	0.10	6
B				14.2	(SI)	(1322)	100			
114A		14 50.0	43 53	14.9	I	0	0	5.20	0.10	5
B				14.4	S	0	0			
115A	NGC5771	14 50.1	30 1	14.6	(OS)	0	0	4.20	0.10	5
B	NGC5773			14.5	S	0	0			
116A	IC1066	14 50.6	3 31	14.2	S	0	0	2.20	0.10	6
B	IC1067			13.6	S	0	0			
117A	IC1075	14 52.6	18 16	14.9	S	0	0	4.90	0.10	5
B	IC1076			13.9	(S)	0	0			
118A	ARP 302	14 54.7	24 48	(15.0)	(S)	0	0	0.74	0.10	8
B	VV 340			(15.0)	(SI)	0	0			
119A		14 54.9	19 53	14.7	S	0	0	2.80	0.10	5
B				14.0	S	0	0			
120A	NGC5820	14 57.3	54 6	13.0	EO	(3445)	100	3.80	0.10	5
B	NGC5821			14.9	S	0	0			

TABLE I (CONTINUED)

BINARY GALAXY DATA

(1) IDENTIFICATION		(2) ALPHA	DELTA	(3) MAG	(4) TYPE	(5) VEL	(6) ERR	(7) SEP	(8) ERR	(9) AP
121A		15 4.0	1 46	(13.8)	E	1937	61	0.80	0.20	4
B	NGC5846			(12.1)	E	1796	55			
122A	NGC5851	15 4.6	13 4	14.9	(S)	16434	78	1.10	0.10	5
B	NGC5852			14.7	S	16396	72			
123A	NGC5857	15 5.2	19 46	13.6	S	4673	43	2.10	0.10	7
B	NGC5859			13.1	S	4676	30			
124A		15 5.6	1 25	14.9	(S)	13583	49	2.90	0.10	5
B				14.7	S	13350	36			
125A		15 14.5	7 12	14.8	E	10385	40	7.60	0.10	1
B				14.9	(S)	10355	38			
126A	NGC5929	15 24.3	41 51	(14.0)	ED	2594	29	0.49	0.10	8
B	NGC5930			(13.6)	S	2872	26			
127A	NGC5953	15 32.2	15 21	(13.5)	D	2125	43	0.80	0.15	9
B	NGC5954			(13.5)	S	2033	39			
128A	NGC5992	15 42.6	41 16	14.2	S	0	0	2.40	0.10	6
B	NGC5993			13.9	S	9564	58			
129A	NGC6008	15 50.8	21 16	14.2	S	0	0	3.20	0.10	4
B				15.0	(S)	0	0			
130A		15 54.8	42 1	15.0	(S)	0	0	1.30	0.10	6
B				14.3	(OS)	(10516)	100			

TABLE I (CONTINUED)

BINARY GALAXY DATA

(1) IDENTIFICATION		(2) ALPHA	DELTA	(3) MAG	(4) TYPE	(5) VEL	(6) ERR	(7) SEP	(8) ERR	(9) AP
131A	NGC6018	15 55.2	16 2	14.6	D	0	0	5.00	0.10	6
B	NGC6021			14.1	E	0	0			
132A	NGC6052	16 3.0	20 41	(15.0)	(SI)	4621	57	0.27	0.10	8
B	ARP 209			(14.7)	(S)	4662	50			
133A		16 4.0	41 28	15.0	(OS)	2221	25	1.60	0.10	5
B				13.6	(OS)	2129	43			
134A	VV 215	16 4.1	15 49	(15.0)	E	12176	106	0.53	0.15	4
B				(15.0)	E	12449	55			
135A	NGC6090	16 10.4	52 35	(15.0)	(I)	8898	25	0.22	0.20	7
B				(14.6)	(I)	8820	37			
136A	NGC7499	23 8.0	7 17	15.0	D	11796	44	5.10	0.10	1
B	NGC7503			14.9	E	11037	74			
137A	NGC7518	23 10.6	6 5	14.5	S	838	190	6.70	0.10	6
B				14.8	S	1081	78			
138A	NGC7537	23 12.1	4 14	13.8	S	2789	46	3.10	0.10	6
B	NGC7541			12.7	S	2580	83			
139A	NGC7557	23 13.2	6 25	15.0	EO	3808	55	4.70	0.10	4
B	NGC7562			13.0	E	3718	51			
140A	NGC7671	23 24.9	12 10	14.3	D	4427	94	6.00	0.10	5
B	NGC7672			14.8	S	4603	93			

TABLE I (CONTINUED)

BINARY GALAXY DATA

(1) IDENTIFICATION		(2) ALPHA	DELTA	(3) MAG	(4) TYPE	(5) VEL	(6) ERR	(7) SEP	(8) ERR	(9) AP
141A	NGC7681	23 26.2	17 1	15.0	(OS)	7704	47	6.30	0.10	3
B				14.2	O	7216	68			
142A	NGC7679	23 26.4	3 14	13.2	O	5381	44	4.50	0.20	6
B	NGC7682			14.3	S	5346	33			
143A	NGC7731	23 39.0	3 28	14.3	S	2972	100	1.70	0.10	6
B	NGC7732			14.5	SI	3045	65			
144A	NGC7783	23 51.6	0 6	(14.7)	(OS)	7165	34	0.80	0.10	6
B	ARP 323			(15.0)	(S)	6855	65			
145A	NGC7824	0 2.6	6 34	14.5	S	3290	86	9.20	0.10	5
B				14.7	S	3235	56			
146A		0 28.7	8 11	15.0	E	4913	184	1.40	0.10	3
B				14.6	S	4501	34			
147A	IC1698	1 22.6	14 35	14.9	O	5508	110	1.70	0.20	2
B	IC1700			14.3	E	5890	192			
148A	NGC631	1 34.4	5 36	15.0	E	4112	52	8.10	0.10	5
B	NGC632			13.5	O	3412	36			
149A	IC162	1 46.1	10 16	14.2	(S)	5129	83	2.50	0.10	1
B	VV 54			14.8	(E)	4921	40			
150A		1 48.9	8 1	14.2	E	5246	105	2.90	0.10	6
B				15.0	E	5092	82			

TABLE I (CONTINUED)

BINARY GALAXY DATA

(1) IDENTIFICATION		(2) ALPHA	DELTA	(3) MAG	(4) TYPE	(5) VEL	(6) ERR	(7) SEP	(8) ERR	(9) AP
151A	NGC770	1 56.5	18 45	14.2	S	2608	124	3.60	0.10	5
B	NGC772			11.3	S	2589	87			
152A	IC195	2 1.0	14 29	14.3	D	8713	34	2.20	0.10	7
B	IC196			14.2	S	8676	69			
153A	IC208	2 5.8	6 7	14.8	S	0	0	4.50	0.10	6
B	NGC825			14.5	S	3199	107			
154A	IC211	2 8.6	3 35	14.5	S	3142	115	4.50	0.10	5
B	NGC851			14.7	D	3265	84			
155A	NGC1024	2 36.7	10 36	13.8	S	3642	81	7.00	0.10	4
B	NGC1029			14.1	DS	3582	103			
156A	IC330	3 29.7	0 9	15.0	S	0	0	5.20	0.10	4
B	IC331			14.9	E	6701	48			

hereafter UGC) when available, and from an inspection of glass copies of the Palomar Sky Survey otherwise. The latter are indicated by parentheses. Table II gives an explanation of the notation used.

Column 5: Radial velocities. The velocities in parentheses are taken from the UGC and are corrected by the usual method (de Vaucouleurs 1964) to the rest frame of the Local Group. The determination of the other velocities is described in §IV.

Column 6: Radial velocity uncertainties. The one standard deviation uncertainty in each UGC radial velocity is assumed to be 100 km s^{-1} except for pair 85 (M51-M52) where de Vaucouleurs' (1964) estimated uncertainty is used. The determination of errors in the new velocity material is described in §IV.

Column 7: Separations. The angular separation of the two components was measured on a 5x enlargement of the Palomar Sky Survey image of the system. It is expressed in minutes of arc. The distribution of observed angular separations is shown in Figure 1.

Column 8: Separation uncertainties. An estimate of the one standard deviation uncertainty in the angular separations is given. These errors arise primarily from difficulty in locating the galactic nuclei within the usually overexposed central regions.

TABLE II

MORPHOLOGICAL TYPE NOTATION

	Type	Table I Abbreviation
Early	Elliptical	E
		EO*
	Lenticular (SO)	O
		OS*
Late	Spiral/Barred Spiral	S
		SI*
	Irregular	I
	Peculiar or Unclassified	U

*Intermediate or uncertain.

FIGURE 1

Observed distribution of angular separations. The number N of the 156 binary galaxy systems with a component angular separation θ_{12} is plotted in one arc minute bins.

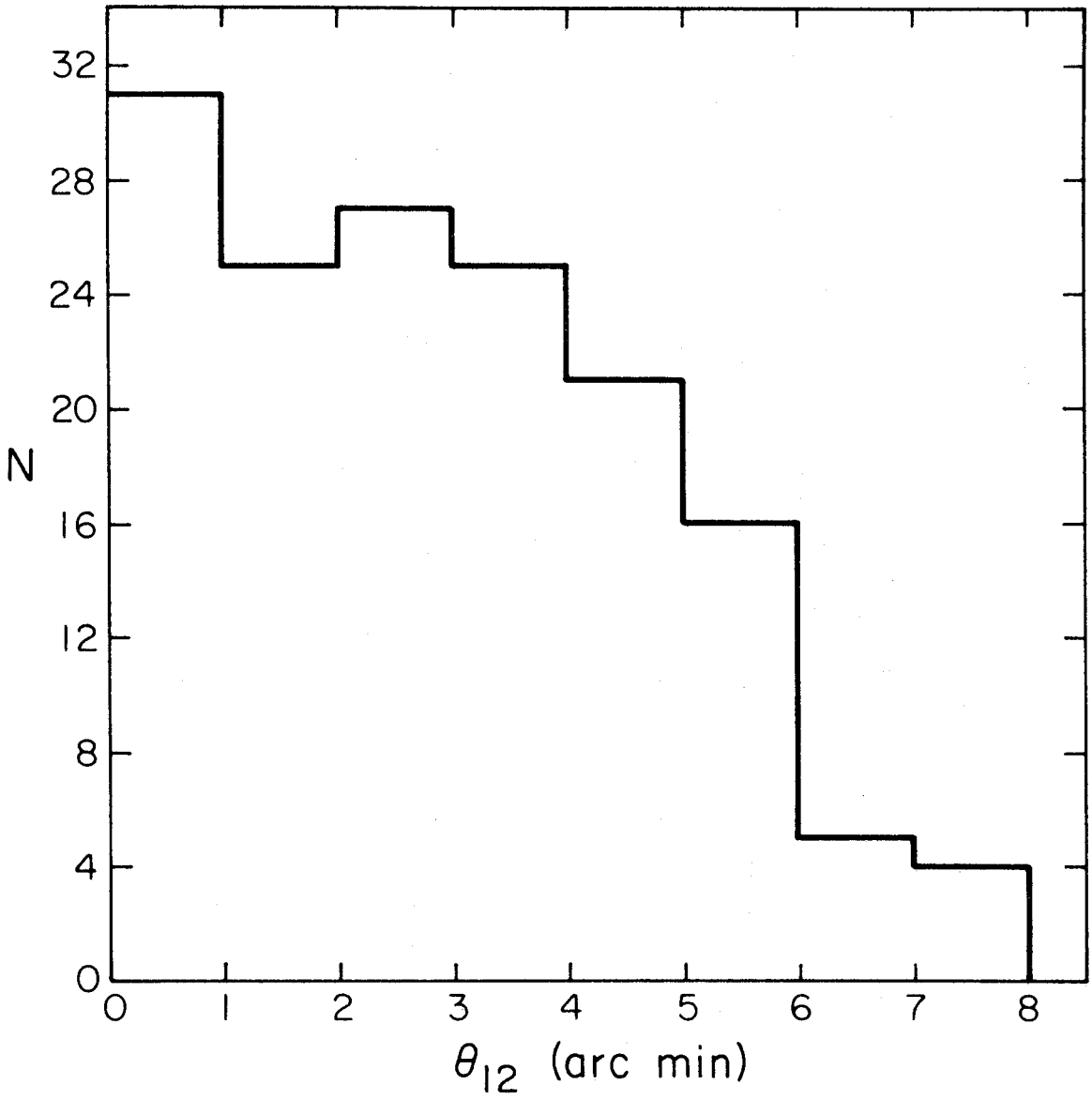
32
28
24
20
16
12
8
4
0
N
0
1
2
3
4
5
6
7
8
θ_{12} (arc min)

Column 9: Appearance. Each system was inspected on a Palomar Sky Survey print and assigned a subjective rank (from 1 to 9) intended to reflect its appearance. Pairs with similar magnitudes, angular separations relatively small compared to the component angular sizes, prominent tidal features, and a generally convincing appearance of association were given high numbers. Pairs lacking the above properties and/or which have nearby faint ($m_{pg} > 15.0$) companions or bright companions only slightly more distant than $5\theta_{12}$ were given low numbers. Any pair rated 3 or higher would probably be called a binary system by the intuitive criteria of someone simply inspecting the field.

IV. RADIAL VELOCITY OBSERVATIONS

The sample of binary galaxies described in the previous section may be analyzed to obtain statistical masses and mass-to-light ratios only if accurate radial velocities are available for a representative and sufficiently large subset of the systems. Velocities available in the literature are unsuitable because they are insufficient in number, embody unknown selection effects, and are probably not accurate enough. Therefore, an observational program designed to obtain a suitable set of radial velocities was undertaken.

During the spring and fall of 1974 and the spring of 1975, spectrograms of 116 galaxies were obtained with a

two-stage image-tube spectrograph at the Ritchy-Chretien focus of the 60-inch (1.5 m) telescope at Mount Palomar. Also during the spring of 1975, spectrograms of 20 more galaxies were obtained with a two-stage image-tube spectrograph at the 2.1 m (84-inch) reflector at Kitt Peak National Observatory. These galaxies constitute both components of 66 binary systems and one component of a further 4 systems. A second spectrum was obtained for 12 of the galaxies to check the repeatability of the velocity determinations.

The Mount Palomar spectra have a dispersion of $\sim$ 140 Å/mm; the KPNO spectra, $\sim$ 100 Å/mm. All of the spectra cover a wavelength range extending from the atmospheric UV cutoff up to $\sim$ 6000 Å. The spectra typically contained 3 to $\sim$ 12 useful lines of the sort normally seen in galaxy spectra at these resolutions (Ca H & K, Na D, G band, [O II], [O I], Balmer lines, Mg triplet, Ca 4226, etc.) A slit of 2 arc sec width was used except on nights of bad seeing when this was increased to 3 arc sec. The slit was oriented east-west and centered on the galaxy's nucleus for each exposure. Whenever possible, the spectra of the two components of a single binary system were obtained in sequential exposures.

In order to assure that the radial velocities were obtained for an unbiased subset of the full sample while maintaining some flexibility at the telescope, the following

procedure was adopted: The 156 systems in the sample were divided into groups according to their right ascension with a bin size of one hour. At any particular time while observing, some convenient group was chosen; however, within a group priority was given to the easternmost, previously unobserved pair. Thus, the observed systems were selected on the basis of their positions in the sky and not their intrinsic properties. Therefore, no further selection effects were introduced in choosing the radial velocity sample from the full sample.

A slightly unconventional technique was used to obtain radial velocities from the spectrograms. A digitized version of each object's spectrum and the associated comparison spectra was generated by scanning each plate with a microdensitometer using a 20μ slit and a 6μ step size. Using programs supplied by T. Williams (1975), the digitized spectra were stored on magnetic tape and later analyzed to produce a list of absorption and/or emission line wavelengths plus an uncertainty in the wavelength (typically $\sim$ 1 to 3 Å), and a line strength (or significance) for each line. These data were analyzed using an algorithm described in the Appendix to give an unbiased radial velocity and an estimate of its one standard deviation uncertainty for each galaxy. Each velocity was corrected for the earth's motion around the sun and then to the Local Group rest frame

(de Vaucouleurs 1964). The results are given (no parentheses) in columns (5) and (6) of Table I. The distribution of corrected radial velocities is shown in Figure 2.

The duplicate spectra obtained for 12 galaxies were used to test the accuracy (or, at least, reproducibility) of the velocity determinations and the validity of the error estimates. Let v_1 and v_2 be the results of the two velocity measurements on a particular galaxy and σ_1 and σ_2 the respective estimated uncertainties. Then, define

$$\Delta V = |v_1 - v_2| \tag{6}$$

and

$$\Delta V_E = (\sigma_1^2 + \sigma_2^2)^{\frac{1}{2}} \tag{7}$$

The distributions of ΔV and ΔV_E are shown in Figure 3. In all 12 cases, $\Delta V/\Delta V_E \leq 1.5$. Also, root mean square values of ΔV and ΔV_E are 56 km s^{-1} and 82 km s^{-1}, respectively. The corresponding implied mean errors in a <u>single</u> velocity determination are 40 km s^{-1} and 58 km s^{-1}. These results indicate that the procedures described in the previous paragraph and in the Appendix are satisfactory although the estimated velocity uncertainties might be too large by $\sim$ 50%.

In addition, 35 of the galaxies observed in the program have previously determined velocities listed in the <u>UGC</u>. Except for two rather large discrepancies, the root mean square difference between the program velocities and the <u>UGC</u>

FIGURE 2

Observed distribution of radial velocities. The number N of radial velocities v_r (from Table I) is plotted with a bin size of 1000 km s^{-1}.

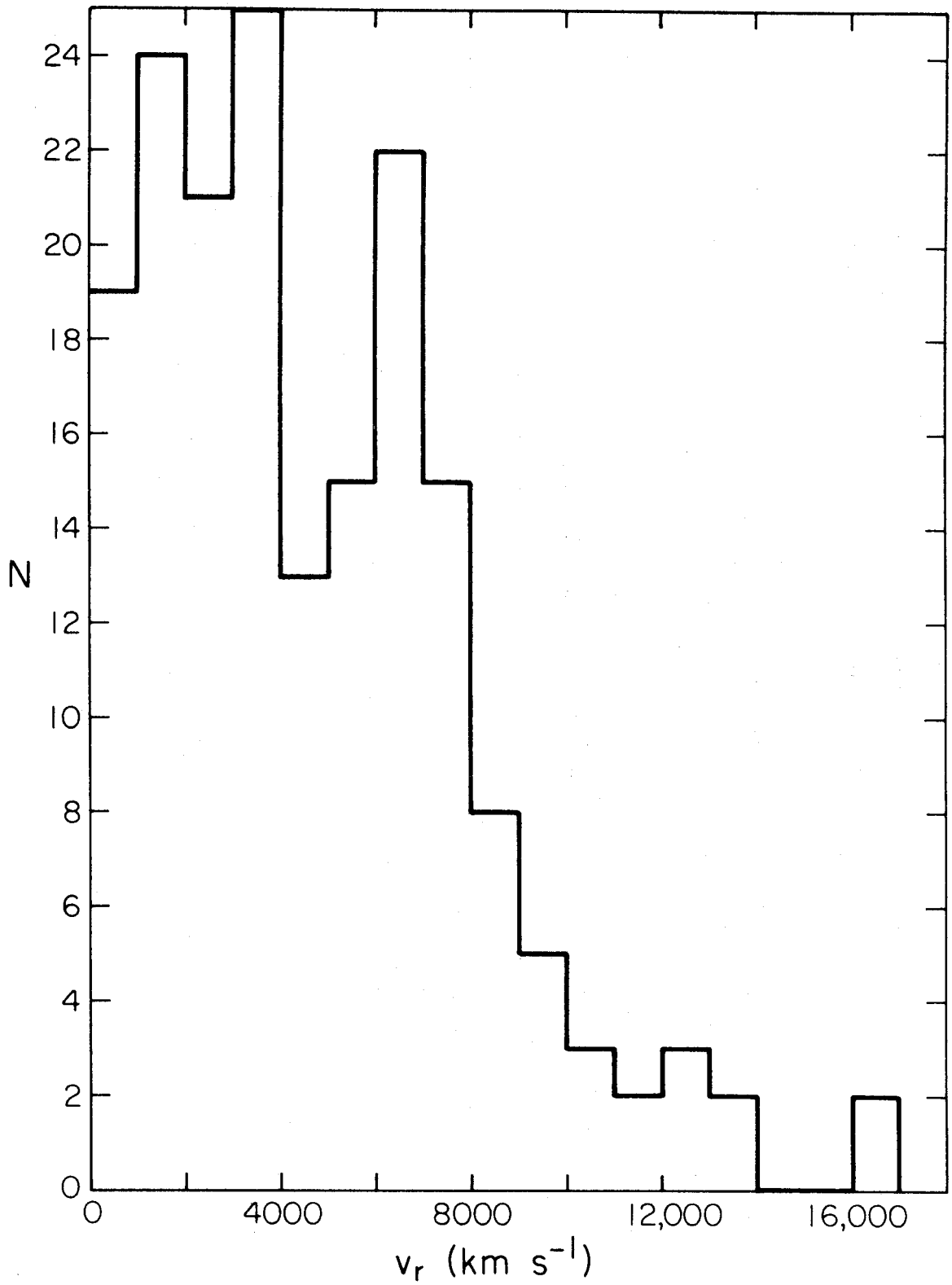
N
0
2
4
6
8
10
12
14
16
18
20
22
24
0
4000
8000
12,000
16,000
v_r (km s^{-1})

FIGURE 3

Distributions of ΔV and ΔV_E. Twelve of the 136 galaxies in the radial velocity sample were observed twice. For these twelve galaxies, two independent velocity determinations were performed. The solid curve shows the number of galaxies $N(\leq V)$ for which the two determinations differed by less than V. The broken curve shows the $N(\leq V)$ curve expected from the adopted (see Appendix) uncertainties in the 24 individual velocity determinations. The data suggest that the errors were, if anything, over-estimated.

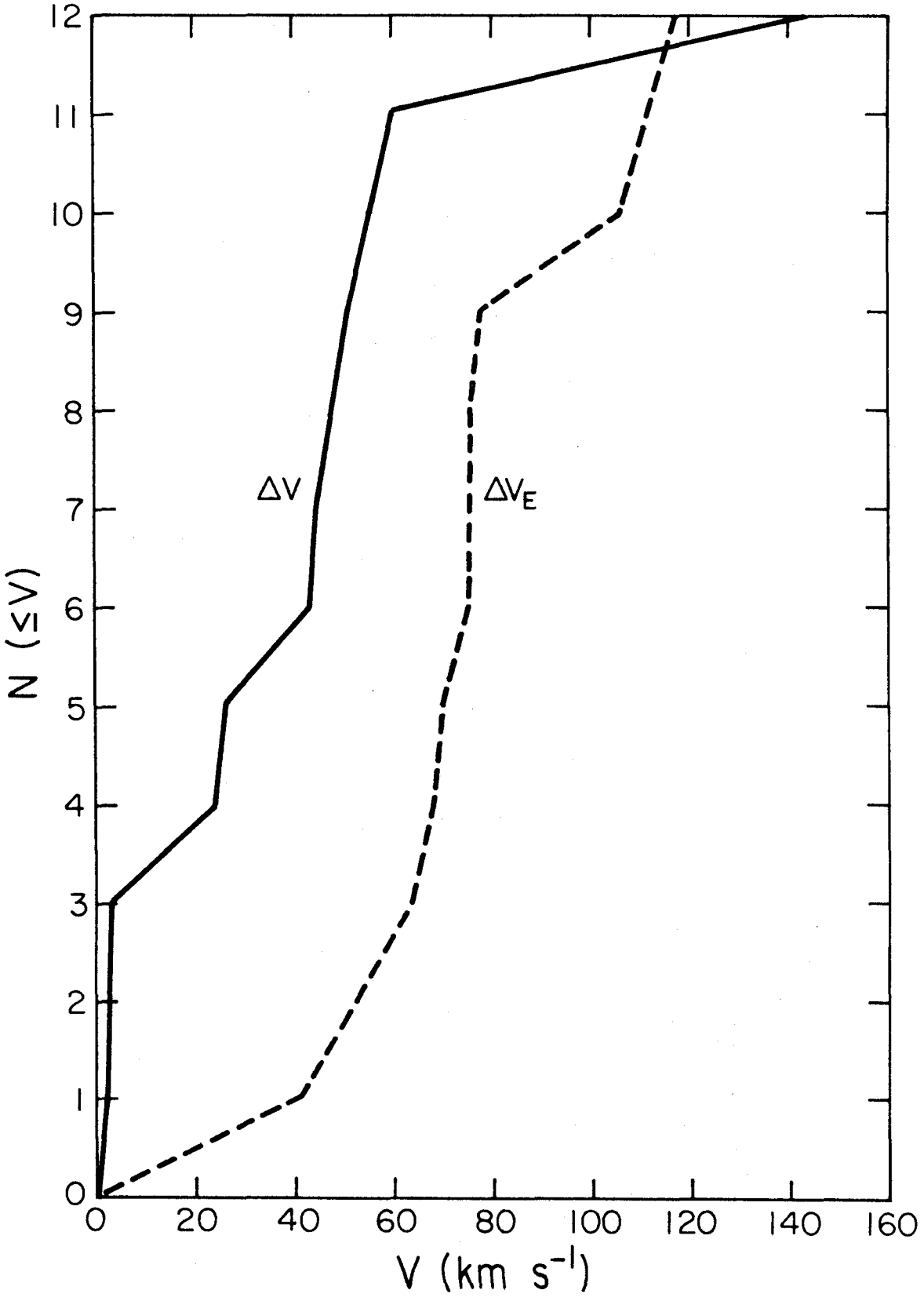
12
11
10
9
8
7
6
5
4
3
2
1
0
N (≤V)
ΔV
ΔV_E
0
20
40
60
80
100
120
140
160
V (km s^-1)

velocities is $\sim$ 100 km s^{-1} with no apparent systematic shift.

V. SUMMARY

In order to obtain a statistical estimate of galaxian masses and mass-to-light ratios from the binary galaxy method, a well-defined statistical sample of binaries is required. Equations (1) and (2) define selection criteria by which such a sample can be drawn from a catalog of galaxies. Using $\theta_c = 8'$ and $x = 5$, a sample of 156 binary systems is selected from the CGCG. Positions, apparent magnitudes, morphological types, velocities, angular separations, and appearance ratings are listed for these systems. An observational program has produced accurate velocities for an unbiased subset of 66 binary systems. These data are well suited to the estimation of mass-to-light ratios reported in PII.

APPENDIX TO CHAPTER 1

RADIAL VELOCITY DETERMINATIONS

The procedure requires the following inputs:

1) A list of measured emission and/or absorption line wavelengths λ^{o}_{i},

2) A list of the one standard deviation uncertainties in these wavelengths σ_i,

3) A list of the line strengths or significances (conveniently expressed in terms of standard deviations from the continuum) S_i,

4) A list of candidate line wavelengths λ^{c}_{i},

5) A list of weights or priorities assigned to the candidate lines w_i,

6) A range of redshifts to be searched.

The N (typically 3 to 10) strongest (greatest S_i) observed lines are chosen, and the pseudo-cross correlation ζ between these and the M candidate lines is calculated for each z in the redshift range by

$$\zeta(z) = \frac{1}{(2\pi)^{\frac{1}{2}}} \sum_{i=1}^{N} \sum_{j=1}^{M} \frac{w_j}{\sigma_i} \exp\left[-\frac{1}{2\sigma_i^2}\left((1+z)\lambda^{c}_{j}-\lambda^{o}_{i}\right)^2\right] \quad \text{(A1)}$$

The value of z associated with the maximum value of $\zeta(z)$ is adopted as a preliminary estimate of the redshift, and the half width at half maximum of the peak, as its uncertainty.

This preliminary redshift is used to shift all of the observed lines back to their approximate rest wavelengths. This list of unredshifted observed lines is now compared

to the list of candidate lines and any match within 3σ is considered an identification. Each identification yields an estimate of the redshift from that line alone.

Starting with the strongest (most significant) lines and proceeding toward the weakest (least significant), the individual line redshifts are combined one by one to give a $1/\sigma^2$ - weighted mean redshift. As each line is added, two estimates of the uncertainty of the mean redshift are computed, one based on a formal error propagation from the σ_i's and one based on the actual scatter in the individual line redshifts. The larger of the two (they are typically of the same order) is adopted. The mean redshift which corresponds to the minimum value of this adopted uncertainty is the final estimate of the redshift. Thus, the algorithm determines the optimum (i.e., smallest error) redshift for each spectrum.

The above procedure using data from digitization and line finding programs provided by T. Williams (1975) has successfully determined accurate redshifts for both galaxies (see text) and a wide variety of stars. It has many advantages over conventional techniques including objectivity, repeatability, speed, and high information usage. The independence from unconscious observer biases and the estimation of accurate uncertainties in each redshift are particularly useful in the determination of small velocity

differences between objects with large total velocities.

REFERENCES

de Vaucouleurs, G., and de Vaucouleurs, A. 1964, Reference Catalogue of Bright Galaxies (Austin: University of Texas Press).

Holmberg, E. 1954, Medd. Lund Astr. Obs., Ser I, 186, 1.

Huchra, J. 1975, preprint.

Jenner, D. C. 1974, Ap. J., 191, 55.

Nilson, P. 1973, Uppsala Astr. Obs. Ann., Vol. 6 (Uppsala General Catalog of Galaxies), (UGC).

Noerdlinger, P. D. 1975, Ap. J., 197, 545.

Page, T. 1952, Ap. J., 116, 63.

———— 1961, in Proceedings of the Fourth Berkeley Symposium on Mathematical Statistics and Probability, ed. J. Neyman (Berkeley: University of California Press), p. 277.

———— 1966, in Proceedings of the Fifth Berkeley Symposium on Mathematical Statistics and Probability, eds. L. M. LeCam, J. Neyman, and E. L. Scott (Berkeley: University of California Press), p. 31.

Smart, N. C. 1973, Ph.D. thesis, University of Cambridge.

Turner, E. L. 1976, in press, (PII).

Williams, T. 1975, Ph.D. thesis, California Institute of Technology.

Wolf, R. A. and Bahcall, J. N. 1972, Ap. J., 176, 559.

Zwicky, F., Herzog, E., Wild, P., Karpowicz, M., and Kowal, C. T. 1961-1968, Catalog of Galaxies and Clusters of Galaxies, in 6 vols. (Pasadena: California Institute of Technology), (CGCG).

CHAPTER 2

BINARY GALAXIES:

DYNAMICS AND MASS-TO-LIGHT RATIOS

I. INTRODUCTION

In the past, several authors (Page 1952, 1961, 1966 and references cited therein; Holmberg 1954; Smart 1973) have attempted to estimate the mean mass-to-light ratio M/L of galaxies from an analysis of the dynamics of a sample of binary galaxies. A variety of different methods have been used. The most elaborate study (Page 1966) gave values of M/L for spirals somewhat smaller than conventional rotation curve estimates and in strong disagreement with the massive halo hypothesis (Ostriker, et al. 1974). Also, previous analyses may well have been influenced by selection effects in the binary galaxy sample studied. Such selection effects are very difficult to correct for, unless the sample is chosen by well-defined criteria. For these reasons, it seemed worthwhile to compile a suitable sample (Turner 1976, herafter PI) and to analyze it with particular attention to possible selection effects.

The goal of the analysis presented here is, therefore, to obtain an estimate of the mean M/L of galaxies from the data presented in PI, taking into account the selection effects introduced into the sample by the criteria defined in PI's equations (1) and (2). There are undoubtedly many ways of obtaining this estimate; here an attempt has been made to choose the simplest method which does not introduce any significant biases. Nevertheless, the chosen

method is sufficiently complex that it seems wise to outline the procedure before presenting it in detail:

1) A maximum permitted difference in the radial velocities of the binary components is established. Pairs with larger velocity differences are rejected as spurious (i.e., projected, accidental pairs). (§ II)

2) The ratio of M/L for early type galaxies to that for late types is estimated. (§ II)

3) The radial velocity difference of each pair is scaled to that which would be expected for a pair of late-type galaxies with a fixed total luminosity. (§ II)

4) The observed distribution of projected separations is convolved with the selection criteria of PI to produce the true distribution of projected separations. (§ III)

5) The distribution of 3-dimensional spatial separations is deduced from the true distribution of projected separations and is fit to a power-law model. (§ III)

6) The fraction of systems with projected separations r_p which have spatial separations $r >> r_p$ is calculated. (§ III)

7) Several possible models for the orbital eccentricity of binary galaxies and for the distribution of mass

within the individual galaxies are presented. (§ IV)

8) A set of radial velocity differences and projected separations is generated for each model, assuming that binary systems have fixed (but arbitrary) mass, separations distributed according to the power-law model, and a random spatial distribution. From these, a set of simulated observations are produced by the application of the PI selection criteria and the introduction of random "measurement" errors. (§ IV)

9) In order to choose between the various models, a logarithmic-separation rank-sum test is used to compare the "shapes" of the joint distributions of radial velocity difference and projected separation for the observed and simulated data. (§ V)

10) The best fit M/L and its uncertainty for each model are obtained from a standard rank-sum comparison of the distribution of a mass parameter in the observed and simulated data. (§ V)

In addition, § V interprets these results in terms of a massive halo model and discusses the statistical and systematic uncertainties in the mean M/L. § VI contains a simpler and independent (but less reliable) estimate of the mean M/L, the results of analyzing the present data with Page's (1966) techniques, and a discussion of the import-

ance of selection effects in binary galaxy studies. A summary and brief discussion of important results is given in § VII.

II. OBSERVED PROJECTED SEPARATIONS AND VELOCITY DIFFERENCES

Some of the galaxy pairs in the sample presented in PI consist of galaxies at very different distances projected close together in the sky and are, thus, not physically associated. In order to remove these from the sample, we consider the distribution of radial velocity differences $\Delta v'$ (figure 1a). The solid curve shows the observed distribution of velocity differences $D_O(\Delta v')$; the broken curve is the expected distribution $D_E(\Delta v')$ if the individual galaxy redshifts had been chosen at random from the observed distribution of total radial velocities (figure 2 of PI). We wish to choose a maximum velocity difference Δv_M such that pairs with $\Delta v' > \Delta v_M$ may be rejected as spurious. Figure 1b shows the total number of spurious pairs N_S as a function of Δv_M given by

$$N_S(\Delta v_M) = N_T \int_{\Delta v_M}^{\infty} D_O(\Delta v')\, d\Delta v' \Big/ \int_{\Delta v_M}^{\infty} D_E(\Delta v')\, d\Delta v' \quad , \qquad (1)$$

where N_T is the number of observed pairs. When $N_S(\Delta v_M)$ falls to a constant value, the remaining pairs ($\Delta v' > \Delta v_M$)

FIGURE 1

Maximum velocity difference. a) lower plot: The solid curve shows the observed distribution of velocity difference $\Delta v'$ between binary galaxies. The broken curve shows the distribution expected if all of the binary systems were chance projections. The two distributions agree only for $\Delta v' > 450$ km s^{-1}. b) upper plot: N_S, defined in equation (1), is the total expected number of projected pairs if all systems with $\Delta v' > \Delta v_M$ are assumed to be chance associations. The curve falls to a roughly constant value beyond $\Delta v_M = 450$ km s^{-1}, indicating that $D_O(\Delta v')$ and $D_E(\Delta v')$ are indeed consistent for greater velocity differences.

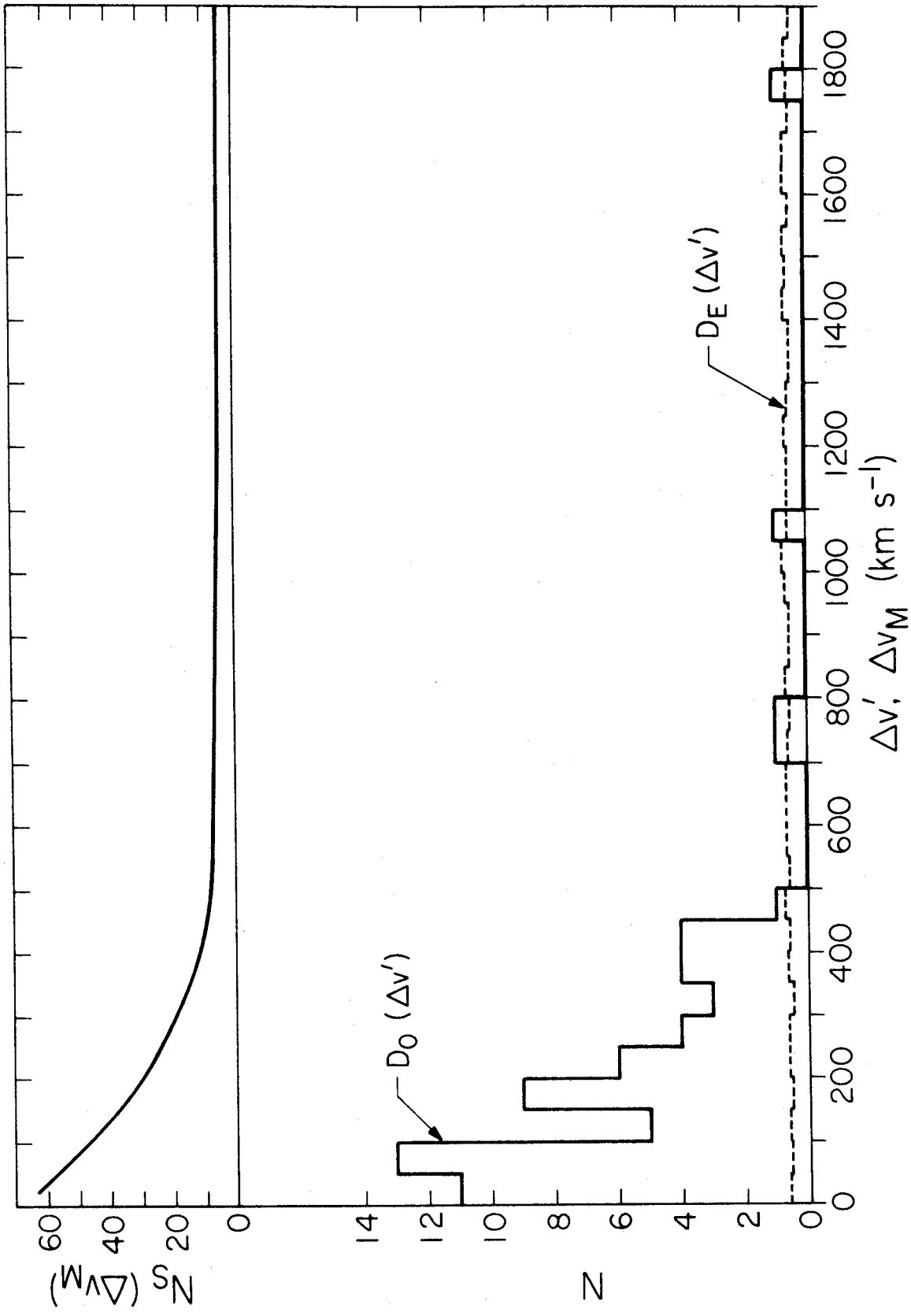
$N_S(\Delta v_M)$
60
40
20
0
N
14
12
10
8
6
4
2
0
$D_O(\Delta v')$
$D_E(\Delta v')$
0
200
400
600
800
1000
1200
1400
1600
1800
$\Delta v'$, Δv_M (km s^{-1})

have a distribution consistent with $D_E(\Delta v')$. From an inspection of both parts of figure 1, $\Delta v_M = 425$ km s^{-1} is adopted. The remainder of the analysis was carried out both with this value of Δv_M and with $\Delta v_M = 500$ km s^{-1}; no significant difference was noted.

After elimination of the spurious pairs, the data were divided into three overlapping samples or classes as described in Table I. Unless otherwise stated, all references to the data and all results refer to the primary class data. The other two classes were subjected to the same analysis as the primary data with very similar results.

It is widely believed that the mean mass-to-light ratios of early and late type galaxies are different. In order to test this assertion and to take any such effects into account in the dynamical analysis, we wish to obtain an estimate of α where

$$\alpha = \langle M/L \rangle_E / \langle M/L \rangle_S \quad , \tag{2}$$

and $\langle M/L \rangle_E$ and $\langle M/L \rangle_S$ are the mean mass-to-light ratios of early and late type galaxies, respectively. Table II of PI defines early and late in terms of the available morphological classifications. Now, for any bound pair of galaxies with radial velocity difference $\Delta v'$, projected

TABLE I

DATA CLASSES

Class	No. of Binaries	Definition*
1 (primary)	59	All pairs for which both velocities were obtained in the program described in § IV of PI plus pair 85
2 (intuitive)	43	All class 1 pairs with appearance ratings ≥ 5
3 (available)	73	All pairs with both velocities available

*All subject to $\Delta v' \leq 425$ km s^{-1}

separation r_p, and total luminosity L, there is a minimum mass-to-light ratio

$$\left(\frac{M}{L}\right)_{MIN} = \frac{\Delta v'^{2}\, r_p}{2GL} \quad . \tag{3}$$

The relation between $(M/L)_{MIN}$ and the true M/L is a function of the direction from which the system is observed, the orbital eccentricity, and the orbital phase. However, if the same selection criteria are used for all systems, then α may be estimated solely from the distributions of $(M/L)_{MIN}$. If f_E is the fraction of the light in a pair coming from early type galaxies, then on the average

$$\left\langle\frac{M}{L}\right\rangle_{S,MIN} [1 + f_E(\alpha - 1)] = \left(\frac{M}{L}\right)_{MIN} \quad , \tag{4}$$

where $\left\langle\frac{M}{L}\right\rangle_{S,MIN}$ is the average minimum M/L of late type galaxies. Calculating f_E, $(M/L)_{MIN}$, and the formal relative error in the latter for each binary system and performing a weighted least-squares fit of equation (4) to these data gives $\alpha = 2.0 \pm 0.5$. This number is poorly determined because there are so few early type galaxies in the sample.

The dynamically interesting parameters of a binary system are

$$\Delta v' = |v_A - v_B| \quad (\text{km s}^{-1}) \quad , \tag{5}$$

$$r_p = 40\ \bar{v}\ \tan\ (\theta_{12}) \quad \text{(kpc)} \quad , \tag{6}$$

$$L = 9.2 \times 10^{-3}\ \bar{v}^2 \left(10^{-0.4m_A} + 10^{-0.4m_B} \right) \quad \text{(L*'s)} \quad , \tag{7}$$

with

$$\bar{v} = \left(v_A\ 10^{-0.4m_A} + v_B 10^{-0.4m_B} \right) / \left(10^{-0.4m_A} + 10^{-0.4m_B} \right) \text{(km s}^{-1}\text{)} \tag{8}$$

taking $H_o = 50$ km s^{-1} Mpc^{-1} and $L^* = 3.4 \times 10^{10}\ L_\odot$. The other symbols are as defined in Table I of PI. Making use of $\Delta v' \sim M^{1/2}$ (valid for any orbital eccentricity and phase) and the assumption of constant M/L (necessary in any case), it is convenient to correct the $\Delta v'$'s to those which would be expected for a system consisting of two late type galaxies with total luminosity L*; this corrected radial velocity difference Δv is calculated from

$$\Delta v = \Delta v'\ [L(1 - f_E + \alpha\ f_E)]^{-1/2} \quad . \tag{9}$$

The errors in r_p and Δv are calculated through a formal error propagation analysis from the errors in the observed quantities (PI). The distributions of r_p and Δv are shown in figures 2 and 3, respectively; the data for each binary system are plotted in the r_p-Δv plane in figure 4. The problem of obtaining a mean galaxian M/L from the binary data is thus reduced to one of constructing one or more models with fixed mass M* and some distribution of orbital

FIGURE 2

Observed distribution of projected separations. r_p is defined by equation (6).

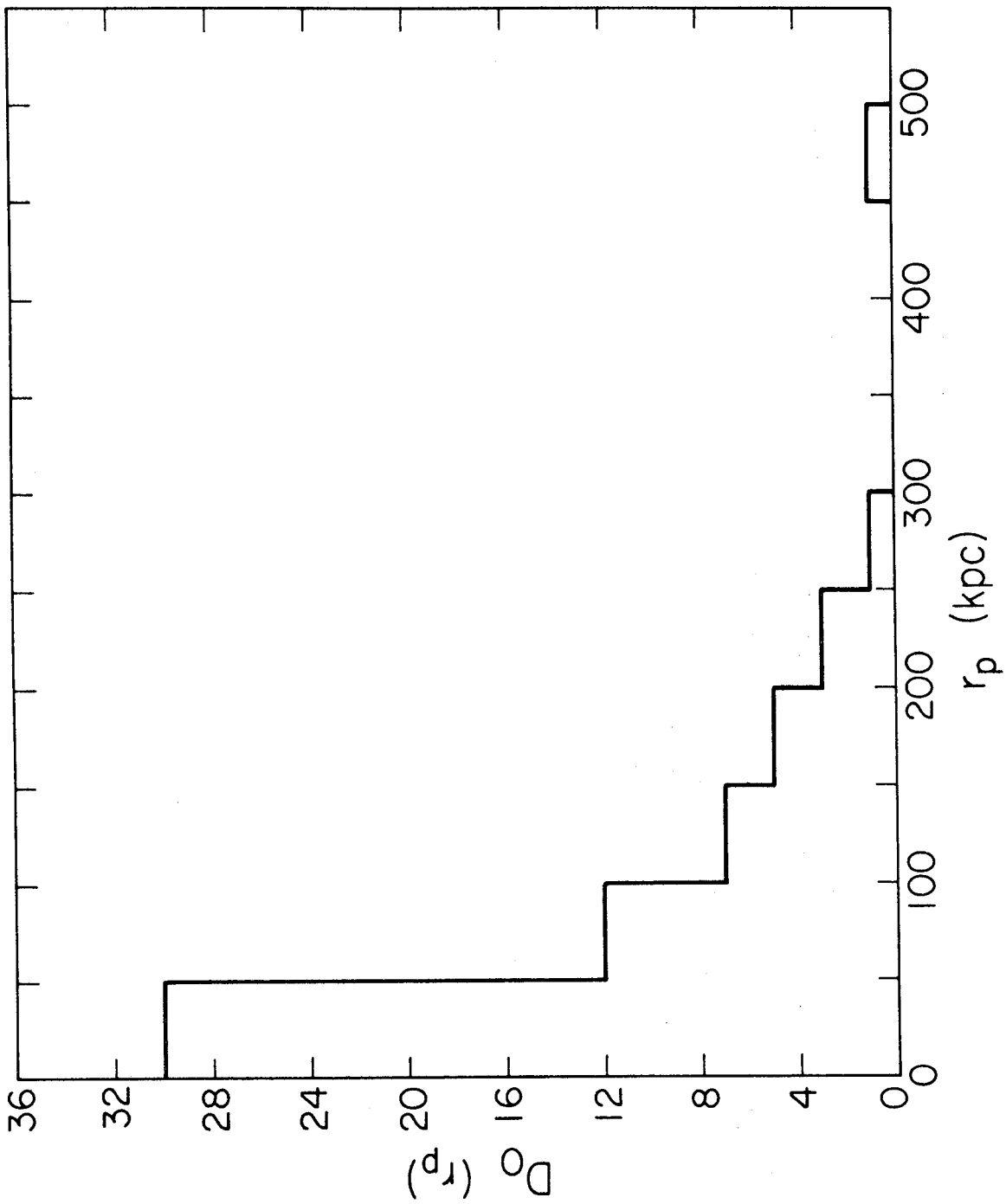
D_O (r_p)
0
4
8
12
16
20
24
28
32
36
0
100
200
300
400
500
r_p (kpc)

FIGURE 3

Observed distribution of corrected velocity differences. Δv is defined by equations (5) and (9).

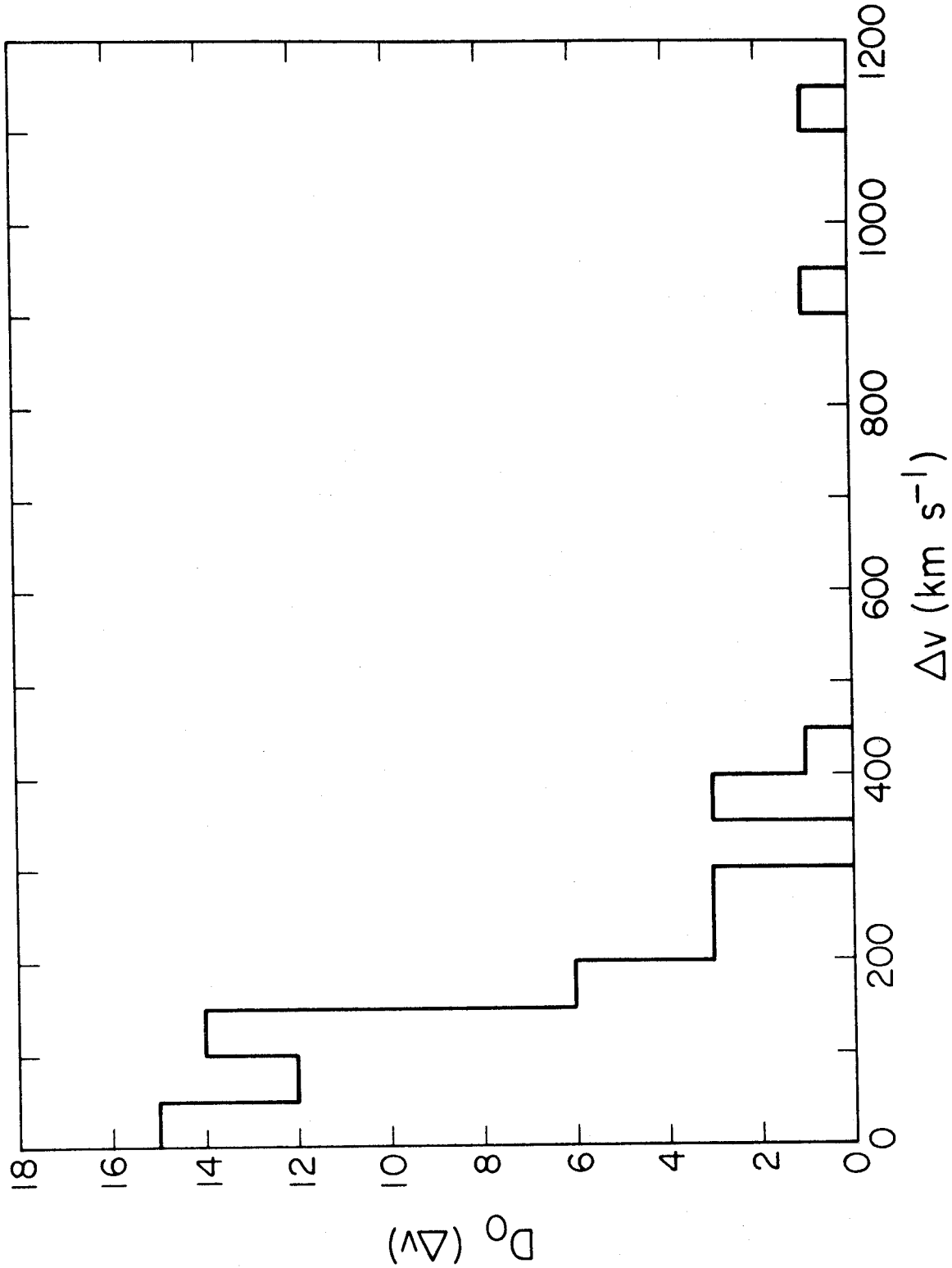
D_0 (Δv)
0
2
4
6
8
10
12
14
16
18
0
200
400
600
800
1000
1200
Δv (km s^{-1})

FIGURE 4

The observed distribution of systems in the r_p-Δv plane. Assuming the correction of $\Delta v'$ to Δv is valid (see text), this set of r_p, Δv points contains <u>all</u> of the dynamical information which can be obtained from the observations. Any acceptable model of binary galaxies must reproduce these data.

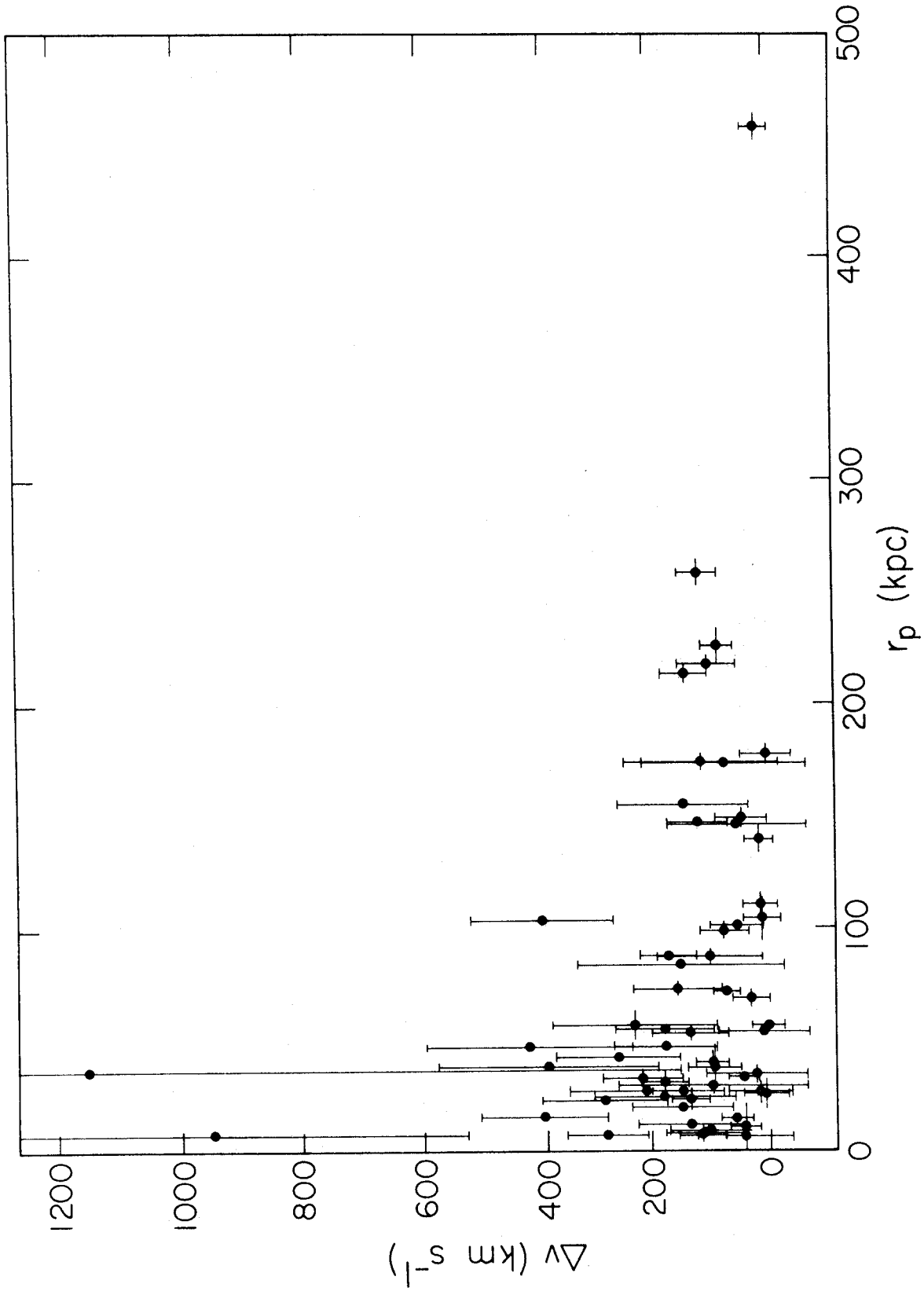
0
100
200
300
400
500
r_p (kpc)
0
200
400
600
800
1000
1200
Δv (km s^{-1})

parameters which, after correction for selection effects and measuring errors, reproduces the distribution of points in figure 4. All such models are consistent with the present observations and give a mean M/L of M*/L*.

III. DISTRIBUTION OF SPATIAL SEPARATIONS

In order to build dynamical models of binary galaxy systems (§ IV), it is necessary to know the distribution of spatial (i.e., 3-dimensional) separations of the components D(r). Fortunately, this problem decouples from the dynamical one, and D(r) can be determined from the observed distribution of projected separations $D_o(r_p)$ (figure 2) and a knowledge of the selection criteria. Clearly, almost any set of selection criteria for binary galaxies favors pairs with small values of r_p. Therefore, the problem divides into two parts: first, determining the true distribution of projected separations $D_T(r_p)$ from $D_o(r_p)$ by removing the selection biases and then, removing projection effects from $D_T(r_p)$ to give D(r).

In the present case, consider the probability $P_A(\theta)$ that a binary system with angular separation θ between the components will pass both criteria (1) and (2) defined in PI, and be accepted into the sample. $P_A(\theta)$ may be calculated if the galaxies in the survey region (see § II of PI) are distributed randomly (broken curve in figure 5);

FIGURE 5

The selection probability. $P_A(\theta)$ is the probability that a binary galaxy system with component angular separation θ would satisfy the selection criteria (1) and (2) of PI. $P_A(\theta)$ is zero for $\theta > \theta_c = 8'$ as a result of criterion (1). $P_A(\theta)$ for $\theta \leq \theta_c$ is the probability that the binary system will be rejected by criterion (2) (having a neighbor nearer than 5θ). The broken curve shows $P_A(\theta)$ if galaxies were distributed randomly in the sky; the solid curve was determined numerically (see text) and takes into account the observed clustering.

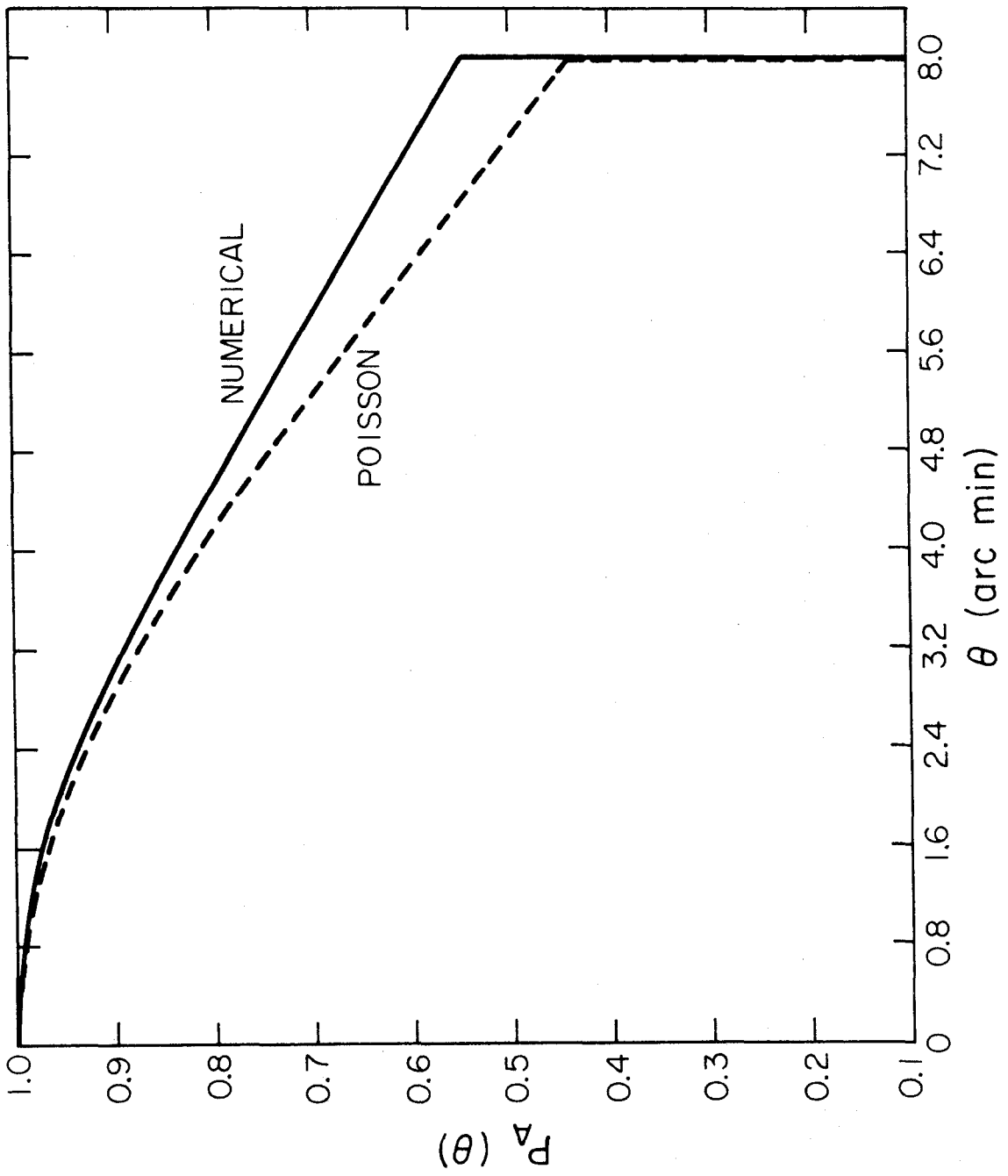
NUMERICAL
POISSON
$P_A(\theta)$
θ (arc min)
1.0
0.9
0.8
0.7
0.6
0.5
0.4
0.3
0.2
0.1
0
0.8
1.6
2.4
3.2
4.0
4.8
5.6
6.4
7.2
8.0

however, since there is obvious clustering $P_A(\theta)$ must be determined numerically. This was accomplished by choosing ~ 7400 randomly distributed points (each representing a possible binary system position) in the surveyed region of the sky [equation (5), PI] and calculating the angular distance to the nearest neighboring galaxy for each point. $P_A(\theta)$ follows trivially (solid line in figure 5) given the assumption of a roughly random distribution for the binary systems alone.

A binary pair with projected separation r_p would be included in the sample over a total effective volume V_{eff} given by

$$V_{eff} = A \int_0^{D_M} D^2 \, P_A[2 \arctan (\frac{r_p}{2D})] \, dD \ , \qquad (10)$$

where A is the size of the survey region in steradians and D_M is the maximum distance at which the fainter component would satisfy the magnitude limit criterion. The integral (10) was evaluated numerically for each pair in the primary sample, and figure 6 (open points) shows a plot of $1/V_{eff}$ versus r_p. Despite the large inherent scatter in $1/V_{eff}$, it is a good estimator of $D_T(r_p)$ and is analogous to the $1/V_M$ estimator for luminosity functions (Schmidt 1968). A least squares power-law fit gives $D_T(r_p) \sim r_p^{-0.51}$.

FIGURE 6

The true distribution of projected separations. The plotted points show two attempts to remove the selection biases from the observed distribution of projected separations. The open points are values of $1/V_{eff}$ determined from equation (10). The filled points with square-root-of-N uncertainties are determined from (11). The line is the best fit of $D_T(r_p) \propto r_p^{-\frac{1}{2}}$ to the open points.

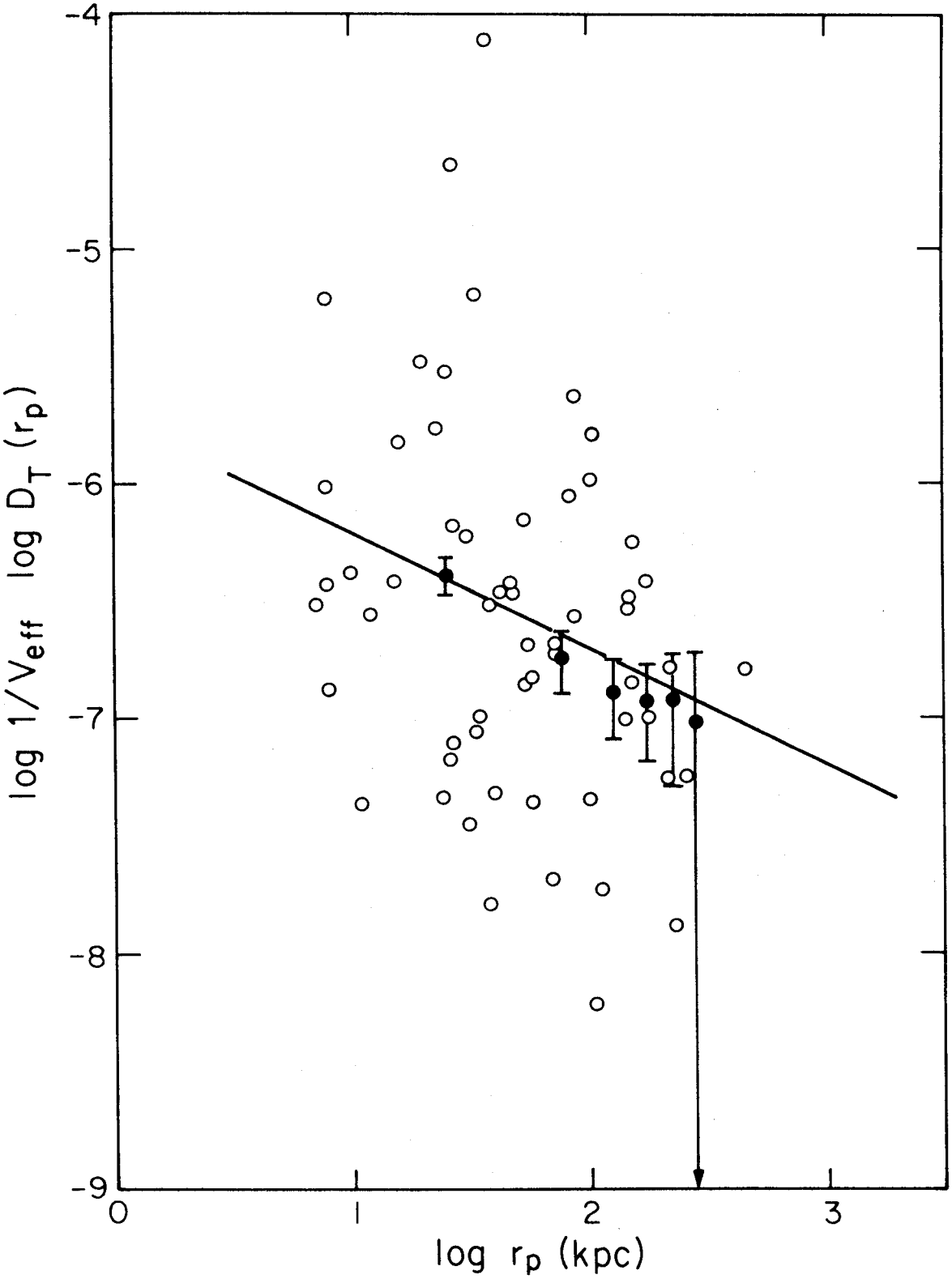
-4
-5
-6
-7
-8
-9
0
1
2
3
log 1/Veff log DT (rp)
log rp (kpc)

If it is assumed that the luminosity of the fainter component in a binary system and the pair's separation are independent, then

$$D_T(r_p) = D_o(r_p)/A \int_o^{\bar{D}_M} D^2 \, P_A\left[2 \arctan\left(\frac{r_p}{2D}\right)\right] dD \ , \qquad (11)$$

where $\bar{D}_M$ is the mean value of D_M ($\sim$ 120 Mpc). The values of $D_T(r_p)$ and square-root-of-N errors are shown as solid points in figure 6; a weighted, least squares fit gives $D_T(r_p) \sim r_p^{-0.57}$.

Since the index in both fits is uncertain by $\gtrsim 0.1$, the agreement is good (of course, both determinations use the same data). For simplicity, we adopt $D_T(r_p) \sim r_p^{-1/2}$.

In the general case, D(r) is obtained from $D_T(r_p)$ by solving the integral equation

$$D_T(r_p) d\, r_p = \int_o^{\infty} D(r) \, P(r, r_p) dr \, dr_p \ , \qquad (12)$$

where $P(r, r_p)dr\, dr_p$, the probability that a system of separation r will have projected separation r_p is

$$P(r, r_p)dr\, dr_p = \frac{2\, r_p}{\pi r \sqrt{r^2 - r_p^2}} \, dr\, dr_p \ , \qquad (13)$$

if the system is viewed from a randomly chosen direction. Fortunately, (12) is trivial in the power-law case; if $D_T(r_p) \sim r_p^{\gamma}$, then $D(r) \sim r^{\gamma}$. Therefore, we are led to

$$D(r) \sim r^{-1/2} \quad . \tag{14}$$

Now, given (14), the fraction $F(\beta)$ of systems with projected separations r_p whose true separation r is $\geq r_p/\beta$ $(0 < \beta \leq 1)$ is

$$F(\beta) = 1 - \left[\int_0^{\arccos \beta} \cos^{1/2} u\,du \Big/ \int_0^{\pi/2} \cos^{1/2} u\,du\right] \quad . \tag{15}$$

If r_p^{max} ($\approx$ 460 kpc in the primary sample) is the maximum observed value of r_p, the fraction ε of the observed systems with $r > r_p^{max}$ is

$$\varepsilon = \int_0^{r_p^{max}} D_o(r_p) F(r_p/r_p^{max})\,dr_p \Big/ \int_0^{r_p^{max}} D_o(r_p)\,dr_p \quad . \tag{16}$$

Evaluating (16) numerically gives $\varepsilon = 0.062$. If ε were $\gtrsim 0.5$, the determination of $D(r)$ would obviously be very questionable; the small value of ε indicates the self-consistency of the analysis (also, see Appendix).

A knowledge of the general shape of $D(r)$ is very critical to the mass determination. In general, the mean value of the angle ϕ between the pair separation vector and the line of sight decreases as $dD(r)/dr$ increases. For the case of a circular orbit with the line of sight lying in the orbital plane, the system's total mass is

$$M_T = \frac{\Delta v^2\, r_p}{G \sin^3 \phi} \quad , \tag{17}$$

a quite strong dependence.

IV. DYNAMICAL MODELS

Using the D(r) obtained in the last section and each of eight models for binary systems, eight sets of simulated r_p and Δv observations are generated for comparison with the real observations (figure 4). The eight models are described in Table II. These models were chosen primarily to span the range of likely possibilities rather than for any reasons of physical plausibility. The procedure which was used to generate 600 simulated r_p, Δv observations for each of the eight models is described below:

1) A separation r between 10 kpc and 1 Mpc is chosen at random from a population distributed according to (14). The results are insensitive to these arbitrary but plausible cutoffs.

2) A value of the orbital phase p randomly distributed between 0 and 1 is chosen and used to calculate the semi-major axis a from

$$a = r/(1 - e \cos E) \quad , \tag{18}$$

where E is determined by solving

$$E - e \sin E = 2\pi p \quad , \tag{19}$$

and e is the appropriate eccentricity (chosen randomly from the distribution given in Table II for model 5).

TABLE II

BINARY GALAXY MODELS

Model	Eccentricity	Total Mass M_T*	Comments
1	0	M'	circular orbit, point masses
2	1	M'	radial orbit, point masses
3	2/3	M'	average eccentricity, point masses
4	$\sqrt{5}/3$	M'	average axis ratio, point masses
5	$P(e)de = 2ede$	M'	phase-space filling orbits, point masses
6	0	$(r/10\ \text{kpc})M'$	circular orbit, large massive halo
7	1	$(r/10\ \text{kpc})M'$	radial orbit, large massive halo
8	0	$(r/10\ \text{kpc})M'$, $r \leq 100$ kpc $10\ M'$, $r > 100$ kpc	circular orbit small massive halo

*$M' = 3.4 \times 10^{10}\ M_\odot$

3) Using the appropriate total mass M_T from Table II, a relative velocity v is calculated using

$$v^2 = GM_T \left(\frac{2}{r} - \frac{1}{a}\right) \quad . \tag{20}$$

In addition, the angle between the relative velocity vector and the separation vector is set by the standard relation for an elliptical orbit.

4) The projection of v onto and r perpendicular to a line with a randomly chosen orientation is calculated to give a simulated Δv and r_p, respectively. If $r_p \leq 5$ kpc, the pair is rejected (because it would probably be too difficult to distinguish the two separate galaxies), and the procedure is begun again with step 1.

5) A distance D is chosen randomly from a distribution shown in figure 7; this distribution is that which would be expected for galaxies with $m_{pg} \leq 15.0$ [equation (5), PI], a luminosity function like that of field and small group galaxies (Schechter 1975; Turner and Gott 1976), and a uniform distribution in space.

6) A number chosen randomly between 0 and 1 is compared to $P_A[2 \arctan (\frac{r_p}{2D})]$ where $P_A(\theta)$ is given by the solid line in figure 5. If the random number is

FIGURE 7

The distribution of distances. $P(D)dD$ is the relative probability of a model binary galaxy system being assigned a distance D. It is derived from a Schechter (1975) luminosity function with $\alpha = -1$ and $L^* = 3.4 \times 10^{10} L_\odot$ (Turner and Gott 1976) for galaxies brighter than 15th magnitude. The binary systems are assumed to fill space uniformly.

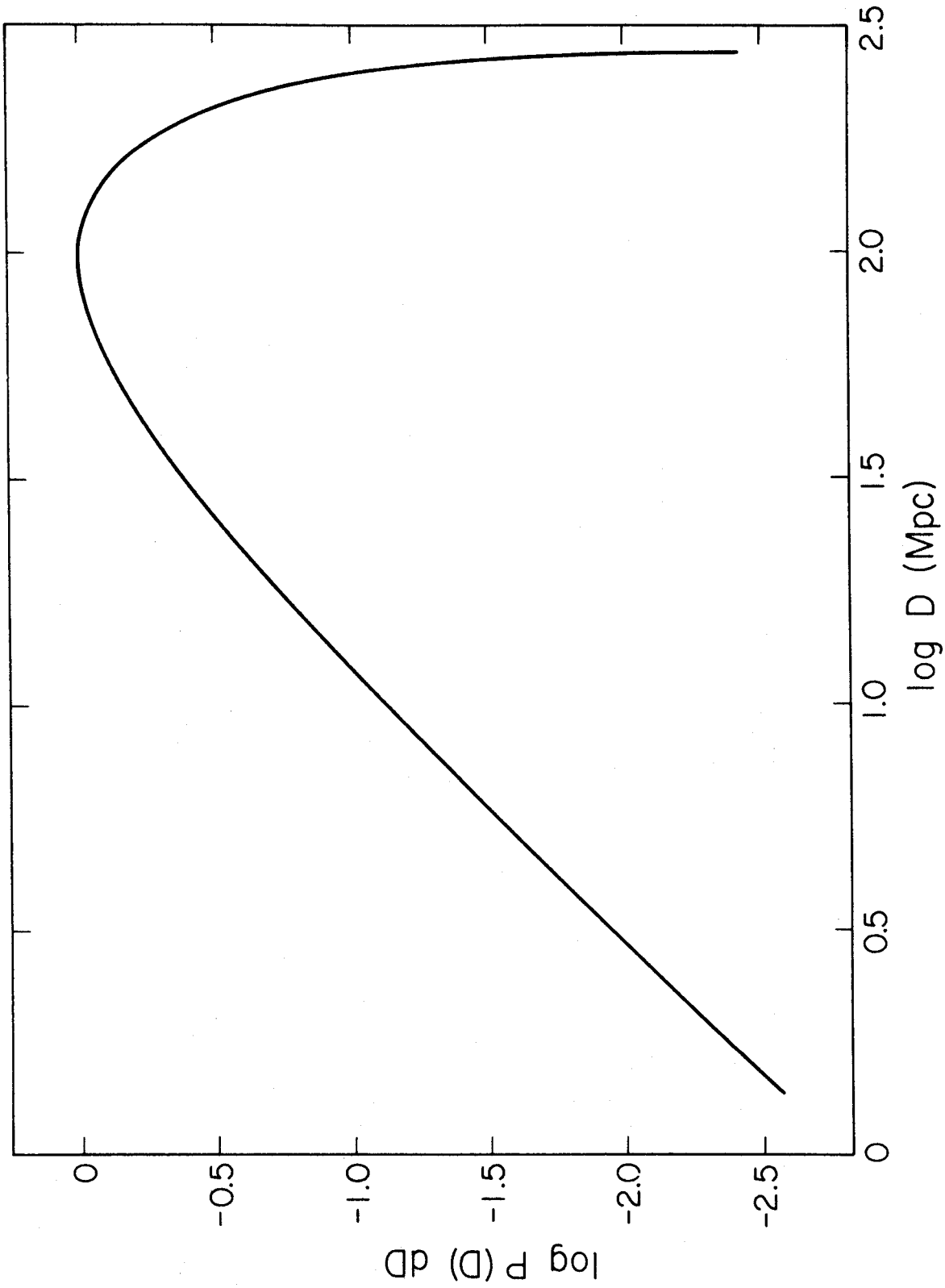
log P (D) dD
0
-0.5
-1.0
-1.5
-2.0
-2.5
0
0.5
1.0
1.5
2.0
2.5
log D (Mpc)

larger, the pair is rejected and the procedure is begun again with step 1; otherwise, the pair is accepted as a member of the simulated sample.

7) An error in both Δv and r_p is chosen randomly from the set of calculated errors in the real, observed Δv's and r_p's (§ II), respectively. These errors are hereafter also associated with the simulated observations.

8) The procedure is repeated until the desired number (600) of simulated observations of r_p and Δv and their uncertainties are accumulated.

Notice that although each model assumed a total or 10 kpc mass of $M' = 3.4 \times 10^{10}\ M_\odot$, the resulting simulated observations can be scaled to those which would result from a total or 10 kpc mass of M^* by multiplying the original Δv by $(M^*/M')^{1/2}$. When (in § V) the simulated and real observations are compared, any such scaling is applied. Each simulated Δv and r_p is then perturbed by an amount chosen randomly from a gaussian distribution with a standard deviation set by the uncertainty associated with the particular Δv or r_p in step 7 above. The simulated observations generated by the above procedure will hereafter by referred to as <u>model data</u>.

V. COMPARISONS OF OBSERVATIONS AND MODELS

Before proceeding to a comparison and matching of the observed and model data, it is useful to pose the problem in a well-defined statistical form: For any population of binary galaxy systems in the sky, there is a function $P(\Delta v, r_p)d\Delta v\, dr_p$ which describes the probability that any particular observed system (given certain selection criteria and observing techniques) will have velocity difference Δv and projected separation r_p. The observed data (figure 4) are a random sampling of this function for the true population of binary systems; the model data similarly represent the various model populations (Table II). The relevant question is then: If the observed and model data were both random samples of the same $P(\Delta v, r_p)d\Delta v\, dr_p$ function, what is the probability P_D of their being at least as different as they in fact are? This type of question is difficult to answer for a function of two variables unless the undesirable alternative of binning is adopted. However, for two sets of observations of a single parameter, the analogous probability can be calculated formally using the powerful, non-parametric rank-sum test (see Appendix for details). Therefore, in what follows, both the observed and model Δv and r_p values will be combined in various

ways to form a single parameter whose observed and model distributions can be compared by a rank-sum test to give P_D. Whenever $P_D << 1$, the model in question can be said to be excluded by the observed data at a confidence level of $1-P_D$. Also, any model with $P_D \gtrsim 0.5$ is completely consistent with the observed data.

First consider the logarithmic separation ℓ_{ij} between the ith and jth point in a set of Δv, r_p data

$$\ell_{ij} = \left[\log^2\left(\frac{\Delta v_i}{\Delta v_j}\right) + \log^2\left(\frac{r_{pi}}{r_{pj}}\right)\right]^{1/2} . \qquad (21)$$

Any set of N samplings of a function $P(\Delta v, r_p)d\Delta v\, dr_p$ can be transformed by (21) into a set of $N(N-1)/2$ samplings of ℓ from a corresponding $P(\ell)d\ell$. The distribution $P(\ell)d\ell$ has the very useful feature that it is independent of the binary system mass. It reflects only the "shape" (but not orientation) of $P(\Delta v, r_p)d\Delta v\, dr_p$ and the number of samplings N. The importance of the "shape" of $P(\Delta v, r_p)d\Delta v\, dr_p$ in distinguishing between the various possible orbital eccentricities has recently been emphasized by Noerdlinger (1975). The observed and model distributions of ℓ were compared using a rank-sum test with the results shown in Table III. The model distributions of ℓ were calculated by randomly dividing each model's 600 points into 10 groups of 59 points each, calculating the ℓ distribution separately for each group,

TABLE III

RESULTS OF LOGARITHMIC-SEPARATION TEST

Model	P_D	One σ P_D Range
1	2.45×10^{-2}	$0.187 - 1.37 \times 10^{-3}$
2	$< 10^{-9}$	$1.20 \times 10^{-8} - < 10^{-9}$
3	0.881	1.0 - 0.313
4	0.944	1.0 - 0.697
5	2.16×10^{-4}	$3.39 \times 10^{-3} - 6.80 \times 10^{-6}$
6	1.59×10^{-6}	$2.67 \times 10^{-4} - 4.00 \times 10^{-9}$
7	$< 10^{-9}$	$6.31 \times 10^{-9} - < 10^{-9}$
8	1.31×10^{-2}	$0.114 - 6.74 \times 10^{-4}$

and then adding the 10 distributions together. The ranges in P_D shown in Table III were calculated by noting the change in P_D when every observed data point was perturbed by its one standard deviation uncertainty.

Table III indicates that the high eccentricity models (2 and 7) are well excluded by the data as are the infinite halo, e = 0 model (6) and, to a lesser but still considerable extent, the phase-space-filling model (5). The low and medium eccentricity models (1, 3, 4, and 8) are all allowed. It should be noted that since the ℓ values calculated from (21) are not independent (N(N-1)/2 numbers determined from 2N independent ones), the assymptotic normalcy of the rank-sum statistic (see Appendix) is not guaranteed. However, numerous numerical experiments testing the above procedure with a variety of two-dimensional distribution functions all show that the normal approximation is quite accurate for $N \approx 50$.

Next, consider the mass parameter m defined by

$$m \equiv \Delta v^2 \, r_p \quad . \tag{22}$$

The distribution $P(m)dm$ corresponding to any $P(\Delta v, r_p)d\Delta v \, dr_p$ is sensitive to both the relative distribution of points in the $\Delta v - r_p$ plane and to the total mass of the binary systems. Using the scaling technique described in

the last paragraph of § IV, a distribution of m values corresponding to any particular late type mass-to-light ratio $\langle M/L \rangle_S$ (i.e., setting $M^* = \langle M/L \rangle_S L^*$ and thus multiplying Δv by $\langle M/L \rangle_S^{1/2}$) can be generated for each model. Comparing these distributions to the observed distribution of m with a rank-sum test gives P_D as a function of $\langle M/L \rangle_S$ and model. These curves are shown in figure 8, and the results are summarized in Table IV. Note that for the massive halo models, the value of $\langle M/L \rangle_S$ refers to a radius of 10 kpc; the total M/L value would be 10 times larger for model 8 and indefinitely larger for models 6 and 7. Models marked with a dagger were previously excluded on the basis of the "shape" test. The analysis in § I indicates that the early type mass-to-light ratio $\langle M/L \rangle_E = \alpha \langle M/L \rangle_S$ where $\alpha = 2.0 \pm 0.5$.

The statistical uncertainties in $\langle M/L \rangle_S$ are satisfactory (20%-30% at the one standard deviation level), but unfortunately, the total mass-to-light ratio varies by a factor of ~ 2 for the various allowed models. The best fit is achieved with model 4 and $\langle M/L \rangle_S = 47^{+14}_{-11}\ M_\odot/L_\odot$. Given the binary data alone, little further can be said.

If, however, additional factors are taken into account, the results presented in Table IV support the massive halo hypothesis of Ostriker and Peebles (1973). Models 1

FIGURE 8

The value of P_D as a function of model and $\langle M/L \rangle_S$. The peak of each curve occurs at the best fit value of $\langle M/L \rangle_S$ for each model (indicated by a number). For models 1-5 the total $\langle M/L \rangle_S$ is plotted; for models 6-8, the 10 kpc value is used. For any particular model, each value of $\langle M/L \rangle_S$ is excluded by the data with a confidence $1-P_D$. The calculation of P_D using a rank-sum test is explained in the text and the Appendix.

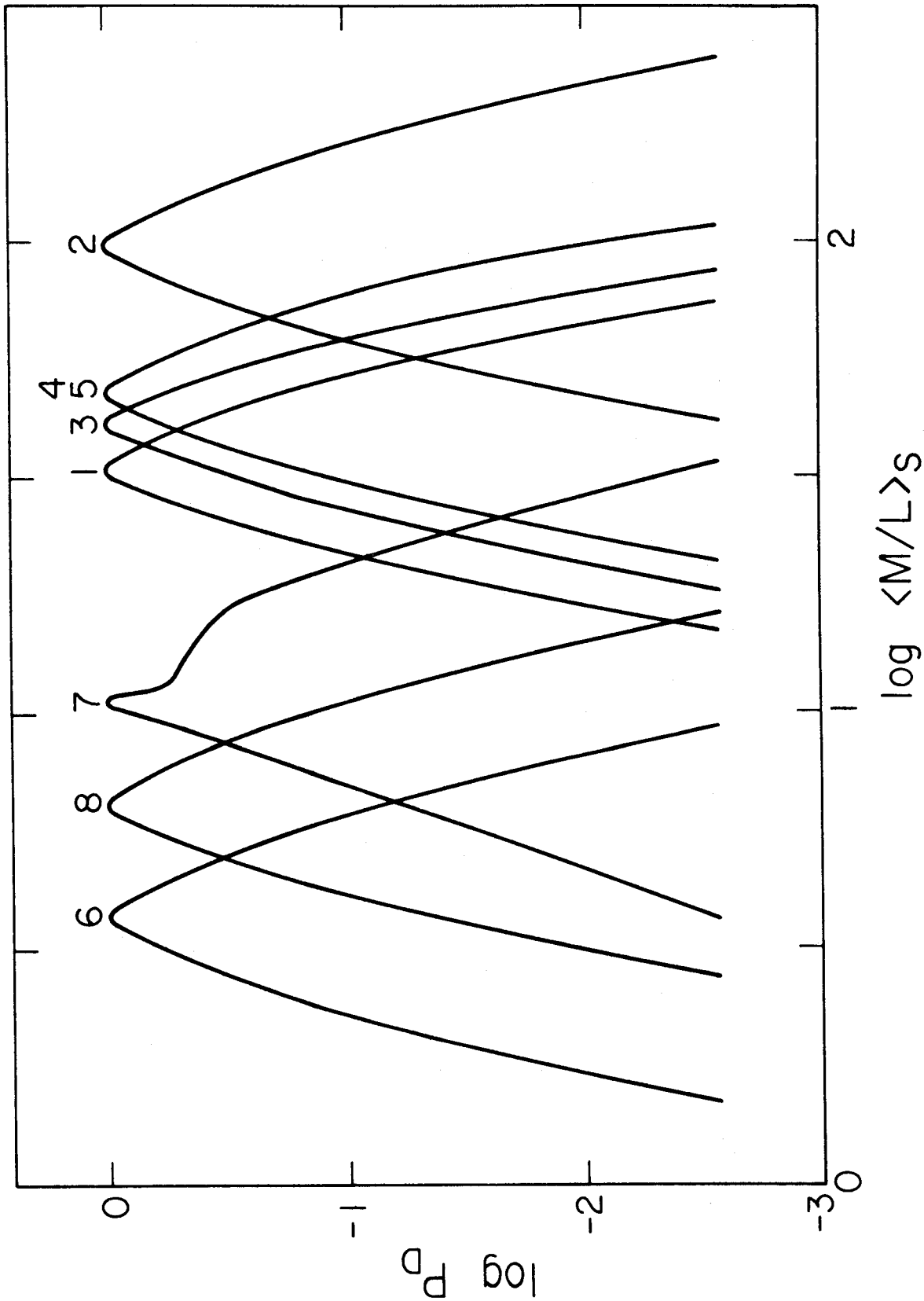
log P_D
0
-1
-2
-3
log <M/L>s
0
1
2
1
2
3
4
5
6
7
8

TABLE IV

BEST-FIT $\langle M/L \rangle_S$ AND ITS UNCERTAINTY

Model	Best $\langle M/L \rangle_S^*$	One σ Range	Three σ Range
1	33	26 - 43	15 - 74
2†	98	74 - 131	42 - 245
3	41	32 - 52	18 - 87
4	47	36 - 61	21 - 102
5†	48	36 - 62	21 - 108
6†	3.7	2.8 - 5.0	1.5 - 9.4
7†	10	8.5 - 16	3.6 - 34
8	6.4	4.8 - 8.6	2.8 - 16

*Total for models 1-5; 10 kpc value for models 6-8.

through 5 which essentially assume that all of the mass is contained in a region small compared to the orbital scales (~ 100 kpc) give M/L values much larger than those derived from conventional rotation curve studies at scales ~ 10 kpc. However, models 6 through 8 which assume that the matter is distributed throughout most or all of the binary system give 10 kpc M/L values in good agreement with rotation curve estimates. Thus, although the present binary data alone do not require it, the most reasonable interpretation of Table IV and figure 8 suggests that late-type (i.e., spiral) galaxies have dark halos containing ~ 10 times the disk mass. The alternative is to simply invoke a mass discrepancy in binary systems similar to that observed in groups and clusters without explaining its origin (if the pairs were unbound, they would separate in ~ 10^9 yrs).

Clearly, the present binary data does not determine the total halo size (and total M/L) very sharply. The very low value of P_D obtained by the infinite halo models (6 and 7) in the "shape" test seems to argue against halos being as large as the largest observed values of r_p (~ 1/2 Mpc); however, these low values of P_D may also reflect incorrect orbital eccentricities (orbits with $0 < e < 1$ for galaxies with halos are too complex to conveniently model). Nevertheless, halos of ~ 100 kpc

radius, total mass-to-light ratios of 65 ± 30, and moderately eccentric orbits seem to be the most likely possibilities. Figure 9 shows 100 randomly selected points from the model 8 data shifted to the best fit 10 kpc $\langle M/L \rangle_S = 6.44$ (for comparison to the observations in figure 4).

VI. OTHER ESTIMATES OF THE MASS-TO-LIGHT RATIO

Given the somewhat complicated nature of the M/L determination presented in the previous sections, it is of interest to try some simpler possibilities.

First, we calculate the minimum mass $\bar{M}_{MIN}$ for both the observed and model data

$$\bar{M}_{MIN} = (2GN)^{-1} \sum_{i=1}^{N} (\Delta v_i^2 - \sigma_{\Delta v_i}^2)\, r_{pi} \quad , \tag{23}$$

where N is the number of binary systems (observed or modeled). Notice that in (23) the velocity measurement errors are statistically removed from the pair velocity differences. Now, if the result for the observed data is $\bar{M}^O_{MIN}$ and that for any particular model is $\bar{M}^M_{MIN}$, a total or 10 kpc mass-to-light ratio $\langle M/L \rangle_S$ is obtained by

$$\langle M/L \rangle_S = C_M\, \bar{M}^O_{MIN}/L^* \quad , \tag{24}$$

where $C_M = M'/\bar{M}^M_{MIN}$. For the observed primary data

FIGURE 9

Simulated observations for the best fit limited halo model. This figure is exactly analogous to Figure 4 except that the points are 100 simulated observations (see §IV) of binary systems in which the individual galaxies are assumed to have halos containing $\sim$ 90% of the mass. $\langle M/L \rangle_S = 64.4$ $M_\odot/L_\odot$ is used.

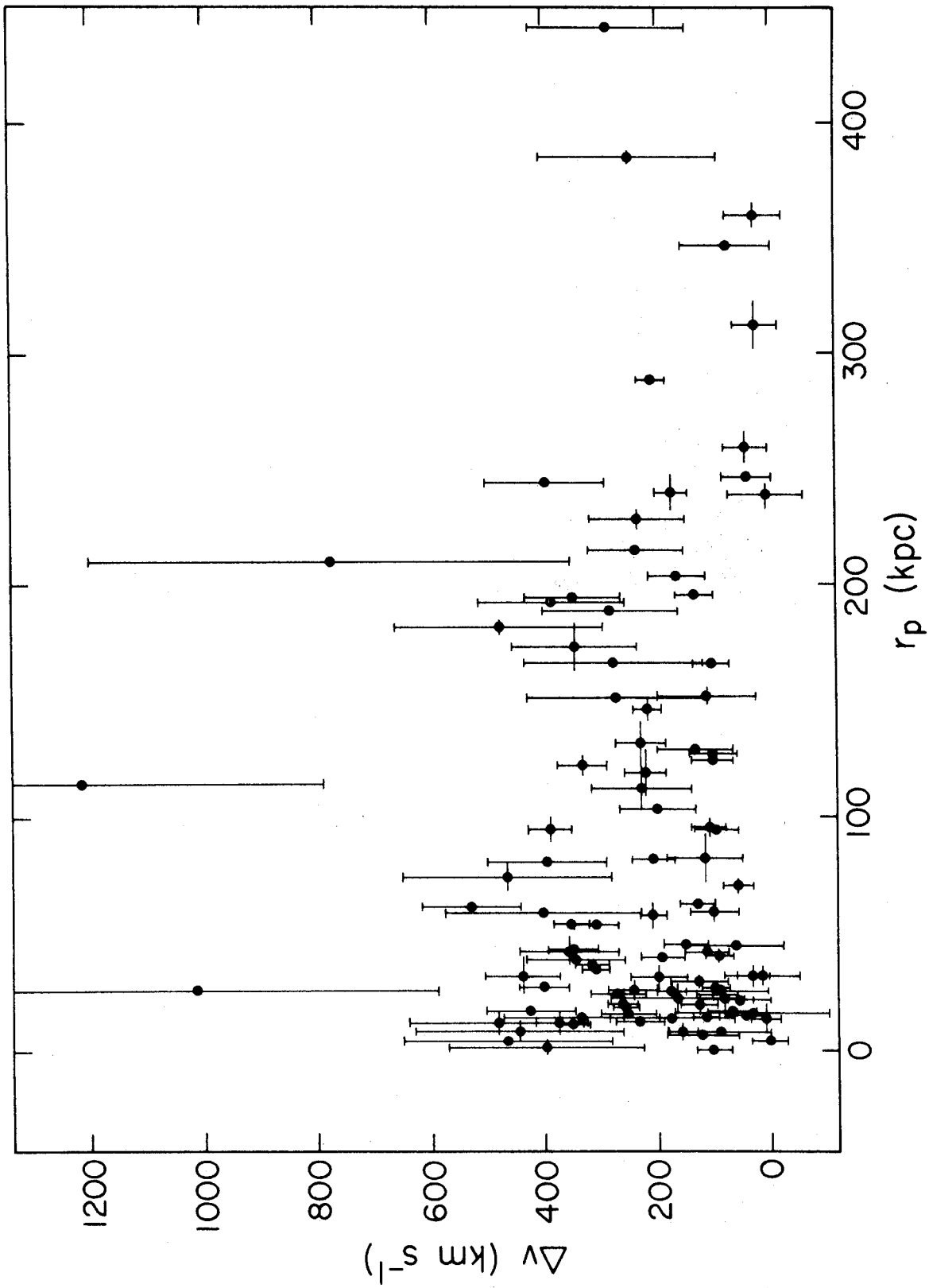
1200
1000
800
600
400
200
0
ΔV (km s⁻¹)
0
100
200
300
400
r_p (kpc)

TABLE V

CORRECTION TO MEAN MINIMUM MASS

Model	Correction Factor C_M	$\langle M/L \rangle_S$ *
1	8.04	32
2	19.1	76
3	10.0	40
4	11.0	44
5	10.8	43
6	0.504	2.0
7	1.14	4.5
8	1.26	5.0

*Total for models 1-5; 10 kpc value for models 6-8.

$\overline{M}^{o}_{MIN}/L^{*} = 3.97\ M_{\odot}/L_{\odot}$. The values of C_M and the resulting $\langle M/L \rangle_S$ are given in Table V. These results agree well with those given in Table IV and, thus, independently confirm the best fit values obtained with the rank-sum test. This method, which essentially consists of using the model data (§ IV) to estimate a correction factor C_M to the observed mean minimum mass-to-light ratio, has several disadvantages which offset its relative simplicity: It provides neither a way of discriminating among the various models nor an estimate of the statistical uncertainty in $\langle M/L \rangle_S$. Also, the method is (like all mean methods) very sensitive to the inclusion or exclusion of a single system with a particularly large minimum mass; the rank-sum test method, by contrast, makes equal use of each measurement.

The values of total M/L derived above and in § V are considerably larger than those found by Page in his studies of binary galaxy systems. In order to determine the source of these differences all of the data in Table I of PI (except pairs with $\Delta v > 425$ km s^{-1}) have been re-analyzed using the same technique and formulae described by Page (1966). The resulting mass-to-light ratios are 3.3 $M_{\odot}/L_{\odot}$ for all pairs combined (74 systems), 2.2 $M_{\odot}/L_{\odot}$ for pure spiral and irregual pairs (44 systems), and 5.9 $M_{\odot}/L_{\odot}$ for pure elliptical and SO pairs (only 9 systems). The pure spiral and irregular result agrees

well with Page's result of 1.6 $M_\odot/L_\odot$ and is ~ 15 times smaller than model 1 (e = 0 and point masses, as Page assumed) values in Tables IV and V. This leads to the conclusion that the large M/L's obtained in the present study are mainly the result of a different method of analysis, not a different data base. The most likely source of the factor of ~ 15 difference is that Page's method assumes an isotropic distribution of separation vectors (see discussion at end of § III) giving $\langle \sin \phi \rangle = 2/\pi$ corresponding to $\phi \approx 40°$. If equation (17) applied exactly, then a true $\langle \sin \phi \rangle = 0.26$ corresponding to $\phi \approx 15°$ would account for the difference. Clearly almost any selection criteria will favor small values of ϕ. In general, the removal of selection effects (requiring the use of well-defined selection criteria) can make a large difference in the derived mass-to-light ratios. This point has probably received insufficient attention in previous studies.

VII. DISCUSSION AND CONCLUSIONS

A number of conclusions can be drawn (with varying degrees of certainty) from the analysis presented in this paper. These are listed below with comments:

1) The total mass-to-light ratio of late-type (i.e., spiral) galaxies in binary systems is quite large

(perhaps ~ 65 $M_\odot/L_\odot$) compared to conventional rotation curve values (~ 5 $M_\odot/L_\odot$). This result extends the familiar "missing mass" problem for groups (Burbidge and Sargent 1971; Rood et al. 1970; Gott and Turner 1976) and clusters (Rood et al. 1972; Oemler 1973) to binary systems. The indicated but rather less certain M/L for early-type (elliptical and SO) galaxies is twice as great (~ 130 $M_\odot/L_\odot$).

2) This mass discrepancy can be understood if spiral galaxies possess dark halos of ~ 100 kpc radius containing ~ 10 times the disk mass. While the size and mass of these halos cannot be sharply determined by the present data, there is some evidence against halos larger than a few hundred kpc. Also halos with less than ~ 3 times the disk mass could not account for the full discrepancy. In view of the other evidence (Ostriker and Peebles 1973; Ostriker et al. 1974; Kalnajs 1972), the heavy halo hypothesis seems to offer the best (but certainly not an exclusive) explanation of the data. Alternative explanations require one or more of the following: other (non-halo) sources of invisible mass, the existence of unbound and young (~ 10^9 yrs) binary systems, a non-velocity interpretation of redshifts, an unconventional theory

of dynamics, or a serious error in the present data or analysis.

3) The best model for the eccentricity of binary galaxy orbits lies between the extremes of $e = 0$ and $e = 1$; the latter is probably excluded by the data. Even a phase-space-filling distribution of orbits seems to have too many highly radial members. Unfortunately, moderate eccentricity orbits of galaxies with massive halos are too complex to model reliably. In any case, it is probably impossible to fully untangle the effects of orbital eccentricity and halo size with the present data and may prove difficult even with much more or better data.

4) A proper analysis of binary galaxy data must take careful account of selection effects in the sample studied. This in turn requires that the sample be chosen using well-defined selection criteria. A neglect of these factors can lead to systematic errors of a factor $\gtrsim 10$ in the resulting M/L values. Earlier binary galaxy mass determinations probably suffered from such difficulties.

Some or all of the conclusions given above might be substantially modified or, in extreme cases, invalidated if any of the following possibilities were realized:

1) the mass-to-light ratio of galaxies varies widely in a systematic or random way,
2) the true population of binary galaxies possesses characteristics very different from those of any of the Table II model populations,
3) galaxies in binary systems have intrinsic properties quite different from those of other galaxies,
4) the distribution of binary galaxy separations is, for some reason, very different from (14).

Other implicit and explicit assumptions (a uniform distribution of binary systems in space, etc.) could be incorrect but seem quite likely to be valid.

Given the intriguing but somewhat uncertain nature of the present results, there is little doubt that binary galaxies deserve further attention, both observational and theoretical.

APPENDIX TO CHAPTER 2

THE RANK-SUM TEST

AND

A NUMERICAL VERIFICATION OF $D(r) \sim r^{-1/2}$

The rank-sum test is a standard statistical technique (Dixon and Massey 1969; Noether 1967) for comparing two sets of observations of a single variable x in order to determine whether both sets could have been drawn from the same population $f(x)dx$. The two sets of data are combined and the individual observations of x are ranked in increasing order (i.e., rank of lowest x = 1, rank of second lowest x = 2, ..., rank of highest x = N_1+N_2, where N_1 and N_2 are the number of observations in the two sets of observations, respectively). Now let the rank-sum statistic T' be defined as the sum of the ranks of the observations in set 1 where $N_1 \leq N_2$. Then, if both sets of observations were made on the same population, the expected value of T' is

$$\mu_{T'} = \frac{N_1(N_1 + N_2 + 1)}{2} \quad , \tag{A1}$$

and if both N_1 and N_2 are greater than ~ 10 the distribution of T' about $\mu_{T'}$ will be very close to a gaussian with

$$\sigma_{T'}{}^2 = \frac{N_1 N_2(N_1 + N_2 + 1)}{12} \quad . \tag{A2}$$

Thus, the probability P_D that two random sets of data drawn from the same population would match as poorly as

the actually observed sets is

$$P_D(z) = 1 - (2\pi)^{-1/2}\sigma_{T'}^{-1}\int_{-z}^{z}\exp[-z^2/2]dz \quad , \qquad (A3)$$

where $z = |\mu_{T'} - T'|/\sigma_{T'}$ (a tabulated function).

The primary advantage of the rank-sum test is its non-parametric nature (i.e., it makes no assumptions about $f(x)dx$ and is completely independent of it). Also, it is a very powerful test, requiring only 5% more observations than the optimum t-test to give the same power in distinguishing two normal populations and 20% less for some non-normal ones (Dixon and Massey 1969).

The technique can be usefully illustrated to test the validity of §§ III and IV of this paper. § III presents an analytic removal of selection and projection effects from $D_o(r_p)$ to give $D(r) \sim r^{-1/2}$. In § IV this $D(r)$ is used in a computer model of the selection and observation processes to produce 4800 simulated observations of binary systems. Comparing these $N_2 = 4800$ model observations of r_p (figure A1) to the $N_1 = 59$ real ones (figure 4) with a rank-sum test gives

$$\begin{aligned} \mu_{T'} &= 143{,}370 \\ \sigma_{T'} &= 11{,}930 \\ T' &= 133{,}017 \\ z &= 0.97 \\ P_D(z) &= 0.33 \quad . \end{aligned} \qquad (A4)$$

FIGURE A1

The modeled distribution of observed projected separations. The modeling process (§IV) simulated observations of 4800 binary systems chosen (using criteria (1) and (2) of PI) from a family whose distribution of spatial separations is described by equation (14). The resulting model distribution of r_p is compared to the observed distribution (Figure 2) in the text of the Appendix.

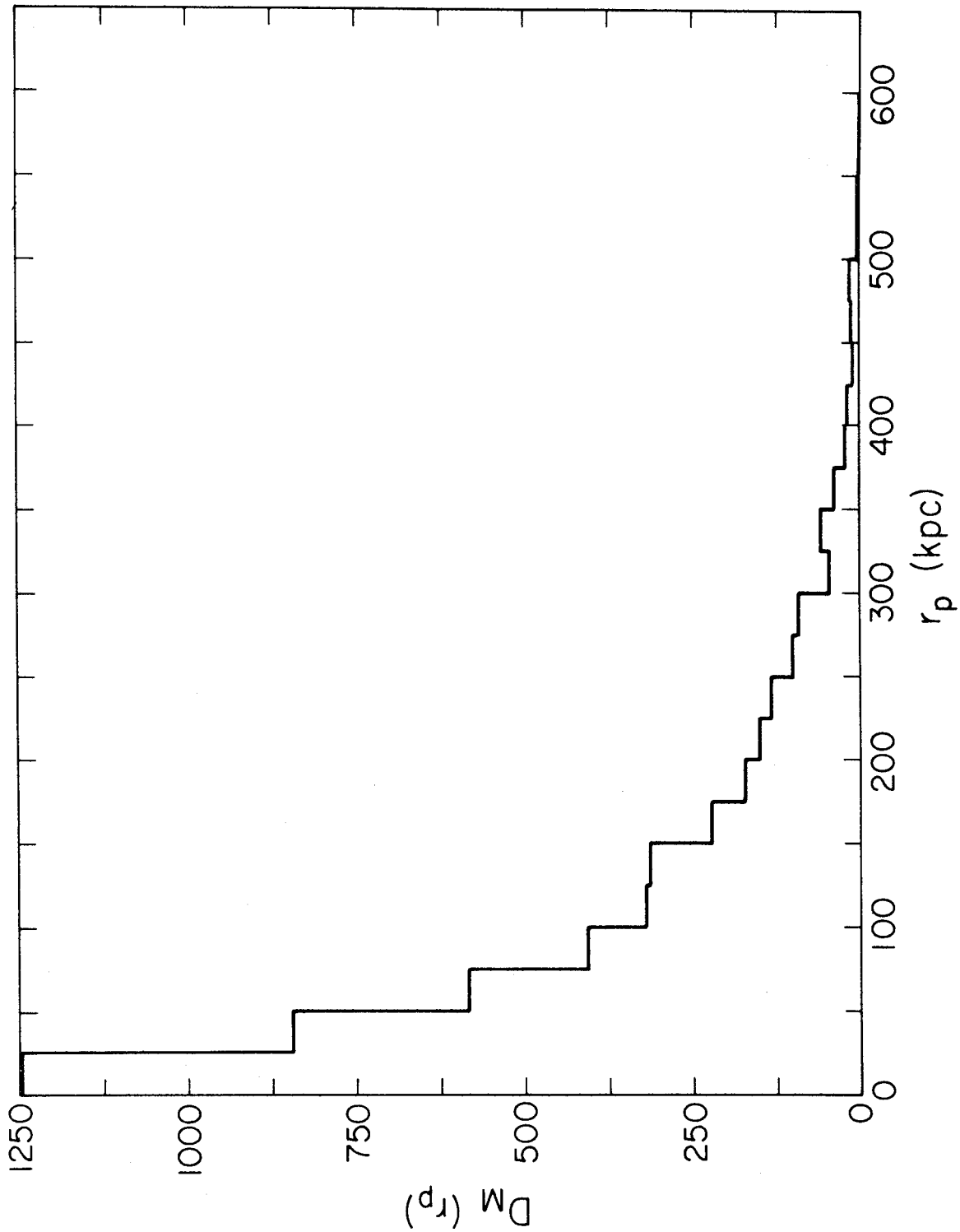
1250
1000
750
500
250
0
D_M (r_p)
0
100
200
300
400
500
600
r_p (kpc)

The large value of $P_D(z)$ confirms the self-consistency of §§ III and IV.

REFERENCES

Burbidge, E. M., and Sargent, W. L. W. 1971, in Nuclei of Galaxies, ed. D. J. K. O'Connell (New York: American Elsevier Publishing Company), p. 351.

Dixon, W. J., and Massey, F. J. 1969, Introduction to Statistical Analysis, (New York: McGraw-Hill Book Company).

Gott, J. R., and Turner, E. L. 1976, in preparation.

Holmberg, E. 1954, Medd. Lund Astr. Obs., Ser I, 186, 1.

Kalnajs, A. J. 1972, Ap. J., 175, 63.

Noerdlinger, P. D. 1975, Ap. J., 197, 545.

Noether, G. E. 1967, Elements of Nonparametric Statistics, (New York: John Wiley and Sons, Inc.).

Oemler, A. 1973, Ph.D. thesis, California Institute of Technology.

Ostriker, J. P., and Peebles, P. J. E. 1973, Ap. J., 186, 467.

Ostriker, J. P., Peebles, P. J. E., and Yahil, A. 1974, Ap. J. Lett., 193, L1.

Page, T. 1952, Ap. J., 116, 63.

Page, T. 1961, in Proceedings of the Fourth Berkeley Symposium on Mathematical Statistics and Probability, ed. J. Neyman (Berkeley: University of California Press), p. 277.

Page, T. 1966, in Proceedings of the Fifth Berkeley Symposium on Mathematical Statistics and Probability, eds. L. M. LeCam, J. Neyman, and E. L. Scott (Berkeley: University of California Press), p. 31.

Rood, H. J., Page, T. L., Kintner, E. C., and King, I. 1972, Ap. J., 175, 627.

Rood, H. J., Rothman, V. C. A., and Turnrose, B. E. 1970, Ap. J., 162, 411.

Schechter, P. 1975, preprint.

Schmidt, M. 1968, Ap. J., 151, 393.

Smart, N. C. 1973, Ph.D. thesis, University of Cambridge.

Turner, E. L. 1976, in press, (PI).

Turner, E. L., and Gott, J. R. 1976, in preparation.

CHAPTER 3

GROUPS OF GALAXIES:

A CATALOG

I. INTRODUCTION

Galaxies occur in a wide variety of bound systems ranging from binary pairs through small groups to rich clusters. These systems in turn possess a wide range of densities with typical separations between bright ($L \geq L^*$) galaxies varying from $\leq$ 10 kpc up to $\sim$ 1 Mpc. Among the most common of these systems are small, loose groups containing of order 10 bright galaxies with separations $\geq$ 100 kpc. Such systems probably contain a substantial fraction of all galaxies (de Vaucouleurs 1975, van den Bergh 1962, Karachentseva 1973). Familiar examples include the Local Group and the M81 group.

Unfortunately, loose groups are somewhat difficult to identify (and therefore study) in the sky precisely because they are neither dense nor populous. For this reason, a catalog of groups of galaxies is extremely useful, as witnessed by the large number of studies (e.g., Rood et al. 1970, Field and Saslaw 1971, Gott et al. 1973, Turner and Sargent 1974, Jackson 1975) prompted by de Vaucouleurs' (1975) unpublished but widely circulated list of groups. The problems in compiling such a catalog arise both from the uncertainty in any particular group's membership and from the difficulty in consistently identifying each group's existence. de Vaucouleurs (1975) has suggested that such groups might be suitably defined as enhancements in the volume

number density of galaxies and might be identified as enhancements in the surface number density of galaxies on the sky. To date, however, all group catalogs (de Vaucouleurs 1975, Holmberg 1937, Sandage and Tammann 1975) have been based on a detailed, but somewhat subjective, consideration of a variety of data (e.g., redshift, position, magnitude, appearance) concerning the candidate galaxies.

In the present paper, a new catalog of groups is presented; this catalog, in contrast to earlier ones, has been generated by the "blind" application of a precisely defined group identification procedure. This procedure only considers the positions of galaxies in the sky. As a result, it sometimes makes absurd "mistakes" (e.g., assigning a dwarf spheroidal member of the Local Group to the same group as a galaxy with $cz = 4000$ km s^{-1}), but these are usually too obvious to be misleading. In addition, the shortcomings of the groups defined by our naive method are offset, we feel, by their objectivity (no unconscious observer biases), homogeneity, and completeness. These attributes are critical in any statistical study of group properties. Also, the present catalog extends to fainter magnitudes (14th) than the previous studies. It is not our intention to claim that such (objective) group identifications can replace the conventional (subjective) ones, but rather that they provide a useful additional technique.

The group identification procedure and the sample of galaxies to which it has been applied are described in §II. The groups, various available data, and comments are given in §III. Data and comments on the galaxies not assigned to groups are contained in §IV. §V briefly discusses the uses and significance of these results.

II. GROUP IDENTIFICATIONS AND MEMBERSHIP

The sample of galaxies to be searched for groups is defined by

$$\begin{aligned} \delta &\geq 0° \\ b^{II} &\geq 40° \\ m_{pg} &\leq 14.0 \end{aligned} \qquad (1)$$

with all positions and magnitudes taken from the Catalog of Galaxies and Clusters of Galaxies (Zwicky et al. 1961-1968, hereafter CGCG). The sample contains 1087 galaxies and is shown in Figure 1. This sample is likely to be quite homogeneous and complete since the CGCG extends well beyond each of the three limits (1). Also, the accuracy of the CGCG magnitude scale has recently been confirmed by extensive, multi-aperture, isophotal, photoelectric photometry (Huchra 1975).

The following group identification procedure has been applied to the sample defined by (1):

1) For each galaxy in the sample, we consider the surface density ρ of galaxies in a circular region of angular

FIGURE 1

The 1087 CGCG galaxies which satisfy (1). This map shows a sterographic projection of the north galactic cap about the north celestial pole (NCP). Each point represents one galaxy, although many are too close together to distinguish at this scale. Although much clustering is apparent, the exact location and definition of individual groups is far from straightforward.

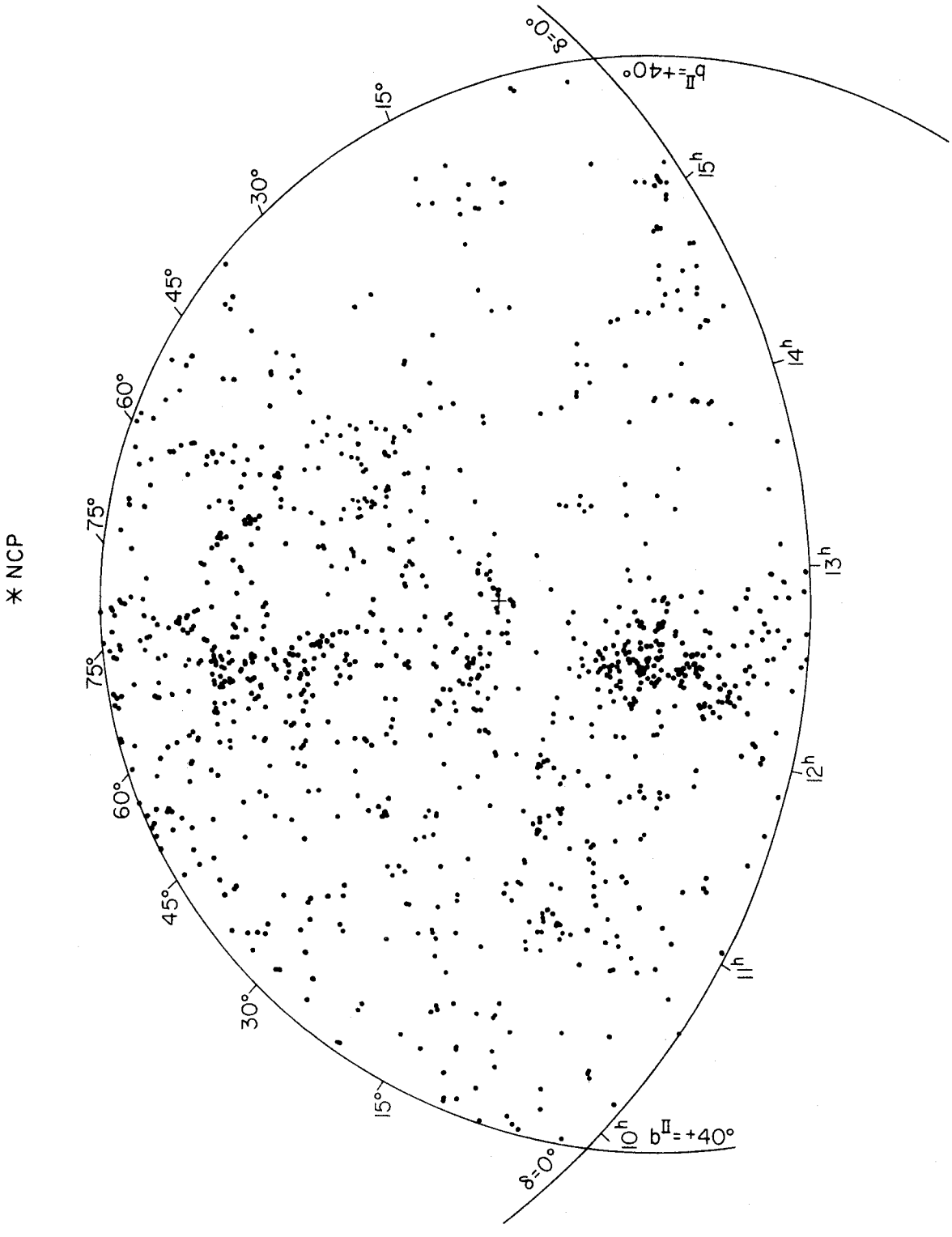
* NCP
δ=0°
b^{II}=+40°
15°
30°
45°
60°
75°
15h
14h
13h
12h
11h
10h
b^{II}=+40°
δ=0°

radius θ centered on the galaxy.

$$\rho(\theta) = \frac{1}{2\pi} N(\leq\theta)/(1 - \cos\ \theta) \qquad (2)$$

where $N(\leq\theta) - 1$ is the number of galaxies within an angular distance θ of the galaxy being considered.

2) For each galaxy, we then choose the largest possible angle θ_c such that

$$\rho(\theta\leq\theta_c) \geq f\ \bar{\rho} \qquad (3)$$

where $\bar{\rho}$ is the mean surface density of galaxies in the sample (594 galaxies per sterradian for our sample) and f is a surface density enhancement factor. Here we have used $f = 10^{2/3}$ in hopes of identifying groups with volume density enhancements ≥ 10 as suggested by de Vaucouleurs (1975). For computational reasons θ_c has only been determined to an accuracy of 0°.25.

3) For any galaxy with $N(\leq\theta_c)>1$, a circle of angular radius θ_c centered on the galaxy is drawn on a map (similar to Figure 1) of the sky. Galaxies whose nearest neighbor is more distant than $\sim (\pi f\bar{\rho}/2)^{-\frac{1}{2}}$ (about 0°.75 here) have $N(\leq\theta_c) = 1$ and have no circle drawn about them.

4) When steps 1 through 3 are completed for each galaxy in the sample, a map of the sky showing all of the resulting circles is prepared. The circles fall into many (103) distinct (i.e., non-overlapping) clumps; each

clump contains from 2 up to $\sim$ 200 overlapping circles. The outside boundary of each clump of circles roughly approximates an iso-surface-density-enhancement contour; that is, the mean surface density of galaxies within the boundary is $\approx f\bar{\rho}$. Each of these distinct clumps of circles is identified as a separate group with a boundary defined by the perimeter of the region of overlapping circles.

5) All galaxies lying within a particular group's boundary are considered (at least tentatively) to be members. Any galaxy lying outside all of the group boundaries is considered a field galaxy and not assigned to any group.

The group identifications and boundaries generated by the above procedure for the sample of galaxies defined by (1) are shown in Figure 2. A total of 737 galaxies are assigned to groups; 350, to the field. It should be noted that although the procedure was designed to locate loose groups, it also identifies large clusters, binary pairs, and generally any system which has a surface number density of galaxies $\geq f\bar{\rho}$. All of these systems will, hereafter, be referred to as groups.

Before proceeding to a consideration of the individual groups (§III) and field galaxies (§IV), it is useful to consider several general properties of the results of the above procedures:

FIGURE 2

The group boundaries. On a map identical to Figure 1, the group boundaries (iso-surface-density-enhancement contours) generated by the procedure described in §II are shown. The identifying numbers correspond to those in Table I.

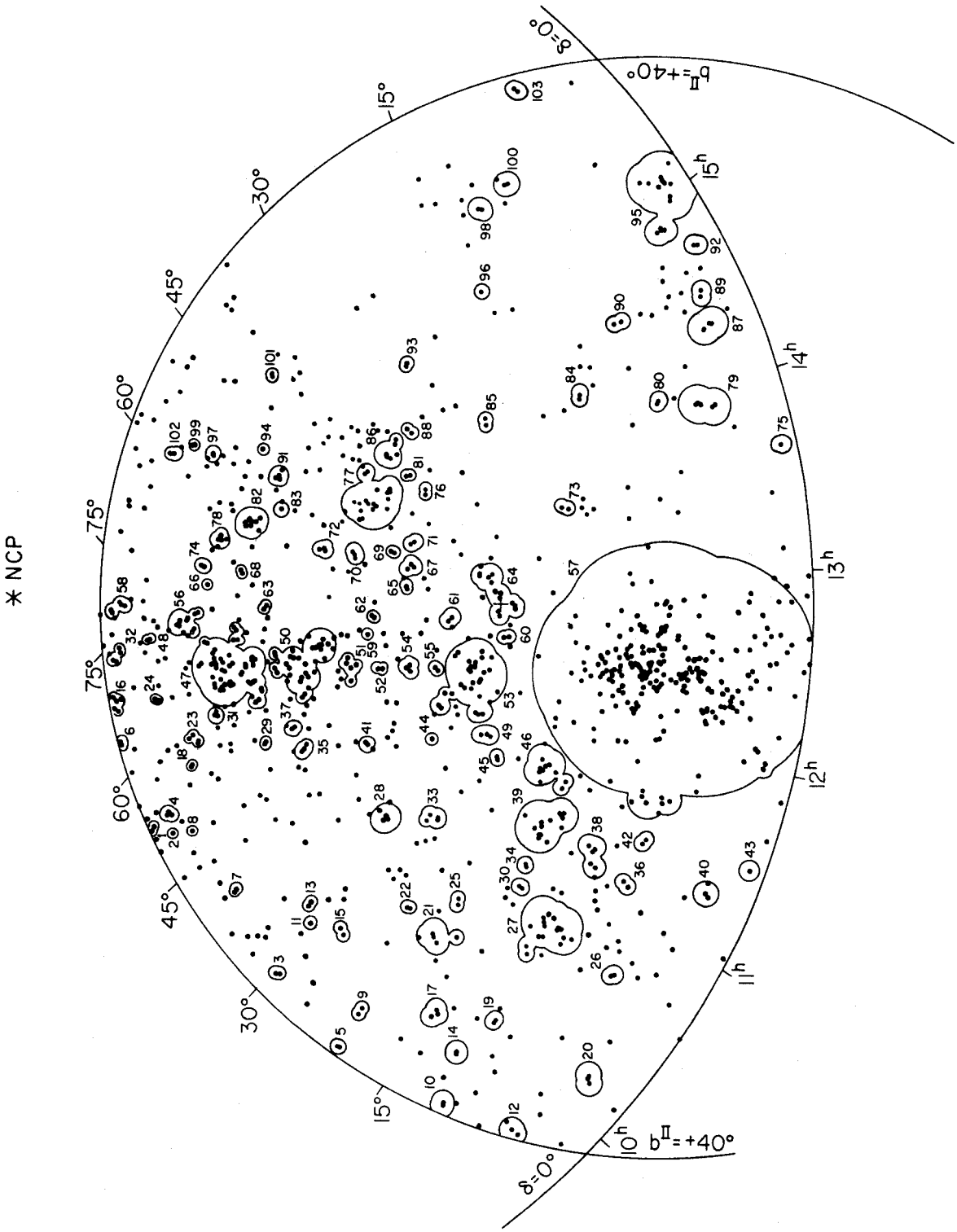
* NCP
δ=0°
15°
30°
45°
60°
75°
15h
14h
13h
12h
11h
10h
b^{II}=+40°

1) It is worth emphasizing again that these groups, defined on the basis of galaxy positions alone, will contain some bogus members as a result of chance projections. On average, about 1/f of the group members should be such foreground and background objects.

2) If all galaxies were characterized by a luminosity function

$$\Phi(L/L^*)d(L/L^*) = \Phi^* (L/L^*)^{-1} e^{-L/L^*} d(L/L^*) \qquad (4)$$

(Schechter 1975, Turner and Gott 1976) where L* is a characteristic luminosity, then a homogeneous spherical group of radius r and volume-density enhancement γ at a distance d would on average give rise to a surface-density enhancement β.

$$\beta = \frac{4}{\Gamma(3/2)} rd^2 \, Ei(d^2) \, (\gamma-1) + 1 \qquad (5)$$

where Ei is the exponential integral and both r and d are measured in units of the distance at which a galaxy of luminosity L* has an apparent magnitude equal to the sample's limiting magnitude (Gott and Turner 1976b). Equation (5) assumes that there is no clustering of group centers. Since the right-hand side of (5) has a maximum at d = 0.66 (corresponding to $\sim$ 60 Mpc for the present sample if $L^* = 3.4 \times 10^{10} L_\odot$) groups at about this distance will be more readily identified than nearer or farther ones.

3) The definition of field galaxies used here is similar but not identical to the definition of "single" galaxies used in Turner and Gott (1975). Having no neighbors within 0?75 is a necessary but not sufficient condition for being a field galaxy, whereas it is both necessary and sufficient to being a "single". In other words, a galaxy with no neighbors within 0?75 can still lie within a group boundary and, thus, be considered a group member.

4) The group identifications and membership assignments generated by the above procedure depend on the somewhat arbitrarily chosen value of f. Clearly, if f is too large, there will be no groups; if it is too small ($\sim$1) there will be only one group containing most or all of the galaxies. Choosing a "correct" value for f is not straightforward; it depends on the desired group properties. For instance, one might wish to set f so that all resulting groups were at least dense enough to be bound, have stopped expanding, be virialized, et cetera. In the present case, $f = 10^{2/3}$ was chosen in order to explore de Vaucouleurs' (1975) suggested definition of a group and in hopes of producing systems in reasonable accord with the usual intuitive identifications. The resulting groups almost all have crossing times considerably shorter than the Hubble

time (Gott and Turner 1976a) and are, therefore, probably bound and relaxed (Gott et al. 1973).

III. GROUP DATA

Table I gives a list of members for each group generated by the procedure described in the last section. Also given are magnitudes, morphological types, and radial velocities for the individual galaxies. The nature, source, and reliability of these data are described below:

Column 1: Identification. The NGC or IC (abbreviated N and I, respectively) number of each galaxy is given, if available. Galaxies without NGC or IC numbers are designated by a Z followed by a 4 to 6 digit number. The 3 least significant digits specify the order of the galaxy in the CGCG field given by the higher order digits (e.g., Z106018 = 18th galaxy in CGCG field No. 106).

Column 2: Apparent magnitude. The CGCG magnitude of the galaxy is listed. These magnitudes have a one standard deviation uncertainty of $\sim$ 0.3 magnitudes and are about $\sim$ 0.35 magnitudes fainter than Holmberg magnitudes (Huchra 1975). Notice that in the case of some very close pairs of galaxies a composite magnitude is given.

Column 3: Morphological type. Simplified morphological types adapted from classifications by Nilson (1973; hereafter UGC) are listed. The simple classification scheme is described in Table II. These classifications, made from an

TABLE I

GROUP CATALOG

(1) ID	(2) MAG	(3) TY	(4) VEL	(1) ID	(2) MAG	(3) TY	(4) VEL
			GROUP 1				
Z264033	13.6	S	0	Z264047	13.7	S	0
			GROUP 2				
N2769	13.8	S	0	N2771	14.0	S	0
			GROUP 3				
N2783	13.9	E	0	N2789	13.8	OS	0
			GROUP 4				
Z264088	14.0	I	0	Z264091	13.4	S	0
N2800	14.0	E	0				
			GROUP 5				
N2804	14.0	O	0	N2809	13.9	O	0
			GROUP 6				
N2805	11.9	S	2023	N2814	14.0	I	1780
N2820	13.1	S	1799				
			GROUP 7				
N2844	13.6	OS	0	N2852	14.0	U	0
			GROUP 8				
N2854	13.8	S	0	N2856	13.9	S	0
			GROUP 9				
N2903	9.8	S	507	N2916	12.3	S	0
			GROUP 10				
N2911	13.6	U	2978	N2914	13.7	S	3208
N2919	13.6	S	0				
			GROUP 11				
N2964	12.0	S	1284	N2968	13.1	I	1552
			GROUP 12				
N2987	13.9	S	0	Z35050	14.0	O	0
N2990	12.5	S	0				
			GROUP 13				
N3003	12.3	S	1429	N3021	12.6	S	1483

TABLE I (CONTINUED)

GROUP CATALOG

(1) ID	(2) MAG	(3) TY	(4) VEL	(1) ID	(2) MAG	(3) TY	(4) VEL
			GROUP 14				
N3016	13.7	S	0	N3020	13.2	S	0
N3024	13.7	S	0				
			GROUP 15				
N3026	13.8	I	0	N3032	13.0	O	1500
			GROUP 16				
N2959	13.7	S	0	N2976	10.9	S	169
N3031	8.1	S	88	N3034	9.2	I	322
N3077	10.7	I	-26				
			GROUP 17				
N3041	13.1	S	0	N3053	13.7	S	0
N3060	13.8	S	0				
			GROUP 18				
N3073	13.8	O	0	N3079	11.2	S	1240
			GROUP 19				
Z64069	14.0	S	0	Z64073	11.3	E	0
			GROUP 20				
N3156	12.8	O	0	N3166	11.2	OS	1200
N3169	11.9	S	1116				
			GROUP 21				
N3162	12.2	S	1361	N3177	12.8	S	1118
N3185	12.9	S	1142	N3187	13.8	S	1491
N3189	11.9	S	1255	N3193	12.4	E	1273
N3226	13.3	E	1232	N3227	12.2	S	1005
			GROUP 22				
N3209	13.9	E	0	Z124004	14.0	U	0
			GROUP 23				
N3182	13.0	OS	0	N3206	12.7	S	1270
N3220	13.7	U	0	N3225	13.3	S	0
			GROUP 24				
N3259	12.9	S	1984	N3266	13.5	O	0

TABLE I (CONTINUED)

GROUP CATALOG

(1) ID	(2) MAG	(3) TY	(4) VEL	(1) ID	(2) MAG	(3) TY	(4) VEL
			GROUP 25				
N3287	12.9	I	0	N3301	12.2	0	1241
			GROUP 26				
N3356	13.3	S	0	N3362	13.6	S	0
			GROUP 27				
Z65058	13.9	I	0	N3300	13.4	0	0
N3338	12.1	S	1202	Z65089	13.8	S	0
N3346	12.8	S	0	N3351	11.2	S	643
N3367	12.0	S	2753	N3368	10.0	S	800
Z66015	14.0	S	0	N3377	10.7	E	593
N3379	9.6	E	746	N3384	10.0	0	636
N3389	12.0	S	1203	N3391	13.5	U	0
N3412	10.8	0	735	N3419	13.4	0	2859
			GROUP 28				
N3395	12.1	S	1622	N3396	12.6	I	1611
N3413	13.1	S	0	N3424	13.2	S	0
N3430	12.2	S	1709	N3442	13.2	U	0
			GROUP 29				
Z241029	13.9	0	0	Z241037	14.0	U	1500
			GROUP 30				
N3455	13.1	S	1006	N3457	13.0	U	0
			GROUP 31				
N3440	14.0	S	0	N3445	12.8	I	2069
N3458	13.2	0	0	N3488	13.7	S	0
			GROUP 32				
N3348	12.0	E	3010	N3364	13.8	S	0
N3403	13.3	S	1403	N3516	12.3	0	2777
N3562	13.2	E	0				
			GROUP 33				
N3486	11.2	S	1067	N3504	11.5	S	1473
N3510	13.6	S	670	N3512	12.9	S	1449
			GROUP 34				
N3501	13.8	S	0	N3507	11.4	S	0

TABLE I (CONTINUED)

GROUP CATALOG

(1) ID	(2) MAG	(3) TY	(4) VEL	(1) ID	(2) MAG	(3) TY	(4) VEL
			GROUP 35				
N3478	13.7	S	0	Z241061	13.4	U	6000
Z241072	13.0	S	0	Z241065	14.0	S	0
			GROUP 36				
I676	13.4	O	0	I2637	13.9	U	0
			GROUP 37				
Z242009	13.6	S	0	N3583	11.6	S	0
N3595	13.0	U	0				
			GROUP 38				
N3559	13.7	S	0	I677	13.6	S	0
N3593	11.8	S	429	N3623	9.6	S	640
N3627	8.9	S	591	N3628	11.5	S	730
			GROUP 39				
N3598	13.5	EO	0	N3599	13.0	EO	0
N3605	12.7	EO	599	N3607	10.2	E	840
N3608	11.7	E	1117	Z96026	13.6	U	0
N3626	11.2	OS	1361	Z96032	14.0	S	0
N3646	11.5	S	4198	N3655	11.6	S	0
N3659	12.7	SI	0	N3681	12.2	S	1220
N3684	12.1	S	1329	N3686	11.6	S	930
N3691	13.1	U	0				
			GROUP 40				
N3630	12.8	OS	0	N3640	11.8	E	1199
N3664	13.6	S	1253				
			GROUP 41				
N3652	12.6	S	0	N3658	13.3	EO	0
N3665	11.6	EO	2010				
			GROUP 42				
N3692	12.9	S	0	N3705	11.5	S	0
			GROUP 43				
N3719	13.8	S	0	N3720	13.7	U	0
			GROUP 44				
N3786	13.5	S	2737	N3788	13.2	S	2327

TABLE I (CONTINUED)

GROUP CATALOG

(1) ID	(2) MAG	(3) TY	(4) VEL	(1) ID	(2) MAG	(3) TY	(4) VEL
			GROUP 45				
N3798	13.9	C	0	N3812	13.9	E	0
			GROUP 46				
Z97C26	13.9	U	0	N3768	13.7	O	0
N3801	13.3	O	0	N3805	13.8	EO	0
N3816	13.6	O	0	N3821	13.8	S	0
N3827	13.6	U	0	N3842	13.3	E	0
N3862	14.0	E	0	N3884	14.0	S	0
			GROUP 47				
N3610	11.4	O	1864	N3613	11.6	EO	2150
N3619	12.6	OS	1744	N3625	13.9	S	0
N3631	11.0	S	1162	N3642	11.9	S	1725
N3656	13.4	U	0	N3657	13.1	U	0
N3669	12.9	I	0	N3674	13.1	O	0
Z291071	14.0	S	0	N3683	12.7	U	0
I694	11.8	U	3212	N3690	11.8	U	3097
Z291C75	12.6	S	0	N3718	11.8	OS	1128
N3725	13.6	S	4500	N3729	12.2	S	0
N3733	13.2	S	0	N3737	13.9	U	0
N3738	11.5	I	0	N3756	12.1	S	0
N3757	13.5	O	0	N3762	13.3	S	0
N3770	13.5	S	0	Z292013	14.0	U	0
N3780	12.2	S	0	N3796	13.4	S	0
N3804	13.8	S	0	N3809	13.6	O	0
N3835	13.0	S	0	N3838	12.7	O	0
Z292026	13.5	U	0	Z292029	13.9	S	0
N3888	12.6	S	2400	Z292030	13.9	U	0
N3894	12.9	O	0	N3895	14.0	S	0
N3898	11.7	S	1135	N3921	13.4	U	6023
N3945	11.6	O	1337	N3958	13.1	S	0
N3963	12.2	S	0	N3972	12.9	S	0
N3978	13.2	S	0	N3982	11.6	S	0
N3990	13.6	O	817	N3998	11.2	O	1177
N4030	11.5	O	1507	N4041	11.6	S	1312
N4149	13.9	S	0	N4161	13.7	S	0
N4290	12.8	S	0	N4335	13.7	E	0
			GROUP 48				
Z334049	13.8	U	0	N3679	13.5	SI	0

TABLE I (CONTINUED)

GROUP CATALOG

(1) ID	(2) MAG	(3) TY	(4) VEL	(1) ID	(2) MAG	(3) TY	(4) VEL
			GROUP 49				
N3900	12.5	S	1666	N3902	14.0	S	0
N3912	13.2	SI	0				
			GROUP 50				
N3769	11.7	S	804	N3811	13.0	S	3000
N3870	13.2	O	660	N3877	11.8	S	0
N3893	10.6	S	1065	N3896	14.0	U	0
N3917	12.5	S	0	N3922	13.8	OS	0
N3928	13.1	U	1500	N3949	10.9	S	743
N3953	10.8	S	1041	Z269018	14.0	S	0
N3985	13.0	S	0	N4010	13.1	SI	0
N4026	11.5	O	956	N4047	12.8	S	0
N4068	13.3	I	0	N4085	12.8	S	0
N4088	11.2	S	812	N4096	11.6	S	0
N4100	11.7	S	0	N4102	11.8	S	985
N4144	12.3	S	0	N4157	11.9	S	0
N4217	12.4	S	0	N4218	13.2	U	0
N4220	12.4	S	1051	N4242	11.9	S	724
N4248	13.9	S	0	N4258	9.6	S	543
N4288	13.6	S	0	N4346	12.3	O	0
N4357	13.5	S	0	N4389	12.8	S	0
			GROUP 51				
I749	13.4	S	0	I750	12.7	S	0
N4111	11.4	O	841	N4138	12.1	O	1090
N4143	12.0	O	830	N4183	13.5	S	0
			GROUP 52				
N4145	12.2	S	0	N4151	11.2	S	989
			GROUP 53				
N3986	14.0	S	0	N3994	13.7	S	3126
N3995	12.9	S	3356	N4004	14.0	U	0
N4008	13.1	EO	0	N4017	13.5	S	0
N4062	11.9	S	0	Z158009	14.0	S	0
N4080	14.0	I	0	N4104	13.7	O	0
N4134	13.8	S	0	N4136	12.1	S	434
N4146	13.8	S	0	N4150	12.6	O	236
N4169	12.9	O	0	N4173	13.7	S	0
N4185	13.5	S	0	N4196	13.7	O	0
N4245	12.4	OS	882	N4251	11.5	O	1000
N4253	13.7	S	0	N4274	11.1	S	761

TABLE I (CONTINUED)

GROUP CATALOG

(1) ID	(2) MAG	(3) TY	(4) VEL	(1) ID	(2) MAG	(3) TY	(4) VEL
N4275	13.4	S	0	N4278	11.2	E	622
N4283	13.1	E	1078	N4310	13.5	S	0
N4314	11.5	S	879	N4359	13.9	S	0
N4375	13.9	S	0	N4393	13.8	S	0
N4414	10.9	S	720	N4448	11.9	S	687
			GROUP 54				
N4163	13.7	I	0	N4190	13.5	I	0
N4214	10.3	I	311				
			GROUP 55				
N4203	11.8	O	1008	N4227	13.8	OS	4820
			GROUP 56				
N4081	13.6	S	0	N4108	13.0	S	0
Z315022	14.0	S	0	N4205	13.8	S	0
N4210	13.4	S	0	N4221	13.6	O	0
N4256	12.7	S	2728	N4332	13.2	S	0
N4391	13.8	O	0	N4441	13.5	U	0
N4521	13.0	OS	0	N4545	13.1	S	0
			GROUP 57				
I719	13.6	O	0	N3810	11.4	S	878
N3822	13.7	O	0	N3825	13.8	S	0
I724	13.8	S	0	N3839	13.6	SI	0
N3863	14.0	S	0	Z68055	13.4	S	0
N3869	13.5	S	0	N3872	12.9	E	3012
N3914	13.8	S	0	N3968	13.3	S	0
N3976	12.8	S	0	N4014	13.5	OS	0
N4032	12.7	I	0	I755	13.9	S	0
N4037	13.8	S	0	N4045	13.5	S	0
Z98035	14.0	U	0	N4058	14.0	S	0
N4067	13.2	S	0	N4065	14.0	E	0
N4064	12.5	S	967	N4073	13.8	E	0
N4078	13.9	O	0	N4116	13.0	S	1175
N4123	13.1	S	0	N4124	12.7	O	0
N4152	12.5	S	0	N4158	13.1	S	0
N4168	12.7	E	0	N4179	12.8	O	1148
N4178	12.9	S	140	N4180	13.2	S	0
N4192	11.0	S	-199	N4191	13.9	O	0
N4193	13.4	S	0	N4189	12.7	S	0
N4197	13.8	S	1927	N4206	13.8	S	0
N4207	13.7	U	0	N4212	11.9	S	2047

TABLE I (CONTINUED)

GROUP CATALOG

(1) ID	(2) MAG	(3) TY	(4) VEL	(1) ID	(2) MAG	(3) TY	(4) VEL
N4215	13.0	OS	0	N4216	11.2	S	-43
N4224	13.3	S	0	N4234	13.4	I	2024
N4235	13.2	S	0	N4233	13.2	O	0
N4237	12.3	S	0	N4239	13.5	E	0
N4241	13.6	O	0	N4246	14.0	S	0
N4254	10.2	S	2397	N4255	13.5	O	0
N4261	12.0	E	2093	N4260	13.1	S	1827
N4264	13.9	O	0	N4262	12.3	O	1280
N4268	13.9	OS	0	N4269	13.9	OS	0
N4267	12.4	O	1180	N4270	13.3	O	2237
N4273	12.3	S	2192	N4281	12.5	O	2492
N4293	11.6	OS	695	N4294	12.6	S	306
N4298	12.2	S	0	N4300	13.9	S	0
N4299	12.8	I	103	N4302	13.4	S	0
N4303	10.9	S	1559	N4307	13.4	S	0
N4305	13.8	S	0	N4312	12.9	S	0
N4313	13.2	S	0	N4316	14.0	S	0
N4321	10.6	S	1552	N4324	12.5	O	1605
N4330	14.0	S	0	N4339	13.1	E	1173
N4336	13.6	OS	0	N4343	13.5	S	0
N4342	13.0	S	613	N4340	12.4	O	0
N4344	13.7	O	0	N4350	11.5	O	1123
N4352	14.0	O	0	N4351	13.5	S	0
N4360	13.9	E	0	N4365	11.5	E	1083
N4371	12.1	O	896	N4374	10.8	O	878
N4378	13.2	S	0	N4376	13.9	I	0
N4377	12.5	O	1270	N4379	12.6	O	0
N4380	13.4	S	0	N4383	12.3	U	0
N4382	10.2	O	712	N4385	13.4	O	1225
N4387	13.2	E	435	N4390	13.7	S	0
N4388	12.2	S	0	N4394	11.9	S	719
N4396	13.7	S	0	N4402	13.6	S	0
N4405	12.9	OS	0	N4406	10.9	E	-367
N4410	13.6	U	0	N4412	13.2	S	0
N4413	13.6	S	0	N4416	13.5	S	0
N4417	12.2	O	0	N4420	12.7	S	0
N4419	11.6	S	0	N4421	12.9	OS	1628
N4424	13.1	S	0	N4425	13.3	OS	1808
N4430	13.4	S	0	N4429	11.4	O	1032
N4434	13.2	E	0	N4438	12.0	S	-105
N4435	11.9	O	796	N4440	13.0	S	0
N4442	11.2	O	493	N4445	13.7	S	0
N4450	11.2	S	1994	I3391	13.9	S	0

TABLE I (CONTINUED)

GROUP CATALOG

(1) ID	(2) MAG	(3) TY	(4) VEL	(1) ID	(2) MAG	(3) TY	(4) VEL
N4451	13.4	U	0	N4452	13.1	O	0
I3392	13.3	S	0	N4455	13.0	SI	0
N4457	11.9	OS	627	N4458	13.3	E	311
N4461	12.2	O	1815	N4459	11.6	O	1042
N4464	13.5	S	1106	N4469	12.6	OS	0
I796	13.9	OS	0	N4470	12.9	S	0
N4472	10.2	E	855	N4473	11.2	E	2171
N4474	12.6	O	1459	N4476	13.3	O	0
N4477	11.9	O	1194	N4478	12.2	E	1407
N4479	13.9	O	753	N4480	13.4	S	0
N4483	13.4	O	0	N4488	13.8	S	0
N4486	10.4	E	1187	N4489	13.2	E	0
N4491	13.7	U	0	Z70141	11.2	E	0
N4497	13.8	O	0	N4496	13.3	S	1775
N4498	12.8	S	0	N4501	10.6	S	2056
I797	13.9	S	0	N4503	12.4	O	0
N4517	12.4	S	1095	I3476	13.5	I	0
N4515	13.3	EO	0	N4516	13.9	S	0
N4519	12.8	S	1125	N4522	13.6	S	0
N4526	10.6	O	396	N4527	12.4	S	1616
N4528	12.9	O	0	N4532	12.3	I	2058
N4535	11.1	S	1854	N4531	13.3	O	0
N4536	12.3	S	1814	N4539	13.5	OS	0
N4540	12.5	S	0	N4541	14.0	S	0
N4548	11.5	S	371	N4550	12.5	O	279
N4551	13.1	E	907	N4552	11.1	E	195
N4561	12.7	S	0	N4564	12.2	E	941
N4568	12.5	S	2204	N4567	12.5	S	2179
N4570	11.8	O	1639	N4569	11.8	S	-367
N4571	13.6	S	0	N4578	12.9	O	2201
N4580	13.1	S	0	N4579	11.5	S	1680
N4581	13.4	E	0	N4586	13.5	S	0
N4595	12.8	S	0	N4596	12.4	O	0
N4600	13.7	O	0	N4599	13.7	S	0
N4606	12.7	S	0	N4608	12.6	O	0
N4612	12.9	O	0	N4621	11.0	E	345
N4620	14.0	O	0	N4623	13.6	OS	0
N4632	12.6	S	1572	N4630	13.4	I	0
N4634	13.6	S	0	N4635	13.7	S	0
N4636	11.8	E	778	N4638	12.2	O	1010
N4639	12.4	S	0	N4643	11.9	O	1325
N4647	12.5	S	1328	N4649	10.3	E	1200
N4651	11.3	S	685	N4654	11.8	S	960

TABLE I (CONTINUED)

GROUP CATALOG

(1) ID	(2) MAG	(3) TY	(4) VEL	(1) ID	(2) MAG	(3) TY	(4) VEL
N4660	12.1	E	948	N4659	13.3	OS	0
N4665	12.4	O	684	N4685	13.8	EO	0
N4689	12.8	S	0	N4694	12.4	O	0
N4698	12.1	S	955	N4701	13.1	S	0
N4710	11.6	OS	1076	N4713	12.3	S	575
N4733	13.2	E	0	N4746	13.3	S	0
N4754	11.6	O	1398	N4762	11.1	O	876
N4765	13.0	U	0	N4771	13.3	S	0
N4772	12.9	S	0	N4779	13.5	S	0
N4795	13.5	OS	0	N4808	12.5	S	650
N4866	11.9	S	1864	N4880	13.3	O	0
N4935	13.9	S	0	N5020	13.4	S	0
			GROUP 58				
N4133	13.1	S	0	N4291	12.3	E	1994
N4319	13.0	S	1878	N4386	12.6	O	1990
Z335017	13.5	E	0	N4589	12.0	E	2003
N4648	12.6	E	0				
			GROUP 59				
N4485	12.4	I	848	N4490	10.1	S	622
			GROUP 60				
N4555	13.5	E	0	N4565	10.3	S	1171
			GROUP 61				
Z155039	14.0	S	0	N4627	13.3	E	0
N4631	9.8	S	646	N4656	10.6	S	775
			GROUP 62				
N4618	11.5	S	618	N4625	13.0	S	0
			GROUP 63				
N4646	13.8	U	0	N4686	13.7	S	0
			GROUP 64				
N4670	12.6	U	1209	N4673	13.7	O	6990
N4692	14.0	EO	7912	N4712	13.5	S	0
N4725	10.2	S	1109	N4747	13.2	I	0
N4789	13.3	EO	8377	N4819	14.0	S	6702
N4839	13.6	E	7455	N4921	13.7	S	5472
N4944	13.3	S	7009	N4952	13.6	E	5886
N4961	13.5	S	2574	N4966	13.9	S	0

TABLE I (CONTINUED)

GROUP CATALOG

(1) ID	(2) MAG	(3) TY	(4) VEL	(1) ID	(2) MAG	(3) TY	(4) VEL
N5000	14.0	S	0				
			GROUP 65				
N4868	12.9	S	0	N4914	12.7	E	0
			GROUP 66				
Z316C11	13.8	OS	0	Z316012	13.7	S	0
			GROUP 67				
N5005	10.6	S	1078	N5014	13.5	S	0
N5033	10.9	S	956				
			GROUP 68				
I875	13.9	O	0	N5109	13.6	S	0
			GROUP 69				
N5107	13.7	U	0	N5112	12.5	S	0
			GROUP 70				
N5103	13.6	U	0	N5123	13.5	S	0
N5145	13.6	S	0				
			GROUP 71				
N5141	13.9	O	0	N5142	14.0	O	0
N5149	13.8	S	0				
			GROUP 72				
N5173	13.5	E	2508	N5194	8.8	S	552
N5195	10.6	I	634	N5198	13.2	E	2605
			GROUP 73				
Z101C61	14.0	I	0	Z102004	13.8	S	0
			GROUP 74				
N5205	13.5	S	0	N5216	14.0	U	0
N5218	13.1	S	0				
			GROUP 75				
N5257	13.7	S	6744	N5258	13.8	S	6569
			GROUP 76				
N5318	13.5	O	0	N5347	13.3	S	0

TABLE I (CONTINUED)

GROUP CATALOG

(1) ID	(2) MAG	(3) TY	(4) VEL	(1) ID	(2) MAG	(3) TY	(4) VEL
			GROUP 77				
N5289	13.5	S	0	N5290	13.0	S	0
N5303	12.9	U	0	N5311	13.7	U	0
N5313	12.4	S	0	N5320	13.1	S	0
N5326	12.9	S	0	N5336	13.6	S	0
N5337	13.4	S	0	N5351	13.1	S	0
N5330	12.4	S	0	N5353	11.8	U	2285
N5354	12.3	U	0	N5355	14.0	U	0
N5362	13.2	S	0	N5371	11.5	S	2682
N5378	13.8	S	0	N5380	13.5	U	0
N5383	12.5	S	2369	N5394	13.7	S	3648
N5395	12.6	S	0	N5406	13.1	S	0
Z215C56	13.9	S	0	N5515	13.7	S	0
N5541	13.4	S	0				
			GROUP 78				
N5322	11.3	E	2061	N5372	13.7	U	0
N5376	12.9	S	0	N5389	13.2	U	0
N5430	12.7	S	0				
			GROUP 79				
N5363	11.4	I	1103	N5364	13.2	S	1359
N5374	13.7	S	0	N5382	14.0	U	0
N5384	14.0	U	0	N5386	13.7	US	0
			GROUP 80				
N5416	13.6	S	0	N5423	13.9	EU	0
			GROUP 81				
N5440	13.4	S	0	N5444	12.8	E	0
			GROUP 82				
N5368	13.8	S	0	N5422	13.1	US	0
N5443	13.2	S	0	N5457	8.7	S	415
N5473	12.5	U	2195	N5474	11.9	S	395
N5475	13.4	S	0	N5485	12.4	U	2137
N5486	14.0	SI	0				
			GROUP 83				
N5480	12.6	S	1859	N5481	13.5	E	2165
N5520	13.3	S	0				

TABLE I (CONTINUED)

GROUP CATALOG

(1) ID	(2) MAG	(3) TY	(4) VEL	(1) ID	(2) MAG	(3) TY	(4) VEL
			GROUP 84				
N5504	13.9	S	0	Z105123	14.0	S	0
			GROUP 85				
N5523	13.4	S	0	N5548	13.1	S	4990
			GROUP 86				
N5529	12.9	S	3879	N5533	13.0	S	0
N5544	13.2	S	3265	N5545	13.2	S	3275
N5557	12.2	E	3296	N5590	13.6	U	0
N5614	12.6	S	3971				
			GROUP 87				
N5560	13.7	S	0	N5566	12.0	S	1581
N5574	13.4	U	1694	N5576	12.3	E	1507
N5577	13.6	S	0				
			GROUP 88				
N5611	13.5	U	0	N5623	13.7	E	0
			GROUP 89				
N5638	12.5	E	1663	I1024	14.0	U	0
			GROUP 90				
N5669	13.2	S	0	N5666	13.5	U	0
			GROUP 91				
N5660	12.2	S	0	N5673	14.0	S	0
I1029	13.7	S	0	N5676	11.7	S	2395
N5689	12.7	S	2355				
			GROUP 92				
N5740	13.2	S	0	N5746	12.3	S	1826
			GROUP 93				
N5789	13.9	S	0	N5798	13.5	I	0
			GROUP 94				
N5797	13.6	US	0	N5804	14.0	S	0
			GROUP 95				
I1067	13.6	S	0	N5770	13.3	U	0
N5774	13.9	S	1534	N5775	13.0	S	1574

TABLE I (CONTINUED)

GROUP CATALOG

(1) ID	(2) MAG	(3) TY	(4) VEL	(1) ID	(2) MAG	(3) TY	(4) VEL
N5806	12.9	S	1309	N5813	12.5	E	1891
N5831	13.1	E	1693	N5838	12.1	O	1441
N5839	13.9	O	0	N5845	13.8	E	0
N5846	11.9	E	1784	Z20061	11.9	E	2304
N5850	13.6	S	2385	N5854	13.1	O	1644
N5864	12.9	O	1639	N5865	13.5	O	0
			GROUP 96				
N5857	13.6	S	4785	N5859	13.1	S	4745
			GROUP 97				
N5905	13.6	S	0	N5906	11.4	S	725
N5908	13.5	S	0				
			GROUP 98				
N5951	13.8	S	0	N5953	12.7	O	2188
N5954	12.7	S	2228				
			GROUP 99				
N5963	13.0	S	0	N5965	13.4	S	0
			GROUP 100				
N5956	13.3	S	0	N5957	13.3	S	0
N5970	12.2	S	2136				
			GROUP 101				
I4562	13.8	E	6036	I4567	13.5	S	0
			GROUP 102				
N5982	12.4	E	3072	N5985	12.0	S	2673
N5989	13.6	S	0				
			GROUP 103				
N6014	13.8	O	0	N6017	13.8	U	0

TABLE I NOTES

In the notes listed below, "UGC" indicates that part or all of the group is identified by Nilson (1973), and "dV" followed by a number indicates that the group is similar to one of de Vaucouleurs' (1975) groups. NGC and IC numbers indicate possible additional group members. A "K" indicates that Kirshner (1975) has obtained new, and, as yet, unpublished redshifts for some or all of the group's members.

2 - UGC

3 - UGC

5 - UGC

6 - UGC, IC 2458, interation

7 - UGC, NGC 2853

8 - UGC, Arp 285, interaction

10 - UGC, Arp 137 and Arp 232

11 - UGC, NGC 2970

12 - NGC 2990 foreground?

14 - UGC, NGC 3019, K

16 - UGC, dV2, M81 group, NGC 3959, NGC 3961

18 - UGC

19 - Z64073 = Regulus system, foreground

20 - UGC, interaction

21 - UGC, dV47, odd distribution of velocities

22 - UGC

23 - NGC 3214

25 - UGC

26 - UGC

27 - UGC, dV11, Leo group plus background objects, clumpy

28 - UGC, dV43, interaction

30 - NGC 3454

31 - UGC, dV28, interaction

32 - NGC 3403 foreground

33 - two pairs projected together

34 - UGC

37 - NGC 3677

38 - dV9, Leo group

39 - UGC, dV 49, NGC 3592, NGC 3649, NGC 3646 background and overluminous?

40 - UGC, NGC 3641

42 - UGC

43 - UGC

44 - UGC, interaction

45 - UGC, NGC 3815

46 - UGC, Abell 1367, NGC 3764, NGC 3832, NGC 3837, IC 2955, IC 732, NGC 3768 and NGC 3801 a separate pair?, K

47 - UGC, dV34, may consist of several sub-systems at different distances, part of Ursa Major cloud

50 - UGC, dV32, part of Ursa Major cloud, several background members

52 - UGC, dV17

53 - UGC, contains NGC 3995 group in the background

55 - projected pair, large velocity difference

56 - UGC, NGC 4512, K

57 - UGC, Virgo cluster, dV18, dV19, dV25, dV26, dV46, includes a number of foreground and background groups

58 - UGC

59 - UGC, interaction

61 - UGC, dV10, NGC 4657, possibly two pairs projected together

62 - UGC, IC 3675

63 - UGC

64 - UGC, the brighter galaxies of the Coma cluster, NGC 4670, 4725, and 4961 are foreground; due to an error in the CGCG magnetic tape, three bright Coma galaxies were omitted.

65 - UGC

67 - UGC

71 - UGC

72 - UGC, two pairs projected together, interaction

74 - UGC, interaction

75 - UGC, interaction

76 - UGC

77 - UGC, probably two groups projected together, K

78 - NGC 5379, K

79 - UGC, two groups projected together?, subclumps

81 - UGC

82 - two groups superimposed

83 - UGC

84 - UGC

86 - UGC, NGC 5589, NGC 5613, NGC 5615, interaction

87 - UGC

89 - UGC

91 - UGC, dV37, K

92 - UGC

93 - UGC

95 - UGC, dV50, NGC 5868, IC 1066

96 - UGC

97 - UGC, NGC 5906 probably foreground, K

98 - UGC, interaction

100 - NGC 5970 may be foreground

101 - UGC

102 - UGC

TABLE II

MORPHOLOGICAL TYPE NOTATION

	Type	Table I Abbreviation
Early	Elliptical	E
		EO*
	Lenticular (SO)	O
		OS*
	Spiral/Barred Spiral	S
		SI*
Late	Irregular	I
	Peculiar or Unclassified	U

*Intermediate or uncertain.

inspection of Palomar Sky Survey prints, vary from reliable to rather tentative.

Column 4: Radial velocity. A radial velocity corrected to the Local Group rest frame is given, if available. These velocities are taken from the literature survey reported in the UGC. Their accuracy varies widely, but a typical uncertainty might be $\sim$ 100 km s^{-1}. In addition to those listed, velocities in several of the groups have been obtained recently by Kirshner (1975) (see Notes section).

Notes: These comments contain a variety of additional information on the individual groups and galaxies calling particular attention to cases of apparent foreground-background contamination.

General properties and parameters of the groups are listed in Table III and described below:

Column 1: Identification. Group numbers corresponding to those used in Table I are given.

Column 2: Position. The mean right ascension and declination (1950) of the galaxies in each group is listed.

Column 3: Number of members. The number of galaxies assigned to each group is tabulated.

Column 4: Number of velocities. The number of galaxies in group with UGC velocities is given.

Column 5: Angular size. The luminosity weighted mean harmonic angular size ϕ of the group is calculated by

TABLE III

GROUP PARAMETERS

(1) Group	(2) Position h^{α} m $^{\circ}\delta$ '	(3) No. of Members	(4) No. of Velocities	(5) Angular Size ϕ	(6) m_{TOT}	(7) $\bar{v}$	(8) σ_v	(9) Faint Members	(10) Rating
1	8 55 52 30	2	0	2.72	12.9	...	...	S	1
2	9 07 50 37	2	0	0.23	13.1	...	...	F	1
3	9 11 30 03	2	0	1.58	13.1	...	...	S	1
4	9 14 52 59	3	0	1.20	12.6	...	...	S	1
5	9 14 20 20	2	0	0.58	13.2	...	...	M	1
6	9 17 64 25	3	3	0.78	11.5	1949	108	S	1
7	9 19 40 22	2	0	1.10	13.0	...	...	S	1
8	9 21 49 26	2	0	0.19	13.1	...	...	S	1
9	9 31 21 50	2	1	7.91	9.7	507	...	F	1
10	9 32 10 24	3	2	0.48	12.4	3088	115	S	1
11	9 40 32 07	2	2	0.59	11.7	1355	118	S	1
12	9 43 5 14	3	0	3.45	12.0	...	...	F	2
13	9 47 33 43	2	2	2.11	11.7	1452	27	N	1
14	9 47 12 59	3	0	0.41	12.3	...	...	S	1
15	9 49 29 07	2	1	3.37	12.6	1500	...	N	1
16	9 49 69 02	5	4	2.91	7.6	141	106	F	1
17	9 52 16 53	3	0	1.95	12.3	...	...	S	1
18	9 58 55 53	2	1	2.28	11.1	1240	...	S	1
19	10 05 12 32	2	0	3.46	11.2	...	...	S	4
20	10 11 3 35	3	2	0.74	10.6	1171	40	S	1
21	10 16 21 37	8	8	0.90	10.3	1217	128	S	2

TABLE III (Cont'd)

(1) Group	(2) Position h^{α} m $^{\circ}\delta$ '	(3) No. of Members	(4) No. of Velocities	(5) Angular Size ϕ	(6) m_{TOT}	(7) $\bar{v}$	(8) σ_v	(9) Faint Members	(10) Rating
22	10 18 25 41	2	0	0.59	13.2	...	...	S	1
23	10 19 57 50	4	1	2.12	11.6	1270	...	S	1
24	10 29 65 10	2	1	1.34	12.4	1984	...	S	1
25	10 33 22 02	2	1	2.48	11.7	1241	...	N	1
26	10 42 6 56	2	0	0.86	12.7	...	...	F	1
27	10 43 13 29	16	10	1.29	8.1	817	413	S	3
28	10 49 33 20	6	3	0.48	10.7	1650	44	S	1
29	10 52 49 57	2	1	0.69	13.2	1500	...	M	1
30	10 52 17 43	2	1	1.34	12.3	1006	...	M	1
31	10 53 57 30	4	1	1.00	11.8	2069	...	F	1
32	10 54 73 08	5	3	2.93	11.0	2689	543	S	3
33	11 00 28 44	4	4	2.31	10.4	1233	236	S	2
34	11 00 18 19	2	0	2.33	11.3	...	...	F	1
35	11 01 45 40	4	1	2.18	12.0	6000	...	M	1
36	11 11 9 36	2	0	2.56	12.9	...	...	N	1
37	11 12 48 04	3	0	3.18	11.2	...	...	M	1
38	11 14 13 04	6	4	1.54	8.3	607	51	S	1
39	11 19 18 08	15	8	1.48	8.9	1380	1031	S	2
40	11 19 3 26	3	2	1.72	11.3	1208	20	M	1
41	11 21 38 38	3	1	1.96	11.1	2010	...	S	1
42	11 27 9 36	2	0	2.68	11.2	...	...	M	1
43	11 30 1 05	2	0	0.14	13.0	...	...	F	1
44	11 37 32 12	2	2	0.21	12.6	2504	203	F	1
45	11 38 25 03	2	0	1.01	13.1	...	...	S	1

TABLE III (Cont'd)

(1) Group	(2) Position h^{α} m $^{\circ}\delta$ '	(3) No. of Members	(4) No. of Velocities	(5) Angular Size ϕ	(6) m_{TOT}	(7) $\bar{v}$	(8) σ_v	(9) Faint Members	(10) Rating
46	11 39 19 47	10	0	2.35	11.2	...	...	M	2
47	11 39 57 54	54	17	4.49	8.1	1762	872	S	2
48	11 43 69 50	2	0	1.66	12.9	...	...	N	1
49	11 47 26 49	3	1	2.13	11.9	1666	...	S	1
50	12 01 49 04	34	13	5.56	8.0	831	343	S	2
51	12 04 43 20	6	3	2.11	10.3	900	110	M	1
52	12 08 39 55	2	1	2.45	10.8	989	...	M	1
53	12 10 29 38	32	12	3.28	8.8	851	553	S	2
54	12 11 36 40	3	1	6.93	10.2	311	...	S	1
55	12 13 33 38	2	2	3.83	11.6	1530	1310	S	4
56	12 17 65 19	12	1	2.81	10.6	2728	...	S	1
57	12 24 10 52	238	94	7.32	6.4	1106	700	M	2
58	12 25 75 04	7	4	1.50	10.5	1980	42	S	1
59	12 28 41 57	2	2	0.65	10.0	646	70	S	1
60	12 33 26 31	2	1	11.97	10.2	1171	...	M	1
61	12 39 32 37	4	2	1.43	9.3	688	60	F	2
62	12 39 41 30	2	1	1.01	11.3	618	...	S	1
63	12 42 54 58	2	0	2.50	13.0	...	...	M	1
64	12 54 27 38	15	11	3.69	9.6	2513	2506	M	3
65	12 58 37 34	2	0	1.28	12.0	...	...	N	1
66	13 07 62 34	2	0	0.21	13.0	...	...	S	1
67	13 10 36 54	3	2	2.62	9.9	1025	60	S	1
68	13 17 57 52	2	0	2.12	13.0	...	...	S	1
69	13 19 38 54	2	0	1.25	12.2	...	...	N	1
70	13 21 43 23	3	0	1.59	12.4	...	...	S	1

TABLE III (Cont'd)

(1) Group	(2) Position h^{α} m ° δ '	(3) No. of Members	(4) No. of Velocities	(5) Angular Size ϕ	(6) m_{TOT}	(7) $\bar{v}$	(8) σ_v	(9) Faint Members	(10) Rating
71	13 23 36 30	3	0	0.48	12.7	...	...	S	1
72	13 28 47 11	4	4	0.54	8.6	615	314	S	4
73	13 29 19 58	2	0	2.39	13.1	...	...	N	1
74	13 30 62 55	3	0	0.53	12.3	...	...	S	1
75	13 37 1 05	2	2	0.11	13.0	6661	88	N	1
76	13 50 33 51	2	0	2.48	12.6	...	...	S	1
77	13 53 40 05	25	4	0.80	9.4	2552	326	M	2
78	13 54 59 44	5	1	3.13	10.7	2061	...	S	1
79	13 55 6 10	6	2	1.63	10.9	1144	94	S	3
80	14 00 9 38	2	0	0.72	13.0	...	...	M	1
81	14 01 35 11	2	0	1.68	12.3	...	...	S	1
82	14 02 55 08	9	4	6.01	8.5	513	405	S	4
83	14 07 50 51	3	2	0.48	11.9	1952	141	F	1
84	14 11 15 58	2	0	2.05	13.2	...	...	M	1
85	14 14 25 28	2	1	2.93	12.5	4990	...	S	1
86	14 16 36 07	7	5	1.24	10.8	3546	319	S	1
87	14 18 3 48	5	3	0.56	11.0	1569	60	S	1
88	14 24 33 22	2	0	2.68	12.8	...	...	S	1
89	14 28 3 20	2	1	2.98	12.3	1663	...	M	1
90	14 30 10 25	2	0	2.56	12.6	...	...	S	1
91	14 31 49 45	5	2	1.74	10.8	2384	18	F	1
92	14 42 2 02	2	1	1.48	11.9	1826	...	S	1
93	14 55 30 17	2	0	1.44	12.9	...	...	F	1
94	14 55 49 53	2	0	0.49	13.0	...	...	M	1

TABLE III (Cont'd)

(1) Group	(2) Position h^{α} m $^{\circ}\delta$ '	(3) No. of Members	(4) No. of Velocities	(5) Angular Size ϕ	(6) m_{TOT}	(7) $\bar{v}$	(8) σ_v	(9) Faint Members	(10) Rating
95	15 00 2 24	16	11	0.77	9.8	1781	323	S	1
96	15 05 19 46	2	2	0.12	12.6	4760	20	F	1
97	15 15 55 56	3	1	4.00	11.1	725	...	F	2
98	15 32 15 17	3	2	0.10	11.8	2208	20	S	1
99	15 33 56 49	2	0	0.59	12.4	...	...	S	1
100	15 34 12 10	3	1	2.34	11.6	2136	...	S	2
101	15 35 43 34	2	1	1.17	12.9	6036	...	S	1
102	15 39 59 39	3	2	0.61	11.3	2836	196	S	1
103	15 54 6 06	2	0	1.41	13.0	...	...	N	1

$$\phi = \left(\sum \ell_i\right)^2 \left(\sum_{i \neq j} \ell_i \ell_j / \theta_{ij}\right)^{-1} \qquad (6)$$

where

$$\ell_i = 10^{-0.4 m_i} \qquad (7)$$

m_i is the apparent magnitude of the i th group member, θ_{ij} is the angular separation between the i th and j th members, the first sum in (6) is over the group members, and the second is over all pairs of members.

Column 6: Total magnitude. The total flux from the galaxies in the group is expressed as a magnitude m_{TOT} where

$$m_{TOT} = -2.5 \log \left(\sum \ell_i\right) \qquad (8)$$

Column 7: Mean radial velocity. For groups in which one or more members have radial velocities v_i, the luminosity weighted mean is

$$\bar{v} = \sum \ell_i v_i / \sum \ell_i \qquad (9)$$

where the sums are only over the members with velocities.

Column 8: Velocity dispersion. For groups with 2 or more velocities, the luminosity weighted velocity dispersion is given by

$$\sigma_v = \left(\sum \ell_i (v_i - \bar{v})^2 / \sum \ell_i\right)^{1/2} \qquad (10)$$

with sums over the members with velocities. The usually small values of σ_v are a good confirmation of the general validity of our group identification procedure.

Column 9: Faint members. Although these groups were chosen solely from galaxies with $m_{pg} \leq 14.0$, the CGCG extends to $m_{pg} \approx 15.7$. The distribution of galaxies with $14.0 < m_{pg} \leq 15.7$ in the CGCG was compared to the group boundaries generated in §II, and each group was classified according to the number of faint galaxies within the boundaries. The classification scheme is described in Table IV.

Column 10: Contamination rating. Each group has been assigned a number from 1 to 4 intended to reflect the apparent degree of contamination by foregound and background galaxies. A group which shows no evidence of contamination is rated 1. Groups which show evidence for some contamination but which are probably not dominated by projected members, are assigned a rating of 2. A rating of 3 indicates that although some physical association probably exists, the system is dominated by foreground or background objects. Groups rated 4 are nearly completely the result of chance projections. These ratings are based on a subjective appraisal of a variety of data including the group's appearance in the sky, the distribution of apparent magnitudes, the distribution of members' radial velocities, and so on. The explanation for high ratings can generally be found in the Notes section of Table I. It is worth emphasizing that in addition to being subjective, these ratings depend on the amount of data available for each particular group. Clearly,

TABLE IV

FAINT MEMBER CLASSIFICATION

Abbreviation	Meaning	$N(m_{pg} \leq 14)/N(m_{pg} > 14)$
N	None	$>> 1$
F	Few	$\gtrsim 1$
S	Some	< 1
M	Many	$<< 1$

foregound and background objects are most easily identified in the groups possessing the most velocity data.

IV. FIELD GALAXY DATA

Table V gives data for the galaxies which were not assigned to groups; the data are exactly like those given for the group galaxies in Table I.

The assignment of a galaxy to the field is probably less reliable than a group membership assignment. It is possible to miss a group either because it is too nearby (large angular separations between members) or because it is too distant (all but brightest member beyond the magnitude cutoff). Those galaxies in Table V which are suspected of actually being group members for one of the above reasons are marked with an asterisk; these suspicions are based on a subjective appraisal of available data similar to that which gave rise to the ratings in column 10 of Table III.

The truly isolated galaxies listed in Table V are an interesting and probably insufficiently studied class of objects (Turner and Gott 1975, Karachentseva 1973). It is hoped that this list will prompt investigations of some of these systems.

V. DISCUSSION

An inspection of Tables I and V reveals a need for a great deal of observational work on both the groups and the field galaxies. Particularly pressing is the need for more

TABLE V

FIELD GALAXIES

(1) ID	(2) MAG	(3) TY	(4) VEL	(1) ID	(2) MAG	(3) TY	(4) VEL
N2684	13.4	U	0	N2693	13.1	E	4998
N2701	12.3	S	0	N2710	13.8	S	0
N2712	12.3	S	1649	Z264057	13.6	S	0
Z180031	14.0	0	0	N2756	13.2	S	0
N2770	12.1	S	0	N2768*	11.1	E0	1495
N2776	12.1	S	2682	N2778*	13.1	E	0
N2782	12.3	S	2514	Z238024	14.0	S	0
N2793	13.9	S	1623	Z121049	14.0	0	0
N2798*	12.9	S	1702	N2832*	13.3	E	6897
N2841	9.9	S	671	Z238045	14.0	SI	0
N2859*	11.8	0	1649	N2862	13.8	S	0
N2870	13.9	S	0	N2880*	12.6	0	1614
N2893*	13.6	S	0	N2918	13.6	E	0
N2939*	13.5	S	0	N2943*	14.0	E	0
N2948	13.8	S	0	Z239019	13.5	U	0
N2954	13.5	E	0	N2958	13.9	S	0
N2955	13.9	S	0	N2950	11.8	0	1475
Z63058	13.8	S	0	Z265042	14.0	S	0
N2998*	13.3	S	0	N3044	12.4	S	1132
N3049	13.5	S	0	N3043	13.3	S	0
N3055	12.3	S	1730	N3070	13.2	E	0
N3067*	12.7	S	1455	Z36012	12.2	I	0
N3094	13.5	S	0	N3098	13.0	OS	0
N3106	14.0	0	0	Z64048	13.6	U	0
Z290008	13.6	U	0	N3111	14.0	E0	0
Z64068	13.5	I	0	Z266024	13.8	S	0
Z266025	13.9	S	0	N3126	13.5	S	0
N3131	14.0	S	0	Z93068	14.0	S	0
Z8063	14.0	S	0	I598	13.8	OS	0
N3153*	13.6	S	0	N3158*	13.4	E	7009
N3184*	10.4	S	418	I602*	13.4	S	0
N3191*	13.9	S	0	N3198*	10.7	S	670
N3239	13.5	I	761	N3246	13.8	S	0
N3245*	11.6	0	1198	I2574	11.2	S	179
N3248	13.9	0	0	N3254*	12.4	S	1170

TABLE V (CONTINUED)

FIELD GALAXIES

(1) ID	(2) MAG	(3) TY	(4) VEL	(1) ID	(2) MAG	(3) TY	(4) VEL
Z266C55	13.2	U	1680	N3274*	13.3	I	0
N3277*	12.3	S	1399	Z266059	14.0	OS	0
N3294	11.5	S	1453	N3306*	13.7	S	0
N3310*	11.0	S	1090	N3319*	12.0	S	832
N3320	13.1	S	0	N3325*	14.0	E	0
N3332	13.7	O	0	Z212042	14.0	S	0
N3344	11.1	S	504	N3353	12.9	U	1098
N3359	11.0	S	1120	N3365	13.6	S	0
N3370	12.4	S	1290	I642	14.0	U	0
N3380*	13.6	S	0	N3385*	13.7	O	0
N3381	12.8	S	0	N3394*	13.1	S	0
Z241022	13.2	U	1800	N3414*	12.1	O	1391
N3423	12.1	S	0	N3427	14.0	OS	0
N3415*	13.2	OS	0	N3406*	13.7	U	0
N3426	13.9	U	0	N3434*	13.4	S	0
N3433*	13.6	S	0	N3432*	11.7	S	594
N3441	13.9	S	0	N3437	12.6	S	0
N3451	13.5	S	0	N3448*	12.2	I	1476
N3462	13.4	O	0	Z66076	13.7	U	0
N3471*	13.0	S	3500	Z184041	13.3	U	0
N3485*	12.8	S	0	N3489*	10.9	O	570
N3492*	14.0	U	0	N3495	13.1	S	831
N3523*	13.8	S	0	N3506*	12.9	S	0
Z184050	13.1	U	0	N3509	14.0	S	7443
N3517*	13.8	S	0	N3521	10.1	S	614
N3524*	13.4	OS	0	N3526	13.7	S	0
N3547*	12.8	S	0	N3549*	12.8	S	0
N3556	10.7	S	763	N3596*	11.7	S	0
N3600*	12.6	S	0	N3611	12.4	S	1603
Z268C16	13.7	S	0	N3615*	14.0	E	0
N3614*	12.7	S	0	N3622	13.7	S	0
N3629	12.9	S	0	N3648	13.5	O	0
N3654	13.4	S	0	N3666*	12.5	S	0
N3668*	13.1	S	0	N3675	10.4	S	727
N3677*	13.5	S	0	N3682	13.4	OS	0

TABLE V (CONTINUED)

FIELD GALAXIES

(1) ID	(2) MAG	(3) TY	(4) VEL	(1) ID	(2) MAG	(3) TY	(4) VEL
N3687	13.0	S	0	N3689	12.9	S	0
N3694	13.5	U	0	N3752	13.7	S	0
Z185080	14.0	S	0	Z314032	13.3	S	0
N3726	11.2	S	998	Z242046	13.9	I	0
N3735	12.4	S	0	N3755	13.9	S	0
N3773	13.1	O	0	N3782	13.1	I	0
N3800*	13.1	S	3469	N3813	12.6	S	0
Z12061	13.7	U	0	N3832*	14.0	S	0
N3853*	13.5	E	0	N3891	13.7	S	0
N3930	13.5	S	0	N3935	14.0	S	0
N3937	14.0	EO	0	N3938*	11.0	S	919
N3941*	11.3	O	969	I745	13.7	U	0
N3971*	13.9	O	0	N3992*	10.7	S	1147
N4013	12.4	S	0	N4020	13.2	S	0
N4051	11.5	S	709	N4125	10.9	E	1504
N4128	12.7	O	2548	N4127	13.5	S	0
N4162	12.6	S	2510	N4194	13.0	U	2684
N4236	10.7	S	185	N4244	10.8	S	269
N4250	13.0	OS	0	Z243069	13.7	OS	0
N4271	13.7	EO	0	N4369	12.3	OS	0
N4384	13.5	S	2400	N4395*	11.7	S	0
N4449*	10.0	I	269	N4460	12.5	O	0
N4494*	10.7	E	1305	N4500	13.2	S	3000
Z216009	13.9	S	0	Z216010	13.7	I	0
Z188007	13.4	S	0	N4525	13.0	S	0
N4534	13.2	S	0	N4559*	10.7	S	852
N4566	13.9	S	0	N4605	10.8	S	276
N4615*	13.8	S	0	N4619	13.5	S	0
N4693	14.0	S	0	N4750	11.8	S	1823
N4736*	8.7	S	362	N4793	12.3	S	0
N4800	12.0	S	832	Z15037	13.6	S	0
N4814	12.4	S	2661	N4826*	8.9	S	352
N4845	12.9	S	0	N4861*	12.8	U	831
N4900	12.8	S	962	N4904	13.2	S	0
N4956	13.5	O	0	N4964	14.0	S	0

TABLE V (CONTINUED)

FIELD GALAXIES

(1) ID	(2) MAG	(3) TY	(4) VEL	(1) ID	(2) MAG	(3) TY	(4) VEL
I4182	14.0	S	0	N4999	13.5	S	0
N5012*	13.6	S	0	N5023	13.2	S	0
N5032*	13.6	S	0	Z245036	14.0	I	0
N5055	9.7	S	600	N5056*	13.6	S	0
N5116	13.7	S	0	N5127*	13.9	E	0
N5144*	13.2	S	3000	N5125*	13.5	S	0
N5129*	13.3	E	0	N5147	12.7	S	1042
N5158	13.8	S	0	N5174	13.7	S	0
N5172	12.7	S	0	N5204*	11.7	S	0
N5190	13.7	S	0	N5217*	14.0	E	0
Z190028	13.8	S	0	N5230*	13.4	S	0
N5243	14.0	S	0	N5250	14.0	0	0
N5248	11.4	S	1144	N5263	14.0	S	0
N5273*	12.7	0	1094	N5279	13.6	S	7708
N5297	12.3	S	0	N5301	13.0	S	1816
N5308	12.5	OS	2199	N5300	13.7	S	0
N5377	12.5	S	1953	N5375	13.2	S	0
I962*	14.0	U	0	N5417	13.8	S	0
N5433*	14.0	SI	0	N5448	12.7	S	2103
N5490*	13.4	E	0	N5492	13.7	S	0
N5491*	13.9	S	0	N5525	14.0	0	0
N5532*	13.3	0	0	N5585*	11.7	S	467
N5582	13.0	E	0	N5607	13.9	U	7800
N5587	14.0	OS	0	N5602	13.5	S	0
Z19012	13.6	S	0	N5603*	14.0	0	0
N5600	11.9	S	0	Z247026	13.9	I	0
N5619*	14.0	S	0	N5631	12.4	OS	2146
N5630	13.6	SI	0	N5633	12.9	S	2484
N5635	13.9	S	3894	Z220019	14.0	S	0
N5641	13.6	S	0	N5653	12.7	S	3648
N5645	12.8	S	0	N5656	12.7	S	0
N5649*	14.0	S	0	N5652	13.8	S	0
N5667	13.1	U	0	N5665	12.6	S	2256
N5675	14.0	S	0	N5678	12.1	S	2472
N5668	12.7	S	1732	N5674	13.7	S	0

TABLE V (CONTINUED)

FIELD GALAXIES

(1) ID	(2) MAG	(3) TY	(4) VEL	(1) ID	(2) MAG	(3) TY	(4) VEL
N5687	13.3	D	2284	N5690	13.1	S	0
N5698	14.0	S	0	N5695	13.9	S	0
N5692	13.3	U	0	N5707	13.3	S	0
N5708	13.9	SI	0	N5701	12.9	D	0
N5731*	14.0	S	0	Z220047	13.8	D	0
Z248C18	13.9	S	0	N5735	13.8	S	0
I1C48	14.0	S	0	N5739	13.7	DS	0
N5751	13.9	S	0	N5772	13.9	S	0
N5783	14.0	S	0	N5784	13.7	D	0
I1076*	13.9	U	0	Z105082	14.0	S	0
N5820*	13.0	ED	3445	N5832	13.3	S	0
N5827	13.7	S	0	N5866*	11.1	D	972
N5875	13.4	S	0	N5876	13.9	S	0
Z318018	13.6	E	0	N5879*	11.9	S	1064
N5894	13.2	SI	0	N5899	12.6	S	2706
N5918	14.0	S	0	N5921	12.7	S	1429
N5928*	13.8	D	0	N5929*	13.0	ED	2683
N5939	13.7	S	0	Z222010	14.0	S	0
N5949	12.7	S	589	N5936	13.0	S	0
I1129	13.7	S	0	N5958	13.2	S	0
N5961*	14.0	U	0	N5966	13.9	E	0
N5962	12.2	S	2088	N5987	13.3	S	0
N5980*	13.3	S	0	N5984*	13.5	S	0
N5993*	13.9	S	0	N5990	13.1	S	0
N5996*	13.2	S	0	N6004	13.4	S	0
Z25C014	13.6	S	0	N6015	11.7	S	889
N6C12	13.1	S	0	I1153	13.6	D	0
I1151	13.4	S	0	Z319036	13.9	E	0
Z223C38	13.6	U	0	I1210	13.8	S	0
I1211	13.8	E	0	N6127	13.0	E	0
N6143	13.9	S	0	N6146	13.8	E	0
N6154	14.0	S	0	N6155	13.0	S	0
N6166*	13.9	E	9082	N6173	14.0	E	0
N6189	13.3	S	0	N6190	13.2	S	0
Z251034	13.9	ED	0	N62C7	11.9	S	1072

and better velocity data. Better photometry as well as more reliable and detailed morphological types would also be very useful.

Despite the shortcomings of the presently available (from the literature) data, a number of interesting statistical investigations of the groups' properties are possible. Three such investigations are currently being published in separate papers of this series. They are studies of the luminosity function of galaxies in small groups (Turner and Gott 1976), the dynamics and virial masses of the groups (Gott and Turner 1976a), and the group multiplicity function (Gott and Turner 1976b). Such statistical studies profit from the well-defined group identification criteria described in §II.

REFERENCES

de Vaucouleurs, G. 1975, in Stars and Stellar Systems, Vol. 9, ed. A. and M. Sandage (Chicago: University of Chicago Press) (in press).

Field, G. B., and Saslaw, W. C. 1971, Ap. J., 170, 199.

Gott, J. R., and Turner, E. L. 1976a, in preparation.

Gott, J. R., and Turner, E. L. 1976b, in preparation.

Gott, J. R., Wrixon, G. T., and Wannier, P. 1973, Ap. J., 186, 777.

Holmberg, E. 1937, Ann. Obs. Lund, No. 6, 1.

Huchra, J. 1975, preprint.

Jackson, J. C. 1975, preprint.

Karachentseva, V. E. 1973, Soobshch. Spets. Astrofiz. Obs., No. 8.

Kirshner, R. P. 1975, private communication.

Nilson, P. 1973, Uppsala Astr. Obs. Ann., Vol. 6 (Uppsala General Catalog of Galaxies), (UGC).

Rood, H. J., Rothman, V. C. A., and Turnrose, B. E. 1970, Ap. J., 162, 411.

Sandage, A., and Tammann, G. A. 1975, Ap. J., 197, 265.

Schechter, P. 1975, preprint.

Turner, E. L., and Gott, J. R. 1975, Ap. J. Lett., 197, L89.

Turner, E. L., and Gott, J. R. 1976, in preparation.

Turner, E. L., and Sargent, W. L. W. 1974, Ap. J., 194, 587.

van den Bergh, S. 1962, Zs. f. Ap., 55, 21.

Zwicky, F., Herzog, E., Wild, P., Karpowicz, M., and Kowal, C. T. 1961-1968, Catalog of Galaxies and Clusters of Galaxies, in 6 vols. (Pasadena: California Institute of Technology), (CGCG).

CHAPTER 4

GROUPS OF GALAXIES:

STATISTICAL PROPERTIES

I. INTRODUCTION

Because small, loose groups are a very common environment for galaxies (e.g., de Vaucouleurs 1975, Holmberg 1937), the average properties of such groups are of considerable interest. The compilation of a new catalog of groups (Turner and Gott 1976, hereafter TG I) offers an opportunity for some preliminary investigations of these properties, even though the available (from the literature) data are not as complete and high quality as might be desired. This paper reports the initial results of studies of the galaxy luminosity function in groups (§ II), the dynamics and virial masses of groups (§ III), and the group multiplicity function (§ IV). § V summarizes the important results and discusses them briefly. Throughout the paper, all quantities are calculated using $H_o = 50$ km s^{-1} Mpc^{-1}.

II. LUMINOSITY FUNCTION

Of the 103 groups identified in TG I, 63 have one or more members with measured radial velocities. Taking the mean radial velocity of each group (table III of TG I) to indicate its distance, a determination of the individual group luminosity functions is possible. However, because most groups possess rather few members, these individual luminosity functions are not very informative. Therefore, in what follows, we have combined the 63 separate group functions into a single composite luminosity function. It

should be remembered, of course, that by using only the groups with radial velocities, some unknown biases may have been introduced.

A galaxy of apparent magnitude m in a group with mean radial velocity $\bar{v}$ has a luminosity L given by

$$L = 6.22 \times 10^{8} \bar{v}^{-2} 10^{-0.4m} L_{\odot} \tag{1}$$

Then let $\phi_i(L)dL$ be the observed luminosity function of the ith group, that is, the number of galaxies in the ith group with luminosities between L and L+dL. Also let L_c be the faintest absolute luminosity which would be visible in a particular group (evaluate (1) with m = 14). We then construct the function Y(L) according to

$$Y(L) = N_L^{-1} \sum_i \phi_i(L)dL \Big/ \int_L^{\infty} \phi_i(L)dL \tag{2}$$

where N_L is the number of groups with $L_c \geq L$. Suppose the brightest galaxy observed in any group has luminosity L′, then the composite group luminosity function $\Phi(L)dL$ is

$$\Phi(L > L')dL = 0 \tag{3}$$

$$\Phi(L')dL = 1 \tag{4}$$

$$\Phi(L < L')dL = Y(L) \int_L^{\infty} \Phi(L)dL \tag{5}$$

In practice, the dL's in equations (2) through (5) are replaced by $\Delta \log L = 0.2$ (i.e., 1/2 magnitude bins), and (5) is solved by numerical iteration. Equations (3) and (4) amount to a normalization of $\Phi(L)$ at the bright end. This procedure is preferable to simply adding the various $\phi_i(L)dL$ because it gives equal weight to each group. Simple addition gives more weight to the groups with more members; if applied to the present data, the result would primarily reflect the luminosity function of group 57 (the Virgo cluster) alone.

The results of applying the above procedure to the 63 groups are shown in figure 1. The error bars are determined from the observed dispersion in Y(L). Since the groups contain both foreground and background projected members, it is expected that these will dominate the calculated $\Phi(L)$ at both the very bright and the very faint ends. Also, there is a good possibility that low luminosity galaxies which tend to have low surface brightnesses might have been missed. Altogether, the results shown in figure 1 are probably not trustworthy outside the indicated "fit interval," $-22.5 \leq M_{pg} \leq -17.5$.

A weighted least-squares fit of the data (inside the fit interval) to a functional form suggested by Schechter (1975)

$$\Phi(L/L^*)d(L/L^*) = \Phi^*(L/L^*)^{\alpha}e^{-L/L^*}d(L/L^*) \qquad (6)$$

FIGURE 1

Group luminosity function. The points show the relative luminosity function of galaxies in groups as determined by the method described in §II. In the range of absolute magnitudes marked "fit interval", the data is probably reliable. The solid curve is a fit of (6) to the data with $\alpha = -1$. The broken curve is Schechter's (1975) rich cluster luminosity function fit in amplitude only.

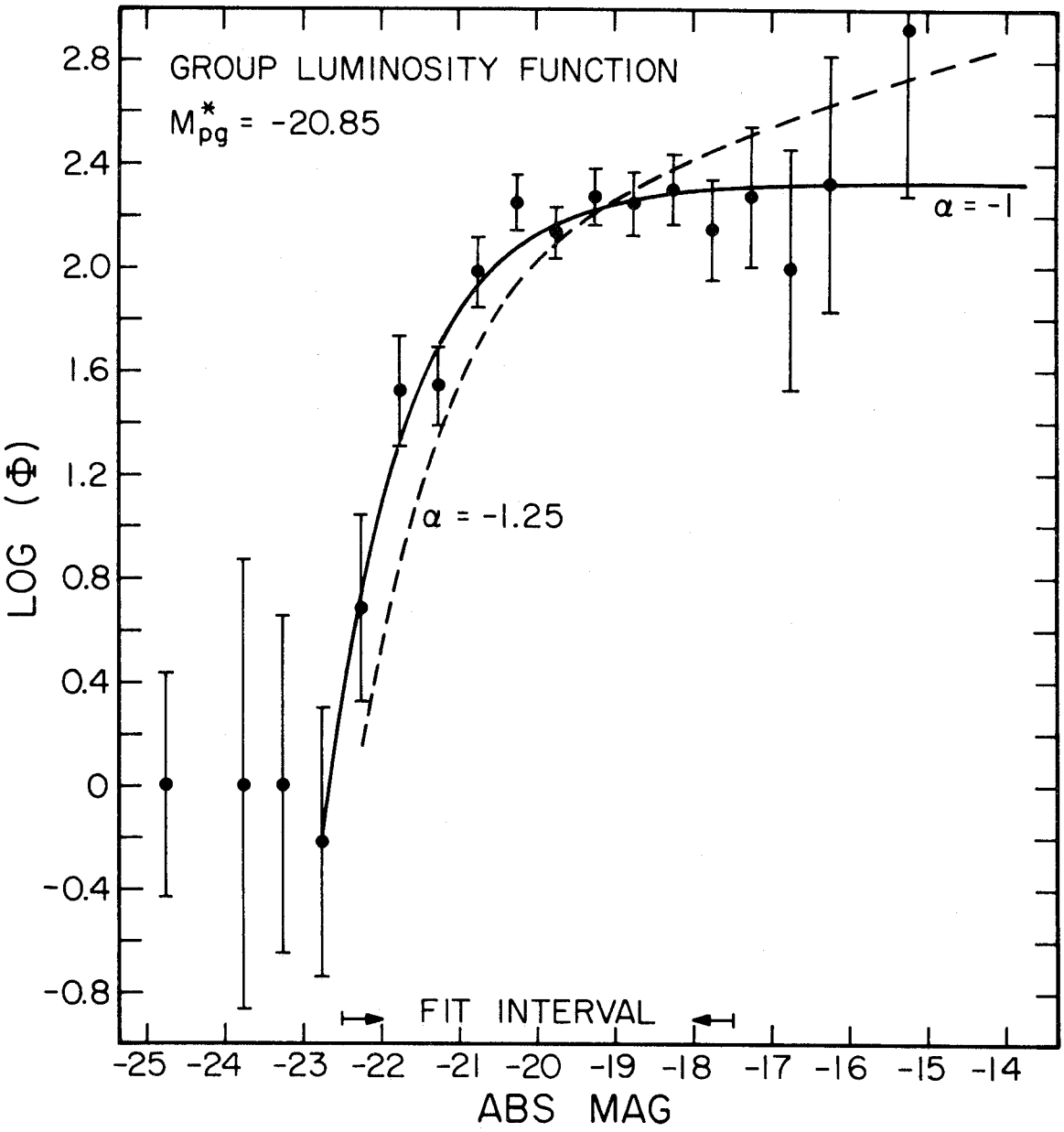
GROUP LUMINOSITY FUNCTION
M^*_{pg} = -20.85
α = -1
α = -1.25
FIT INTERVAL
LOG (Φ)
ABS MAG
2.8
2.4
2.0
1.6
1.2
0.8
0.4
0
-0.4
-0.8
-25 -24 -23 -22 -21 -20 -19 -18 -17 -16 -15 -14

yields $\alpha = -0.83 \pm 0.17$ and $M^*_{pg} = -20.59 \pm 0.26$. If, for simplicity, we constrain $\alpha = -1$, then the fit gives $M^*_{pg} = -20.85 \pm 0.13$ corresponding to $L^* = 3.4 \times 10^{10} L_\odot$. Both fits give a reduced chi-square of 0.63 and are, therefore, equally good. Since the analytic form of (6) is particularly convenient if $\alpha = -1$, the latter fit is adopted and plotted as a solid curve in figure 1.

Schechter (1975) has fit (6) to a composite luminosity function constructed from Oemler's (1974) data for rich clusters and obtained $\alpha = -1.25$ and $M^*_{B(O)} = -20.6$. These values are in fairly close agreement with the above results for small groups. The most significant difference ($\sim 2\sigma$) is in the value of α (slope of the low luminosity tail). It is intriguing that some of Oemler's (1974) clusters seem to have relatively fewer low luminosity galaxies than others (i.e., larger α's). Schechter's rich cluster luminosity function (fitted only in amplitude) is shown as a broken curve in figure 1.

Figures 2 and 3 show the composite luminosity function for early (E and S0) and late (S, SB, and Irr) type galaxies, respectively. These were determined by the same procedure as the total luminosity function (figure 1). Fits of (6) yield $\alpha = -0.79 \pm 0.23$ and $M^*_{pg} = -20.49 \pm 0.30$ for late types and $\alpha = -1.27 \pm 0.24$ and $M^*_{pg} = -21.34 \pm 0.60$ for early types. These results are identical within the errors (2σ); but it is, again, intriguing that the α value for

FIGURE 2

The luminosity function of early-type (elliptical and SO) galaxies in groups. The best fit value of α is -1.27 $\pm$0.24.

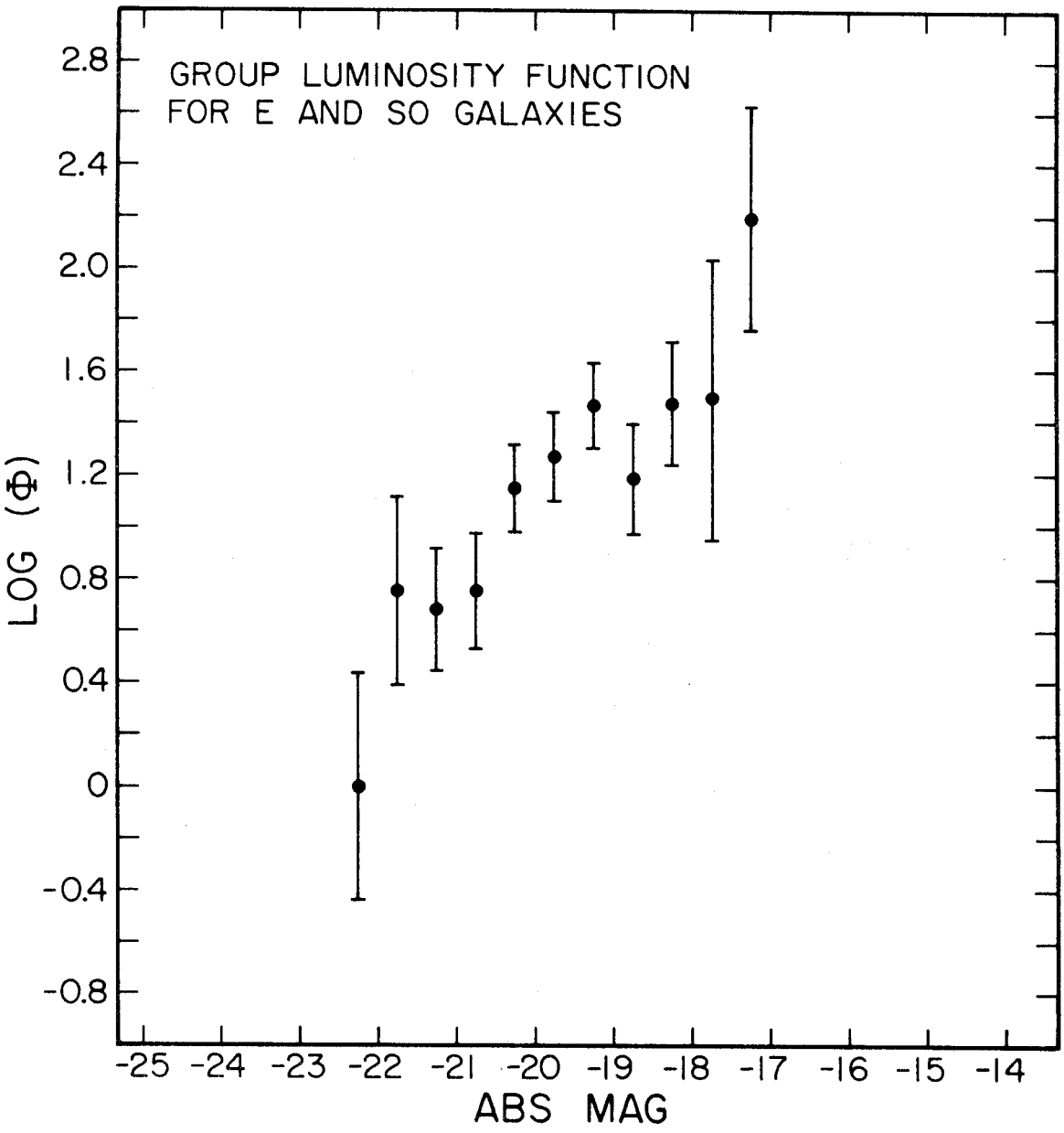
GROUP LUMINOSITY FUNCTION
FOR E AND SO GALAXIES
LOG (Φ)
2.8
2.4
2.0
1.6
1.2
0.8
0.4
0
-0.4
-0.8
-25 -24 -23 -22 -21 -20 -19 -18 -17 -16 -15 -14
ABS MAG

FIGURE 3

The luminosity function of late-type galaxies in groups. The best fit value of α is -0.79 ± 0.23.

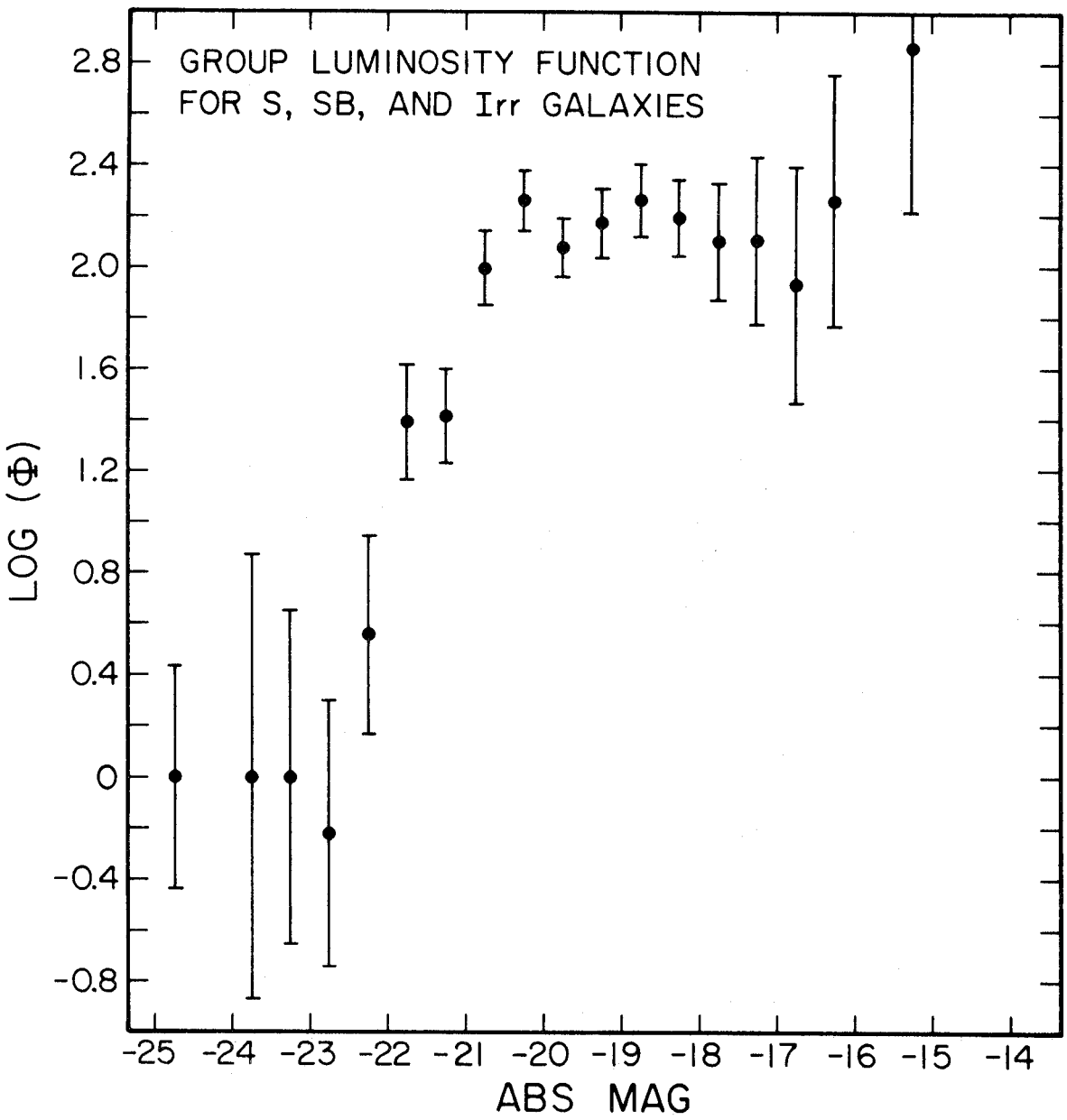
GROUP LUMINOSITY FUNCTION
FOR S, SB, AND Irr GALAXIES
LOG (Φ)
2.8
2.4
2.0
1.6
1.2
0.8
0.4
0
-0.4
-0.8
-25 -24 -23 -22 -21 -20 -19 -18 -17 -16 -15 -14
ABS MAG

early type galaxies agrees so well with Schechter's result for rich clusters (in which early type galaxies are often concentrated).

Assuming that the true luminosity function of galaxies in small groups is well represented by (6) with $\alpha = -1$ and $L^* = 3.4 \times 10^{10}\ L_\odot$ and that the galaxies in any particular group represent a random sampling of that luminosity function (Geller and Peebles 1975, Schechter 1974), it is then possible to use the Schechter and Press (1975) method to estimate the distance and total luminosity of any observed group. They have kindly prepared for us a table (analogous to Table I of their paper but calculated for the above values of α and L^*) relating the distance and total luminosity of a group to m_{TOT} (see Table III of TG I) and the number of members. Their method, which consists of a maximum-likelihood matching of (6) to an observed distribution of apparent magnitudes, also provides an estimate of the rms uncertainty in the distances and total luminosities. Table I gives the results of applying the Schechter and Press method to each of the 103 groups. Figure 4 shows the relation between the luminosity function distance D_{LF} and the observed mean velocity for the 63 groups with velocities; the insert shows the distribution of $\Delta D/\sigma = |D_{LF} - (\bar{v}/H_o)|/\sigma$ where σ is the predicted uncertainty in D_{LF}. Generally, figure 4 supports the validity of the Schechter and Press distance indicator.

TABLE I

LUMINOSITY FUNCTION DISTANCES AND TOTAL LUMINOSITIES

(1) Group	(2) Distance (Mpc)	(3) Relative Error	(4) Total Luminosity(L*)	(5) Relative Error
1	132	0.440	42.0	2.56
2*	281	0.384	1.71×10^5	7.69
3*	227	0.396	5210	5.46
4	172	0.340	374	2.93
5*	...	...	...	...
6	41.1	0.486	2.4	0.864
7*	181	0.412	410	3.88
8*	227	0.396	5210	5.46
9	8.9	0.823	0.5	0.810
10	128	0.362	53.1	2.01
11	33.3	0.627	1.2	0.987
12	71.7	0.420	6.5	1.16
13	33.9	0.625	1.3	0.992
14	103	0.382	19.7	1.58
15	80.5	0.499	5.8	1.55
16	4.8	0.574	0.9	0.496
17	100	0.385	17.7	1.54
18	22.0	0.691	0.8	0.897
19	23.7	0.679	0.9	0.910
20	20.9	0.570	1.2	0.726
21	36.9	0.306	5.6	0.509
22*	...	...	...	...
23	62.8	0.377	6.4	0.920

TABLE I (Cont'd)

(1) Group	(2) Distance (Mpc)	(3) Relative Error	(4) Total Luminosity(L*)	(5) Relative Error
24	65.9	0.526	3.6	1.34
25	35.5	0.618	1.3	1.01
26	93.5	0.480	9.2	1.76
27	13.8	0.269	4.9	0.297
28	39.9	0.347	4.6	0.604
29*	...	...	...	...
30	58.6	0.543	2.8	1.25
31	80.5	0.353	11.7	1.10
32	42.8	0.373	4.2	0.680
33	22.8	0.484	1.7	0.639
34	25.0	0.671	0.9	0.920
35	96.5	0.337	20.6	1.29
36	126	0.446	31.7	2.40
37	32.9	0.514	1.8	0.803
38	8.0	0.484	1.4	0.464
39	21.8	0.253	6.3	0.327
40	35.4	0.505	2.0	0.821
41	29.9	0.526	1.7	0.782
42	24.1	0.677	0.9	0.913
43	166	0.419	190	3.43
44	81.7	0.497	6.1	1.57
45*	288	0.383	3.00×10^5	8.08
46	139	0.195	279	1.22
47	34.0	0.120	34.4	0.191
48	130	0.442	38.2	2.51
49	59.9	0.441	4.4	1.03

TABLE I (Cont'd)

(1) Group	(2) Distance (Mpc)	(3) Relative Error	(4) Total Luminosity (L*)	(5) Relative Error
50	21.7	0.168	14.2	0.217
51	29.6	0.373	3.3	0.552
52	18.3	0.718	0.7	0.871
53	36.1	0.154	21.8	0.253
54	16.1	0.602	1.0	0.699
55	32.7	0.630	1.2	0.982
56	80.3	0.204	34.7	0.632
57	31.4	0.058	139	0.089
58	39.7	0.321	5.4	0.558
59	10.6	0.799	0.5	0.820
60	12.5	0.775	0.6	0.832
61	11.3	0.558	1.1	0.583
62	24.5	0.674	0.9	0.916
63	166	0.419	190	3.43
64	38.1	0.222	10.9	0.376
65	45.9	0.579	1.9	1.11
66	166	0.419	190	3.43
67	13.6	0.622	0.9	0.686
68	162	0.421	156	3.30
69	52.7	0.559	2.3	1.18
70	114	0.373	29.4	1.75
71*	283	0.313	3.04×10^5	6.37
72	7.2	0.603	0.9	0.565
73*	281	0.384	1.71×10^5	7.69
74	98.1	0.387	16.4	1.51
75	166	0.419	190	3.43

TABLE I (Cont'd)

(1) Group	(2) Distance (Mpc)	(3) Relative Error	(4) Total Luminosity (L*)	(5) Relative Error
76	87.9	0.488	7.6	1.67
77	49.0	0.161	25.8	0.322
78	33.3	0.397	3.1	0.624
79	47.2	0.332	5.9	0.647
80	162	0.421	156	3.30
81	59.2	0.542	2.9	1.26
82	11.8	0.369	2.5	0.390
83	59.4	0.442	4.3	1.03
84*	...	...	...	...
85	72.3	0.514	4.4	1.43
86	49.3	0.304	7.3	0.610
87	44.7	0.369	4.5	0.691
88	120	0.451	25.0	2.28
89	56.3	0.549	2.6	1.22
90	81.7	0.497	6.1	1.57
91	36.8	0.387	3.5	0.644
92	40.7	0.597	1.6	1.05
93	142	0.434	62.9	2.79
94*	181	0.412	410	3.88
95	48.5	0.202	16.2	0.401
96	79.8	0.500	5.7	1.54
97	31.1	0.521	1.7	0.790
98	53.6	0.454	3.6	0.971
99	67.6	0.523	3.8	1.37

TABLE I (Cont'd)

(1) Group	(2) Distance (Mpc)	(3) Relative Error	(4) Total Luminosity(L*)	(5) Relative Error
100	46.1	0.472	2.8	0.905
101	130	0.442	38.2	2.51
102	35.2	0.506	2.0	0.819
103*	192	0.408	694	4.20

*Method breaks down; all members have apparent magnitudes near the limit.

FIGURE 4

Luminosity function distances. The Schechter and Press (1975) luminosity function distance D_{LF} for $\alpha = -1$ and $L^* = 3.4 \times 10^{10}\ L_\odot$ is plotted against mean observed radial velocity v_{obs} for 63 groups. The straight line indicates $D_{LF} = v_{obs}\ H_o^{-1}$. The insert shows the distribution of observed over expected deviations from this relation.

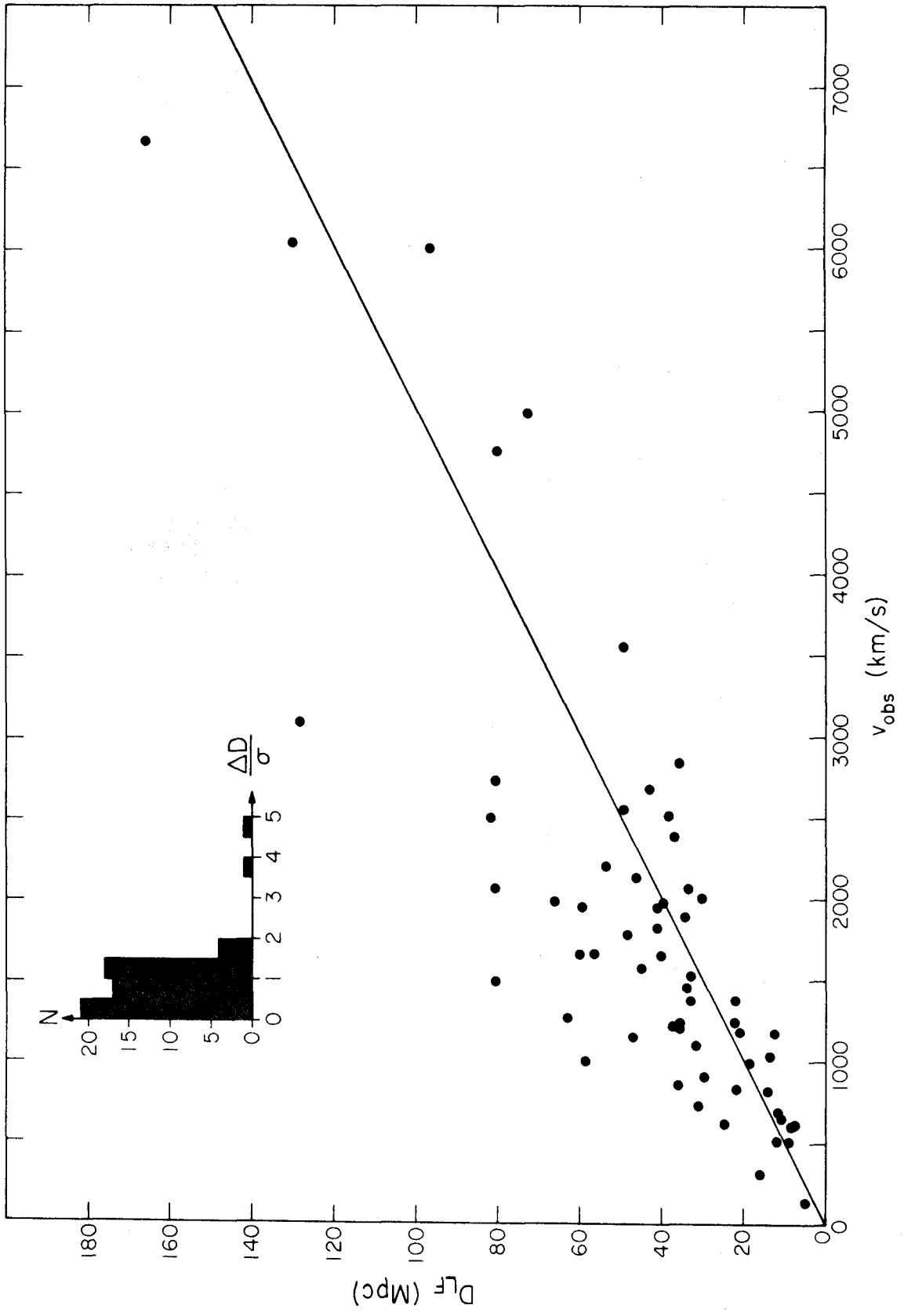
D_{LF} (Mpc)
v_{obs} (km/s)
0
20
40
60
80
100
120
140
160
180
1000
2000
3000
4000
5000
6000
7000
N
0
5
10
15
20
$\frac{\Delta D}{\sigma}$
0
1
2
3
4
5

It is interesting to compare the above luminosity function distances to the far simpler first-brightest-cluster-member distance estimator (Sandage 1972, Sandage and Hardy 1973, Sandage 1975). In figure 5, the absolute magnitude M_1 of the brightest group member is plotted as a function of the group's total luminosity L expressed in units of L*. This total luminosity is

$$L = L_o \, e^{L_c/L^*} \tag{7}$$

where L_o is the total luminosity of the observed members and the exponential correction is for members beyond the survey's limiting magnitude. An inspection of figure 5 reveals that M_1 is, as often emphasized by Sandage (1972, 1975, and references therein), remarkably constant for groups with total luminosities > 10 L*; however, it is poorly defined and a systematic function of the total group luminosity for smaller groups ($L/L^* \leq 10$). This suggests that M_1 may be preferable as a rich cluster distance indicator while the Schechter and Press luminosity function distances are better for small groups.

FIGURE 5

The relation of the brightest group member's absolute magnitude M_1 to the total group luminosity L. The straight line corresponds to all of the group's luminosity being in its brightest member. The curve shows the statistically expected value of M_1 if each group represented a random sampling of the luminosity function (6). The arrow indicates the correction of the Coma cluster point for a foreground galaxy. See the text for further interpretation.

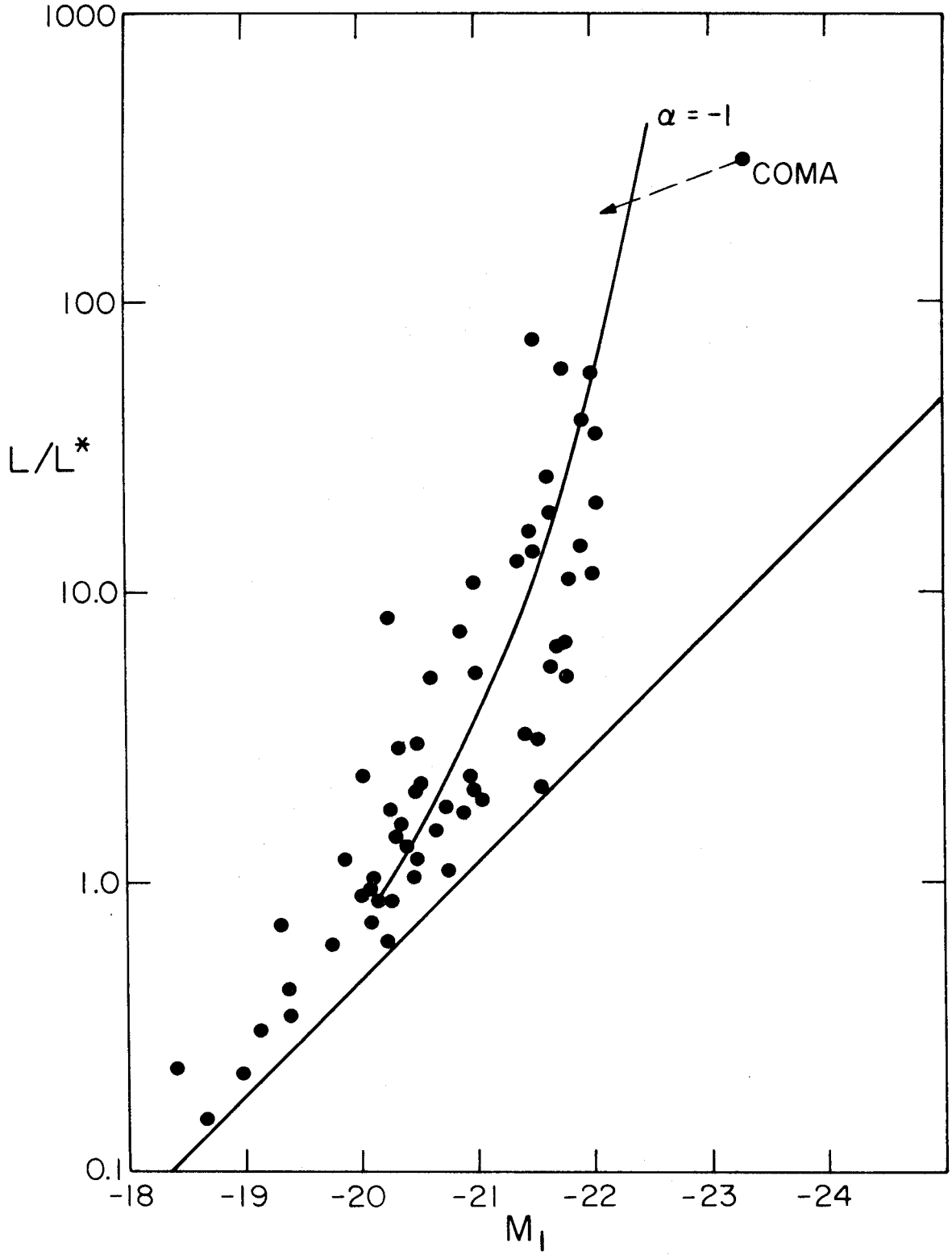
1000
100
10.0
1.0
0.1
L/L*
α = -1
COMA
-18
-19
-20
-21
-22
-23
-24
M1

III. DYNAMICS AND VIRIAL MASSES

In order to study the dynamical properties of a group, it is necessary that a bare minimum of two members have measured radial velocities so that some estimate of the group velocity dispersion σ_v can be obtained. Only 39 of the 103 groups satisfy this requirement; this dynamical sample is quite likely to be biased by redshift selection effects. Moreover, because σ_v is so sensitive to even a single discrepant velocity, the presence of foreground and background members in some groups (TG I) decreases their value for dynamical studies. Although it is possible to remove suspect members (see notes to Table I and ratings in Table III of TG I), this introduces a further selection bias. For the present study, the 39 groups have been used exactly as given in TG I; however, the contamination rating (Table III of TG I) is used to distinguish relatively reliable groups from those heavily influenced by projected members.

For each of the 39 groups, the following dynamically interesting parameters are calculated: the total (3 dimensional) velocity dispersion

$$V = \sqrt{3}\ \sigma_v \quad , \tag{8}$$

the mean harmonic radius

$$R = \pi\ \bar{v}\ H_o^{-1}\ \tan(\phi/2) \quad , \tag{9}$$

the virial mass

$$M_{VT} = \frac{V^2 R}{G} \tag{10}$$

and the crossing time (in units of the Hubble time)

$$\Delta t\, H_o = \frac{3\pi}{5^{3/2}} \frac{\bar{v}}{\sigma_v} \tan(\phi/2) \tag{11}$$

where $\bar{v}$, σ_v, and ϕ are given in Table III of TG I and the various numerical factors account for projection effects (Mathews and Limber 1960, Gott et al. 1973). Also of interest is the total group luminosity L as defined in equation (7) from which the virial mass-to-light ratio M_{VT}/L is calculated. These parameters are listed in Table II.

For groups with contamination ratings of 1 or 2, figures 6 and 7 show the distributions of V versus R, and L versus R, respectively. Performing least-squares power-law fits to these data gives $V \sim R^{0.6}$ and $L \sim R^{0.8}$ (both significant at the 1% or better level) implying $M_{VT}/L \sim R^{1.4}$. However, if the groups rated 2 are excluded, no significant correlations remain for those rated 1; this would give $M_{VT}/L \sim R$. Either of these results could be interpreted as supporting the massive halo hypothesis (Ostriker and Peebles 1973, Ostriker et al. 1974, Kalnajs 1972), but the large scatter of the data casts some doubt on any such conclusion. Moreover, a direct plot of M_{VT}/L versus R (figure

TABLE II

DYNAMICAL PARAMETERS

(1) Group	(2) V(km s^{-1})	(3) R(Mpc)	(4) $\Delta t\ H_o$	(5) M_{VT} ($M_\odot$)	(6) L ($L_\odot$)
6	187	0.830	0.103	6.76×10^{12}	7.22×10^{10}
10	199	0.809	0.094	7.47×10^{12}	9.72×10^{10}
11	204	0.438	0.050	4.26×10^{12}	2.69×10^{10}
13	47	1.677	0.834	8.54×10^{11}	3.06×10^{10}
16	184	0.225	0.029	1.77×10^{12}	1.10×10^{10}
20	69	0.475	0.159	5.31×10^{11}	5.28×10^{10}
21*	222	0.601	0.063	6.87×10^{12}	7.60×10^{10}
27†	715	0.578	0.019	6.88×10^{13}	2.37×10^{11}
28	76	0.432	0.132	5.84×10^{11}	1.02×10^{11}
32†	941	4.327	0.107	8.90×10^{14}	2.57×10^{11}
33*	409	1.563	0.089	6.07×10^{13}	6.98×10^{10}
38	88	0.512	0.135	9.29×10^{11}	1.10×10^{11}
39*	1786	1.118	0.015	8.29×10^{14}	3.55×10^{11}
40	35	1.142	0.766	3.19×10^{11}	2.94×10^{10}
44	352	0.292	0.019	8.41×10^{12}	4.80×10^{10}

TABLE II (Cont'd)

(1) Group	(2) V(km s^{-1})	(3) R(Mpc)	(4) $\Delta t\ H_o$	(5) M_{VT} ($M_\odot$)	(6) L ($L_\odot$)
47*	1510	4.351	0.067	2.31×10^{15}	1.27×10^{12}
50*	594	2.543	0.099	2.09×10^{14}	2.78×10^{11}
51	191	1.042	0.127	8.80×10^{12}	3.90×10^{10}
53*	958	1.534	0.037	3.27×10^{14}	1.47×10^{11}
55†	2269	3.215	0.033	3.85×10^{15}	3.58×10^{10}
57*	1212	4.464	0.086	1.53×10^{15}	2.22×10^{12}
58	73	1.627	0.520	2.00×10^{12}	1.82×10^{11}
59	121	0.231	0.044	7.91×10^{11}	2.70×10^{10}
61*	104	0.541	0.121	1.36×10^{12}	5.57×10^{10}
64†	4341	5.093	0.027	2.23×10^{16}	7.32×10^{11}
67	104	1.476	0.330	3.71×10^{12}	7.22×10^{10}
72†	544	0.184	0.008	1.26×10^{13}	8.83×10^{10}
75	152	0.409	0.062	2.21×10^{12}	1.34×10^{12}
77*	565	1.115	0.046	8.27×10^{13}	9.76×10^{11}
79†	163	1.020	0.146	6.29×10^{12}	3.84×10^{10}

TABLE II (Cont'd)

(1) Group	(2) V(km s^{-1})	(3) R(Mpc)	(4) $\Delta t\ H_o$	(5) M_{VT} ($M_\odot$)	(6) L ($L_\odot$)
82†	701	1.697	0.056	1.94×10^{14}	6.47×10^{10}
83	244	0.508	0.048	7.05×10^{12}	5.05×10^{10}
86	553	2.402	0.101	1.71×10^{14}	6.92×10^{11}
87	104	0.477	0.107	1.20×10^{12}	6.72×10^{10}
91	31	2.280	1.700	5.16×10^{11}	2.21×10^{11}
95	559	0.754	0.031	5.49×10^{13}	2.64×10^{11}
96	35	0.308	0.207	8.60×10^{10}	3.75×10^{11}
98	35	0.127	0.085	3.55×10^{10}	7.46×10^{10}
102	339	0.950	0.065	2.55×10^{13}	2.20×10^{11}

*Contamination rating = 2 †Contamination rating = 3 or 4

See Table III of TGI for details of contamination ratings.

FIGURE 6

Velocity dispersion versus mean harmonic radius (in Mpc) for groups with contamination ratings of 1 (filled circles) and 2 (filled triangles). The best fit power-law is $V \sim R^{0.6}$.

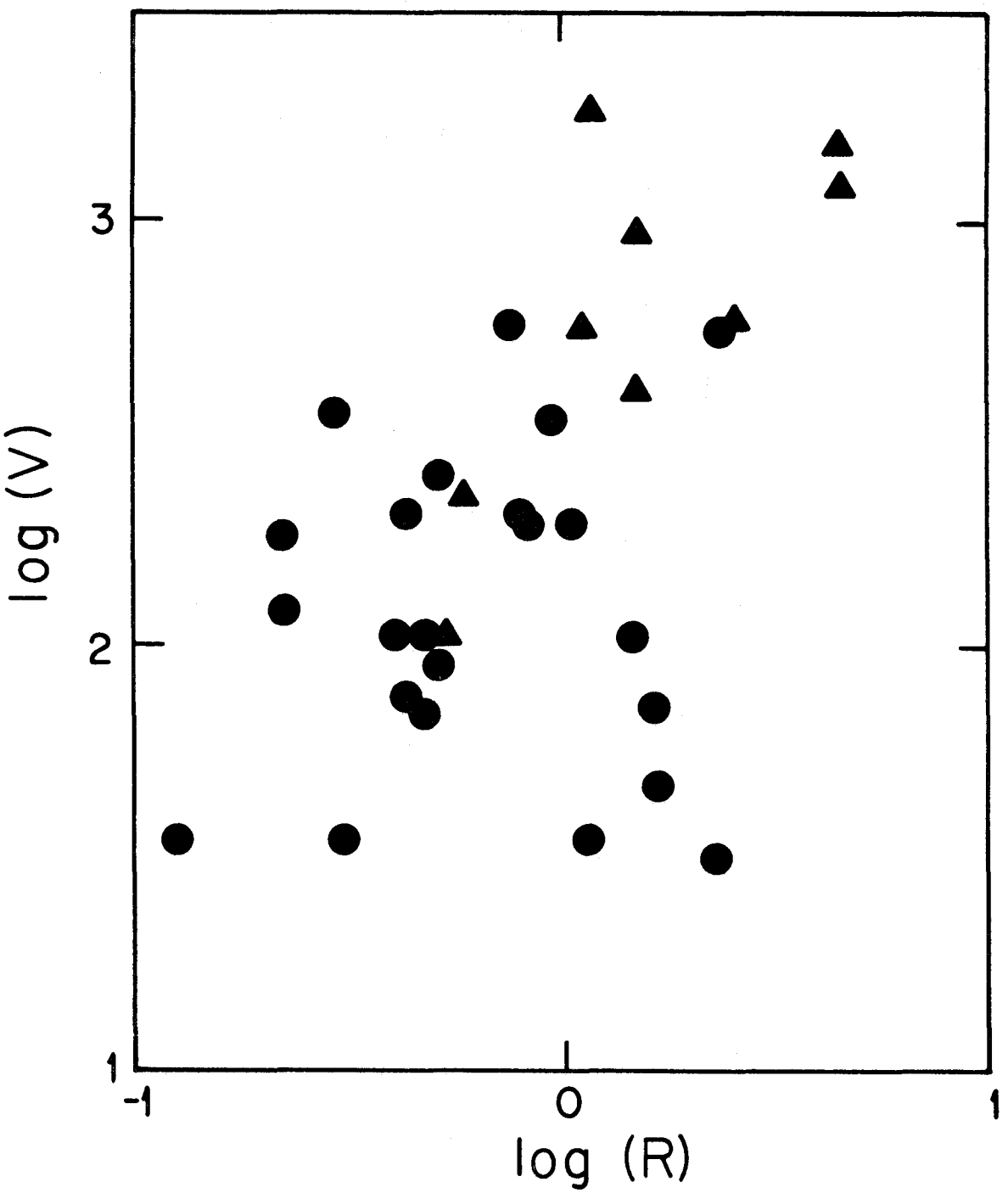
3
2
1
log (V)
-1
0
1
log (R)

FIGURE 7

Total group luminosity versus mean harmonic radius (in Mpc) for groups with contamination ratings of 1 (filled circles) and 2 (filled triangles). The best fit power-law is $L \sim R^{0.8}$.

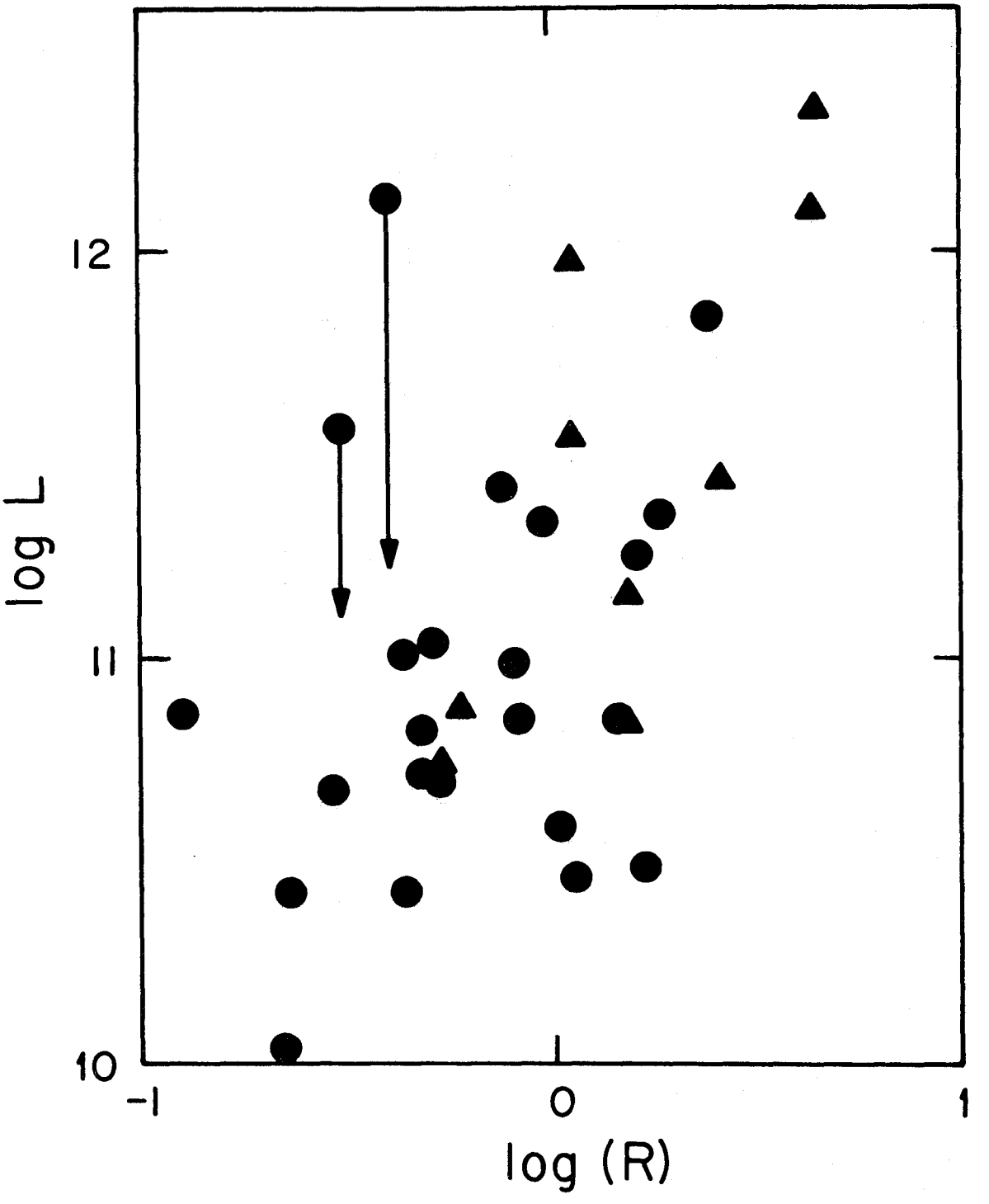
12
11
10
log L
-1
0
1
log (R)

8) for the pure spiral groups shows no apparent correlation; this impression is supported by a formal correlation analysis.

Figure 9 is a plot of M_{VT}/L versus $\Delta t\ H_o$ for all 39 groups with two or more velocities; only the filled points (groups rated 1 or 2) can be considered even moderately reliable, and only they will be discussed below. Although the data are very scattered, several interesting conclusions can be drawn from the general distribution:

1) Unbound groups of galaxies expanding with the Hubble flow (Gott et al. 1973, Turner and Sargent 1974) would be expected to cluster in the region marked "field"; their absence suggests that the TG I groups are nearly all bound.

2) The short crossing times ($\Delta t\ H_o \approx 0.1$) of most of the groups supports the above conclusion and suggests that the groups are probably relaxed.

3) The dynamically inferred volume density enhancements of the groups varies from $\sim 10^2$ to $\sim 10^5$; these correspond to mean intergalactic separations of ~1 Mpc to ~100 kpc respectively.

4) The median value of M_{VT}/L for the groups rated 1 and 2 is $\sim 90\ M_\odot/L_\odot$, perhaps as good an estimate of the characteristic M/L of galaxies as can be obtained from this material.

5) Almost all of the groups (including every group rated

FIGURE 8

Mass-to-light ratio versus mean harmonic radius. Open points are various rotation curve results. Filled circles and the triangle are pure spiral groups from the present sample; "B" indicates binary systems. "LGT" and "LGV" are for Local Group timing and virial analyses, respectively. "GP" is a corrected form of the Geller and Peebles (1973) result. The arrow indicates the M/L needed to close the universe if the luminosity density is 4.7×10^7 $L_\odot$ Mpc^{-3}. For more details, see Gott and Turner (1976). Notice that among themselves the group data (filled points) show no evidence for $M/L \sim R$.

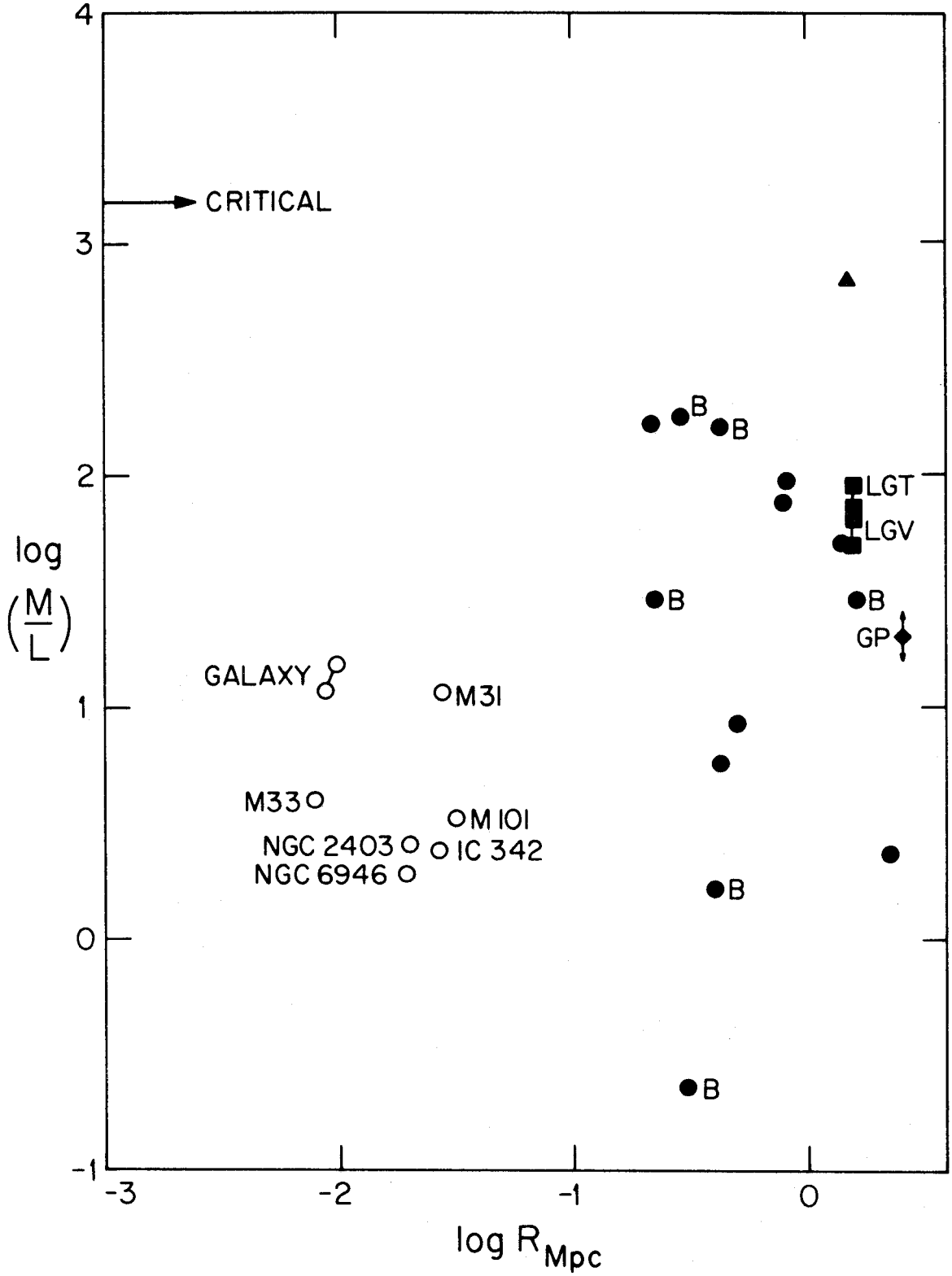
4
3
2
1
0
-1
-3
-2
-1
0
CRITICAL
log (M/L)
log R Mpc
B
B
B
B
B
B
LGT
LGV
GP
GALAXY
M31
M33
M101
NGC 2403
IC 342
NGC 6946

FIGURE 9

Mass-to-light ratio versus crossing time. Contamination ratings of 1, 2, 3, and 4 are indicated by filled circles, filled triangles, open circles, and open triangles, respectively. The "field" point indicates the expected location of unbound groups. The straight lines indicate values of the ratio of the dynamically inferred density in a group to the mean density. The meaning of the arrow is discussed in the caption of Figure 8. The histograms show the distributions of groups rated 1 (filled), 2 (shaded), and 3 or 4 (open), along the two axes. The plot is interpreted in detail in the text.

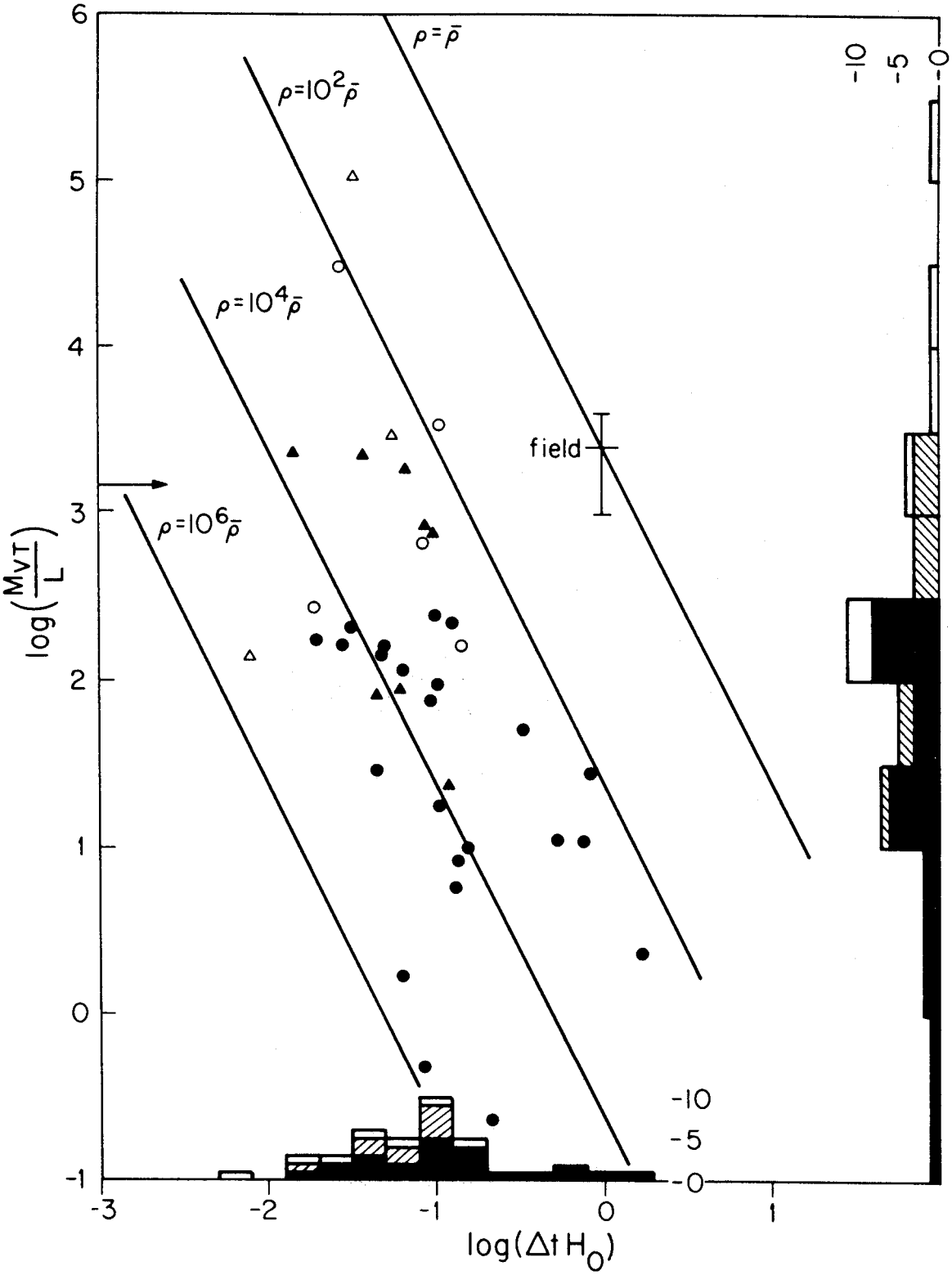
$\rho=\bar{\rho}$
$\rho=10^2\bar{\rho}$
$\rho=10^4\bar{\rho}$
$\rho=10^6\bar{\rho}$
field
$\log\left(\frac{M_{VT}}{L}\right)$
$\log(\Delta t H_0)$
-10
-5
-0

1) have M_{VT}/L values less than the critical mass-to-light ratio (indicated by an arrow) required to bind the universe. Although the plotted arrow is based on a luminosity density of 4.7×10^7 $L_\odot$ Mpc^{-3} (Gott and Turner 1976), the preceding sentence would still be true for the more conventional 1.6×10^8 $L_\odot$ Mpc^{-3} (Shapiro 1971, Oort 1958). In addition, any reasonable errors in the observations and shortcomings of the analysis tend to cause overestimates of M_{VT}/L (Materne and Tammann 1974). Therefore, the data in figure 9 offer little hope of closing the universe with the mass in or around galaxies.

It should be noted that the large scatter of V, M_{VT}/L, and Δt H_o (figures 6, 8, and 9) is almost certainly due to the small number (often only 2 per group) of radial velocities available and is probably not intrinsic. The dynamics of these groups cannot be properly analyzed until more and better velocities are obtained.

IV. MULTIPLICITY FUNCTION

The multiplicity function (Holmberg 1937, de Vaucouleurs 1970) is the distribution of groups with respect to the number of member galaxies. In order to define this concept more clearly, let us define the number of members in a group of total luminosity L to be L/L^*. Consider the function $\rho(L/L^*)\, d(L/L^*)$, the density (cluster centers Mpc^{-3}) of

groups between L/L^* and $L/L^* + d(L/L^*)$. It is essentially the luminosity function of groups as opposed to the luminosity function of galaxies in groups (§II). However, in order to avoid confusion, $\rho(L/L^*)\ d(L/L^*)$ will be referred to as the multiplicity function.

Suppose a complete sample of observed groups with known distances and total luminosities is available, then

$$\rho(L/L^*)\ d(L/L^*) = N(L/L^*)\ d(L/L^*)/\ V_{max} \qquad (12)$$

where $N(L/L^*)\ d(L/L^*)$ is the number of groups with a particular luminosity L and V_{max} is the maximum volume within which they could be observed. If the groups are distributed uniformly in space,

$$V_{max} \approx \frac{2}{3} A\ \overline{D^3} \qquad (13)$$

where A is the solid angle of the surveyed area of the sky and $\overline{D^3}$ is the mean cubed distance to the groups. The concept of V_{max} is, of course, closely related to that of Schmidt's (1968) V_M. In practice, naturally, the $d(L/L^*)$'s in (12) and (13) must be replaced by finite bins.

The above procedure has been used to obtain an estimate of the multiplicity function from the data given in TG I. All groups and field galaxies (considered as groups of ~1) are included in the sample, if they have at least one member brighter than an apparent magnitude of 13.5. Distances and total luminosities [calculated from (7)] are based on

redshifts where they are available and on the Schechter and Press (1975) technique (see §II), otherwise. The 13.5 magnitude cutoff is necessary because the Schechter and Press method breaks down for small groups in which all members have apparent magnitudes near the survey's limit (14th); see Table I for examples of this breakdown. Varying this cutoff between 12 and 13.8 has no substantial effect on the results. The analysis yielded an estimate of $\rho(L/L^*)d(L/L^*)$ which is shown in figure 10 with square-root-of-N errors.

It must be strongly emphasized that the curve in figure 10 may be influenced by substantial systematic errors. It would clearly be preferable to use only redshift distances if they were available; the Schechter and Press method explicitly couples estimates of distance to those of total luminosity. Also, the TG I groups are by no means a complete sample of bound (or relaxed, etc.) systems (see §II of TG I) but only a list of those systems which give rise to substantial surface density enhancements of galaxies on the sky. Nevertheless, the present results probably reflect, at least crudely, the true multiplicity function of (easily) identifiable groups.

Putting aside the misgivings of the previous paragraph temporarily, the derived multiplicity function (figure 10) possesses a number of interesting features. There appears to be a sharp break near $L/L^* \approx 1$, the region in which the systems presumably shift from multigalaxy groups to field

FIGURE 10

The multiplicity function. Using the method described in §IV, the mean density (group centers Mpc^{-3}) of groups ρ has been determined as a function of total group luminosity. The broken curve was drawn through the data points by hand. For the purpose of the multiplicity function alone, the concept of a group has been extended to "groups of one" (i.e., field galaxies). This figure is discussed at some length in the text.

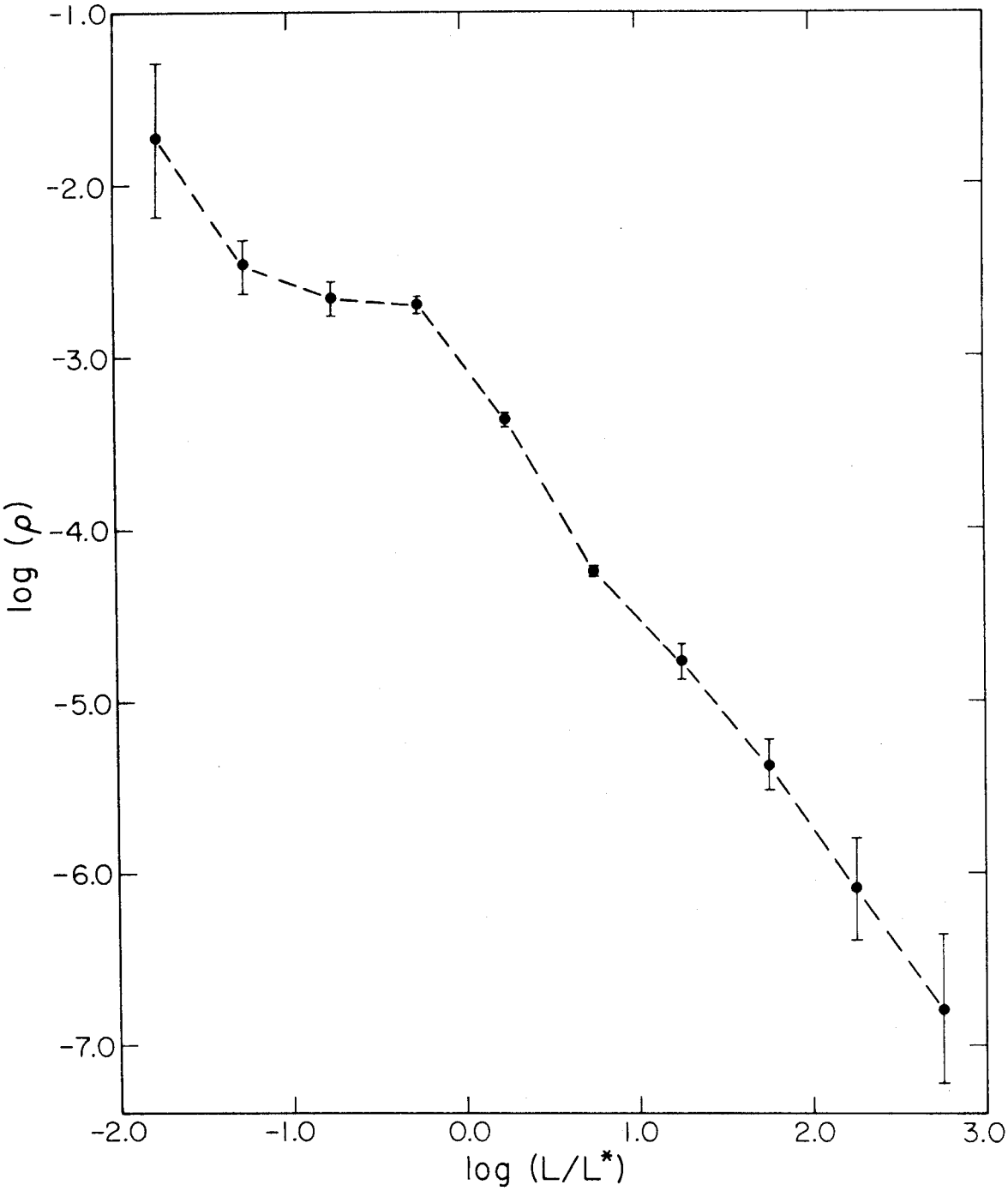
-1.0
-2.0
-3.0
-4.0
-5.0
-6.0
-7.0
log (ρ)
-2.0
-1.0
0.0
1.0
2.0
3.0
log (L/L*)

galaxies (groups of 1). For $L/L^* < 1$ the multiplicity function is not too different from the galaxy luminosity function (§II); while for $L/L^* \geq 1$, it is very well approximated by a power law [$\rho(L/L^*) \sim (L/L^*)^{-7/3}$]. No groups with L/L^* greater than a few hundred are observed in agreement with theoretical expectations (Schechter 1974). The integral of $L\ \rho(L/L^*)\ d(L/L^*)$ yields, not surprisingly, a reasonable estimate of the luminosity density $\sim 1.5 \times 10^8 L_\odot$ Mpc^{-3}. The fractions of this luminosity density arising from groups with $L/L^* \leq 1$, $1 < L/L^* \leq 30$, and $L/L^* > 30$ are 0.56, 0.32, and 0.12 respectively. These numbers emphasize the importance of small groups and field galaxies.

Better and more reliable estimates of the multiplicity function will be of great value to the study of galaxy clustering.

V. SUMMARY

The major results of this statistical study of the TG I groups are summarized below:

1) The luminosity function of galaxies in small groups (figure 1) is well approximated by equation (6) with $\alpha = -1$ and $L^* = 3.4 \times 10^{10}\ L_\odot$ and is quite similar, if not identical, to Schechter's (1975) rich cluster luminosity function.

2) Surprisingly, there is, at best, only marginal evidence for a difference in luminosity function between early

and late type galaxies.

3) The Schechter and Press (1975) luminosity function method probably gives better distance estimates than the brightest-cluster-member method for groups with $L \lesssim 10\ L^*$, while the reverse holds for larger clusters.

4) The TG I groups are likely to be bound and relaxed since they have relatively small virial masses and crossing times compared to those expected for unbound groups.

5) Although the virial mass-to-light ratios in the groups are generally quite high ($\sim 90\ M_\odot/L_\odot$), they are still much smaller than the M/L required to close the universe.

6) The multiplicity function of identifiable groups has an $L^{-7/3}$ dependence for $L/L^* \gtrsim 1$ and turns over (i.e. flattens) for smaller luminosities.

7) The majority of galaxies ($\sim$90%) reside in small groups ($L/L^* \lesssim 30$) or the field.

The above conclusions all rest on a relatively small amount of data drawn from a wide variety of sources in the literature and may, as a result, embody unknown biases. New observational studies of the groups would be of great value in revealing these biases and, undoubtedly, in obtaining new insights.

REFERENCES

de Vaucouleurs, G. 1970, Science, 167, 1203.

de Vaucouleurs, G. 1975, in Stars and Stellar Systems, Vol. 9, ed. A. and M. Sandage (Chicago: University of Chicago Press) (in press).

Geller, M. J., and Peebles, P. J. E. 1973, Ap. J., 184, 329.

———————————————— 1975, preprint.

Gott, J. R., and Turner, E. L. 1976, in preparation.

Gott, J. R., Wrixon, G. T., and Wannier, P. 1973, Ap. J., 186, 777.

Holmberg, E. 1937, Ann. Obs. Lund, No. 6, 1.

Kalnajs, A. J. 1972, Ap. J., 175, 63.

Materne, J., and Tammann, G. A. 1974, Astron. Astroph., 37, 383.

Mathews, W. G., and Limber, D. N. 1960, Ap. J., 132, 286.

Oemler, A. 1974, Ap. J., 194, 1.

Oort, J. H. 1958, Distribution of Galaxies and the Density in the Universe, Institut International de Physique Solvay, Brussels.

Ostriker, J. P., and Peebles, P. J. E. 1973, Ap. J., 186, 467.

Ostriker, J. P., Peebles, P. J. E., and Yahil, A. 1974, Ap. J. Lett., 193, L1.

Sandage, A. 1972, Ap. J., 178, 1.

———————— 1975, preprint.

Sandage, A. and Hardy, E. 1973, Ap. J., 183, 743.

Schechter, P. 1974, Ph.D. thesis, California Institute of Technology.

———————— 1975, preprint.

Schechter, P., and Press, W. H. 1975, preprint.

Schmidt, M. 1968, Ap. J., 151, 393.

Shapiro, S. L. 1971, A. J., 76, 291.

Turner, E. L., and Gott, J. R. 1976, in preparation, (TGI).

Turner, E. L., and Sargent, W. L. W. 1974, Ap. J., 194, 587.